藥學博士 學位論文

TM4SF5/STAT3 signaling axis-mediated development of liver disease

간질환 심화과정에서 TM4SF5/STAT3 의 상호작용과 그 역할에 관한 연구

2017 年 8 月

서울大學校 大學院

藥學科 醫藥生命科學專攻

柳 知 惠

TM4SF5/STAT3 signaling axis-mediated development of liver disease

by

Jihye Ryu

A thesis submitted in partial fulfillment of the requirements

for the degree of

DOCTOR OF PHILOSOPHY

(Pharmacy : Pharmaceutical bioscience major)

under the supervision of Professor Jung Weon Lee

at the college of Pharmacy,

Seoul National University

August 2017

TABLE OF CONTENTS

LIST OF FIGURES

Ⅰ.Chapter 1

Ⅱ.Chapter 2

treatment of SNU761 cells.

Fig. Ⅱ-3.

IL-6 treatment of cells differentially regulates migration and invasive ECM degradation depending on TM4SF5 expression.

Fig. Ⅱ-4.

Suppression of STAT3/JAK signaling inhibited IL-6-mediated FAK phosphorylation of Chang-TM4SF5 cells but did not recover IL-6-suppressed FAK phosphorylation of SNU761-TM4SF5 cells.

Fig. Ⅱ-5.

STAT3 suppression inhibited IL-6-mediated FA formation by Chang-TM4SF5 cells but did not recover the IL-6-suppressed FA formation and ECM degradation by SNU761-TM4SF5 cells.

Fig. Ⅱ-6.

Inhibition of FAK activity did not alter IL-6-mediated pY^{705} STAT3 in Chang or SNU761 cells.

Fig. Ⅱ-7.

Crosstalk between the TM4SF5/FAK and IL-6/STAT3 pathways.

LIST OF ABBREVIATIONS

TM4SF5;	Transmembrane 4 L six family member 5
STAT;	Signal transducer and activator of transcription
SOCS;	Suppressor of cytokine signaling
HC;	Hepatocyte
HSC;	Hepatic stellate cell
HCC;	Hepatocellular carcinoma
HIF1α;	Hypoxia-inducible factor 1-alpha
CD;	Cluster of differentiation
ECM;	Extracellular matrix
NAFLD;	Nonalcoholic fatty liver disease
SREBP;	Sterol regulatory element-binding protein
TGFβ1;	Transforming growth factor beta 1
CCl_4;	Carbon tetrachloride
DEN;	Diethylnitrosamine
KO;	Knock-out

TG; Triacylglycerol

ACC; Acetyl-CoA carboxylase

FFA; Free fatty acid

HFD; High fat diet

TSAHC; 4'-(*p*-toluenesulfonylamido)-4-hydroxychalcone

PCR; Polymerase chain reaction

LAMC2; Laminin gamma 2

Col1a1; Collagen 1A1

α-SMA; Alpha-smooth muscle actin

CM; Conditioned media

FAK; Focal adhesion kinase

FA; Focal adhesion

IL-6; Interleukin-6

CCL2; Chemokine [C-C motif] ligand 2

WT; Wild-type

MCL1; Myeloid cell leukemia sequence 1

IHC; Immunohistochemistry

MMP2; Matrix metallopeptidase 2

NSCLC; Non-small-cell lung carcinoma

RT-PCR; Reverse transcription polymerase chain reaction

qRT-PCR; Quantitative real-time polymerase chain reaction

IHC; Immunohistochemistry

Ⅰ. Chapter 1

Conversion from nonalcoholic fatty to fibrotic and cancerous liver by TM4SF5/STAT3 signaling axis

ABSTRACT

Mechanistic aggravations of the chronic liver malignancy remain unclear. We here investigated roles of TM4SF5 in the liver malignancy progression, using multiple *in vitro* and *in vivo* cellular, animal, and clinical patient tissue models. Transmembrane 4 L six family member 5 (TM4SF5)-transgenic mice revealed fatty, fibrotic, and cancerous phenotypes depending on age increase and disease-prone property. Following chronic inflammation, the hepatocytes accumulated lipids via SOCS1/3-inhibited STAT3 activity. Ligand independent and TM4SF5-mediated STAT3 activity promoted fibrotic expression of collagen I and laminin/laminin γ2 in hepatic stellate cells (HSCs) and hepatocytes, respectively, leading to fibrotic phenotypes. TM4SF5 overexpression led to induction of HIF1α, CD34, and α-fetoprotein, a HCC marker, together with robust STAT3 activity and ECM expression. Altogether, this study supports that TM4SF5-STAT3 signaling could aggravate liver diseases and the laminin induction in hepatocytes also importantly contribute to the malignancy, indicating TM4SF5 as a driving player for the liver diseases.

Keywords : Animal models, Collagen I, Fibrosis, Hepatic cancer, Laminin, Nonalcoholic fatty liver disease (NAFLD), SOCS, SREBP1, STAT3, TM4SF5

Student Number : 2011-21717

1. Introduction

Chronic liver injury can cause inflammation, metabolic dysregulation, and excessive extracellular matrix (ECM) production for fibrosis and further cirrhosis, ultimately leading to liver failure or hepatocellular carcinoma (HCC) [1]. Liver injury occurs due to immune-mediated or direct injury to the hepatocytes, and injured hepatocytes can lead to both cell death (and thereby inflammation) and regeneration of the cells to compensate for the loss of hepatocytes [1,2]. During the battle between injury-mediated cell death and regeneration, inflammation and ECM deposition for cell proliferation prevalently play critical roles. An excessive ECM deposition without reciprocally balanced degradation result in fibrosis with abnormal cell proliferation, which can lead further to cirrhosis with scar tissues and HCC [3]. ECMs in liver is known to be produced mostly by hepatic stellate cells (HSCs) [4], although liver parenchyma hepatocytes comprising the majority at 85% of the liver mass [2] can also produce and alter ECM [1]. Interestingly, deposition of collagen I as the main component of the fibrous septa is not relevant to hepatocyte but to activated-HSCs [5]. Meanwhile, the roles of other hepatic cell types including hepatocytes in ECM remodeling eventually leading to liver fibrosis is recently emerging to be studied [1]. However, it is not clear yet how the hepatocytes can contribute to ECM production while the aggravation of liver malignancy.

Chronic liver injury leads to inflammation, by which further diverse cytokines including TGFβ1 [6], IL-13 [7], and others can be produced for ECM production and fibrosis. Furthermore, other molecules and signaling pathways in different liver cell types can cause inflammation and ECM production, given that mammal ECM consists of about 300 proteins [8], and that effects and responses of hepatocytes may be prevalent because hepatocytes contributes to the majority (approximately 85%) of the liver mass, and because the chronic injury affects primarily the hepatocytes. Therefore, it would be interesting to reveal the signaling molecules or pathways in hepatocytes to induce ECM production as overall perspective for liver diseases from inflammatory fatty liver to fibrotic and cancerous liver.

Transmembrane 4 L six family member 5 (TM4SF5) is a glycosylated-membrane protein with 4 transmembrane domains, similar to the tetraspanins (TM4SFs). TGFβ1 signaling that cross-talks with EGFR pathway causes TM4SF5 expression in CCl_4-mediated fibrotic animal system [9,10]. Different cancer types including liver and prostate cancer show TM4SF5 overexpression [11,12] and cancer metastasis from liver to intestinal area in liver-orthotopic animal model occurs via cross-talks between TM4SF5 and CD44 [13]. TM4SF5 affects c-Src and FAK via direct physical associations [14,15], and STAT3 via c-Src activity, independent of IL6 [16]. Therefore, it is likely that TM4SF5 may play multi-functional roles during development of liver malignancy even from inflammation to HCC, although it has not been

explored so far.

Based on the pivotal observations that TM4SF5 transgenic mice showed nonalcoholic fatty liver disease (NAFLD) and fibrosis, we here investigated how TM4SF5-mediated signaling axis for lipid or ECM metabolisms could promote progression of overall liver diseases. We found that TM4SF5-mediated STAT3 activity for the alternative modulation of lipid or ECM metabolic status could aggravate overall liver malignancy from fatty liver, non-alcoholic steatohepatitis, and fibrosis to cancer.

2. Materials and Methods

1. Cells

TM4SF5-lacking control [hepatocarcinoma SNU449 or SNU761] or TM4SF5 WT-expressing (endogenously expressing HepG2 and Huh7 or ectopically expressing SNU449T_7) cells have been described previously [12]. Cells were purchased from either Korean Cell Bank (Seoul National Univ. Seoul, Korea) or ATCC (Manassas, VA, USA). Stable cells were maintained in RPMI-1640 (WelGene, Daegu, Korea) containing 10% FBS, G418 (250 μg/ml), and antibiotics (Invitrogen, Grand Island, NY).

2. Transfection

siRNA, shRNA, or cDNA plasmids that are properly indicated are transiently transfected for 48 h, using Lipofectamine RNAiMAX or Lipofectamine 3000 following the protocol by manufactures (ThermoFisher Scientific, Waltham, MA, USA).

3. TM4SF5 transgenic or knockout animals

TM4SF5 transgenic mice were generated and confirmed for its expression. pcDNA3-TM4SF5-Flag was digested with *NruI* and *DraIII* and the fragment consisting of the CMV promoter, whole TM4SF5-FLAG sequence, and BGH poly A region was purified and microinjected into fertilized eggs from C57BL/6N mice according to standard procedures (Macrogen, Seoul, Korea).

Two-week-old founders were screened by PCR using the primer set for CMV-F1 (forward primer, 5' CGC TAT TAC CAT GGT GAT GCG 3') and TM4SF5-R1 (reverse primer, 5' AGA CAC CGA GAG GCA GTA GAT 3'). In addition to negative controls, normal mouse genomic DNA or non-transgenic mouse did not have the PCR constructs of 555 bp covering a part of CMV promoter and a part of FLAG-TM4SF5. TM4SF5 transgenic mice with FVB/N disease-prone strain were prepared via breeding between normal FVB/N and TM4SF5 transgenic C57BL/6N mice more than 10 generations, before confirmation of its expression as above. TM4SF5-knockout (*TM4SF5*$^{-/-}$) mice were generated by targeting exon 3-5 coding for the 2nd extracellular loop (EC2) in mouse *TM4SF5* gene (Macrogen), via embryo injection and transfer to normal healthy female C57BL/6N mice of mouse TM4SF5-FLAG digested by Cas9 protein and sgRNAs (i.e., RG1 and 2 for exon3 up and down, respectively; RG3 for intron between exon 4 and 5; RG4 for exon 5). Identification of deletion mutation in F0 founders was performed on tail genomic DNA by a T7E1 assay to see a heteroduplex formation between WT and mutant PCR products (Macrogen). Further, genotyping was performed using primers for Mouse-TM4SF5-FLAG (forward 5′-GTAGTATGCG GGAGGCACTG-3′, reverse 5′- GGGTGACCACTCAGACTTCC-3′).

TM4SF5$^{-/+}$ heterozygotes in F1 little mates were bred to generate *TM4SF5*$^{-/-}$ homozygotes.

4. Chemical-treated animal models

Four-week-old mice (BALB/c) were purchased from Orient. Co. Ltd (Seungnam, Korea). Mice were housed in a specific pathogen-free room with controlled temperature and humidity. All animal procedures were performed in accordance with the procedures of the Seoul National University Laboratory Animal Maintenance Manual and IRB agreement by Institute of Laboratory Animal Resources Seoul National University (ILARSNU). Mice aged 5 weeks ($n \geq 5$) were injected intraperitoneally with or without CCl_4 (Sigma, 1 mg/kg) in 40% olive oil three times a week for 4 or 16 weeks. 4'-(*p*-toluenesulfonylamido)-4-hydroxychalcone (TSAHC) administration (IP at 50 mg/kg in 40% DMSO) was performed the day after each CCl_4 administration. And diethylnitrosamine (DEN) injected(sigma, 50mg/kg) once a week for 28weeks. After 4, 16 or 28weeks, mice were sacrificed with ether, the tissues were resected, and one piece of tissue was immediately frozen in liquid N_2 while a second piece was embedded in paraffin.

5. Primary cell preparation

Primary hepatocytes were isolated from 4-6 weeks-old BALB/C mice (Orient. Co. Ltd Seungnam, Korea) or 52-78weeks C57BL/6 Mice (Macrogen, Seoul, Korea) by perfusion of the liver using collagenase type Ⅱ (Life technologies, Carlsbad, CA, USA). The hepatocytes were cultured William's E Medium(Life technologies, Carlsbad, CA, USA) supplemented with 10%

fetal bovine serum (FBS), primary hepatocyte maintenance supplements (Life technologies, Carlsbad, CA, USA) on collagen-coated plates.

For the isolation of Hepatic stellate cells, nonparenchymal sufficient supernatant was centrifuged in 50%/30% percoll (Sigma-aldrich). The top layer containing Hepatic stellate cells was cultured RPMI 1640 (WelGene, Daegu, Korea) with 10% FBS on collagen-coated plates.

6. Co-culture

Cells were co-cultured using cell culture inserts (SPL, 0.4μm pore size) to separate the cell populations; Primary hepatocytes were plated on the bottom, and primary hepatic stellate cells were plated on the insert. After each incubation, shTM4SF5 is transfected only in the primary hepatocytes. And after 24 hours, change the serum free medium and inserted primary hepatic stellate cells into the well with hepatocytes. After 24h co-culture, the cells were harvested for western blotting.

7. Western blots

Subconfluent cells in normal culture media, or cells transiently transfected with control or siRNA against the indicated molecules for 48 h or animal liver tissues harvested for whole cell or tissue extracts using a modified RIPA buffer, as explained previously [12,16]. The primary antibodies include anti-pY^{397}FAK (Abcam, Cambridge, UK), -pY^{416}Src, -Akt (Santa cruz Biotech., Santa cruz, CA) -p-ERKs, -ERKs (Cell Signaling Technol. Danvers, MA), -

pY^{705}STAT3 (Millipore, Bellerica, MA), -α-tubulin, (Sigma, St Louis, MO), -c-Src, -pY^{577}FAK, -pS^{473}Akt (Santa Cruz Biotech., Santa Cruz, CA), -FAK (BD Transduct. Lab., Bedford, MA), -STAT3 (Millipore, Solna, Sweden), and -collagen I, -laminin γ2 (Santa Cruz Biotech., Santa Cruz, CA), -laminin, -STAT5, -pY^{694}STAT5, -albumin, -pS^{727}STST3, -precursor SREBP1 (Santa Cruz Biotech., Santa Cruz, CA), -mature SREBP1 (Santa Cruz Biotech., Santa Cruz, CA), -PPARγ (Santa Cruz Biotech., Santa Cruz, CA), -PPARα (Santa Cruz Biotech., Santa Cruz, CA), -CD36, -pY^{701}STAT1, -β-actin (Santa Cruz Biotech., Santa Cruz, CA) antibody.

8. Immunofluorescence

Cells in normal culture condition on glass coverslips or transiently transfected for 48 h with siControl or siSTAT3 (Dharmacon, Pittsburgh PA) together with GFP-conjugated control siRNA were immunostained using antibody against pY^{397}FAK or pY^{705}STAT3, in addition to DAPI staining for DNA. Immunofluorescent images were acquired on a microscope (BX51TR, Olympus, Japan). Randomly saved images for 10 fields in each experimental condition were visually counted by two independent individuals. Cells with at least similar or increased spreading area and FA numbers upon IL6 treatment were counted and their mean ± standard deviation values were presented as a graph.

9. Immunohistochemistry

Immunohistochemistry of mouse or human liver tissues that informed consents were obtained from each patient following a IRB approve were performed with primary antibodies for normal rabbit or mouse IgG, TM4SF5 [12], collagen I, pY^{705}STAT3 (Millipore, Solna, Sweden), SREBP (Santa Cruz Biotech., Santa Cruz, CA), laminin (Abcam, Cambridge, UK), and laminin γ2 (Santa Cruz Biotech., Santa Cruz, CA). Alternatively, the tissues were processed for Masson′s Trichrome and hematoxylin and eosin staining as previously described [17], or for double-immunofluorescence stainings for TM4SF5 and either α-SMA or PDGFRα. Incubation with anti-TM4SF5 primary antibody was followed by anti-rabbit IgG conjugated with TRITC, and incubation with anti-α-SMA or -PDGFRα antibodies was followed by anti-mouse or -rabbit IgG conjugated with FITC, respectively. In addition, the nucleus was stained with DAPI.

10. RT-PCR

Total RNA was isolated using TRIzol Reagent (Invitrogen), and complementary DNA (cDNA) was synthesized using amfiRivert Platinum cDNA synthesis master mix (GenDEPOT Inc.) according to the manufacturer′s instructions. The cDNA was subjected to RT-PCR using Dream Taq Green PCR master mix (Thermo Scientific, San Jose, CA).

11. Adipocyte differentiation

Mouse 3T3-L1 preadipocytes were seeded using DMEM supplemented with 10% newborn bovine serum (Gibco), 1% penicillin/streptomycin in 6well plates at a density of $1x10^5$. 2day postconfluent **(**day 0) preadipocytes were treated with adipocyte differentiation medium(MDI medium) containing 1μM Dexamethasone, 0.5mM IBMX, 10μg/ml Insulin (Sigma, USA) for 2 days. After that, the media were replaced with DMEM supplemented with 10% fetal bovine serum (FBS) and insulin (10 μg/mL) for 2 days. The extent of differentiation was determined on day 12.

12. ECM-luciferase assay

To construct a vector for the promoter assay, Lamc2 promoters (encoding regions of -1871 to +388 and -592 to +388) and Col1a1 promoters (encoding regions of -2865 to +89, -2047 to +89 and -845 to +89) were amplified by PCR and cloned into the pGL3-basic vector. Primary cultured hepatocytes or AML12 were seeded in 48well plates using lipofectamin3000 transfection reagent (Invirogen). 24h after transfection, luciferase activity was measured according to manufacturer's protocol using luciferase reporter assay kit (Promega) with a luminometer (Berthold technologies, DE/Centro LB960).

13. Anti-TM4SF5 antibody blockade of liver diseases.

All animal procedures were performed in accordance with the procedures of the Seoul National University Laboratory Animal Maintenance Manual and

Institutional Review Board (IRB) agreement by Institute of Laboratory Animal Resources Seoul National University (ILARSNU). Nude mice (BALB/c-nude, 5 weeks old, male) were obtained Orient. Co. Ltd (Seungnam, Korea). SNU449Cp (control cells) (n=4) and $SNU449T_7$ (TM4SF5-overexpressing stable cells) (n=21) were injected subcutaneously into the back of each mouse. Five million cells resuspended in PBS were mixed with Matrigel on ice before injection. On 8th day after the injection with $SNU449T_7$ cells, tumor-bearing mice were randomized into control and treatment groups (n=7 per group). Ab27 (5 μg/mouse) or Ab79 (16 μg/mouse) anti-TM4SF5 antibodies were intratumorally injected into each mouse at 2 or 3-day intervals for total 5 times. PBS (20 μl/mouse) was injected as a negative control. Body weight and tumor volume were measured before antibody injection. The tumor volumes were calculated as follows: tumor volume = ($a \times b^2$) × 1/2, where a was the width at the widest point of the tumor and b was the maximal width perpendicular to a. On 19th day, mice were sacrificed and photographed. Tumor masses were lysed as described [12] and subjected to immunoblot analysis.

14. Statistical analysis

Student's *t*-tests were performed for comparisons of mean values to determine statistical significance. A *p* value less than 0.05 was considered statistically significant.

3. Results

1. TM4SF5 expression promoted nonalcoholic fatty liver disease (NAFLD).

At 1 year old age, systemic TM4SF5-overexpressing transgenic mice (C57BL/6-Tg^{TM4SF5}) showed severe abdomen obesity and fatty liver phenotypes (Fig.1A). Together with lipid accumulation in livers, collagen I deposition was also obvious, compared with normal wildtype mice (Fig.1B). Thus, TM4SF5 expression significantly caused phenotypes of fatty liver (Fig.1C). Further, Tg^{TM4SF5} mice livers showed elevated levels of hepatic triacylglycerol (TG) and alanine aminotransferase (GOT/ALT), although the level of albumin was maintained, compared with normal wildtype livers (Fig.1D). At molecular levels, acetyl-CoA carboxylase 1 (ACC1) for fatty acid synthesis and matured sterol regulatory element-binding protein 1 (SREBP1) for cholesterol synthesis and uptake were greatly higher in livers of Tg^{TM4SF5} mice over than normal wildtype mice (Fig.1E). In addition to lipid synthesis, molecules related to lipid uptake by hepatic cells were elevated in the Tg^{TM4SF5} mice livers, compared with normal wildtype mice livers, whereas molecules for fatty acid oxidation were not clearly differential. Furthermore, when *TM4SF5* of the primary hepatocytes from Tg^{TM4SF5} mice livers were suppressed by shRNA against TM4SF5, levels of diverse mRNAs including

PPAR$_\gamma$, *CD36*, *FASN*, *SREBP1*, and *FABP1* were reduced, suggesting that TM4SF5 play roles in lipid metabolisms. Further interestingly, laminin level was parallel to the levels of lipid synthesis-related molecules, but STAT3 phosphorylation at Tyr705 (i.e., pY^{705}STAT3) was lower in the Tg^{TM4SF5} mice livers than wildtype mice livers (Fig.1E). Immunohistochemistry also resulted in such a positive correlation between TM4SF5 expression, ECM expression, and lipid droplets and SREBP1 expression, but a negative correlation between TM4SF5 expression and pY^{705}STAT3 (Fig.1F).

Meanwhile, either TM4SF5 transfection or treatment of free fatty acid (FFA) to primary mouse hepatocytes resulted in lipid accumulation (Fig.1G) together with increased mRNA levels of lipid metabolism-related genes (Fig.1H). Among them, *SREBP2*, *FASN*, and *LDLR* mRNAs were elevated via a positive cooperation with IL6 and TM4SF5, but *CD36* and *FABP1* were not depending on IL6 but on TM4SF5 (Fig.1I). When protein levels of SREBP1 and PPARγ increased by TM4SF5 expression or FFA treatment, furthermore, laminin was also elevated (Fig.1J). FFA-treatment-mediated increase in matured SREBP1 protein in TM4SF5-expressing hepatocytes were not observed anymore when the TM4SF5-positive cells were transfected with STAT3 (Fig.1K), indicating that STAT3 activity (pY^{705}STAT3) was inversely correlated with FFA-treatment-mediated SREBP1 maturation. Thus, pY^{705}STAT3 decreased by SREBP1 overexpression (Fig.1L). Therefore, while TM4SF5-mediated lipid accumulation in hepatocytes, an inverse relationship

between SREBP1 maturation and STAT3 might be importantly involved in.

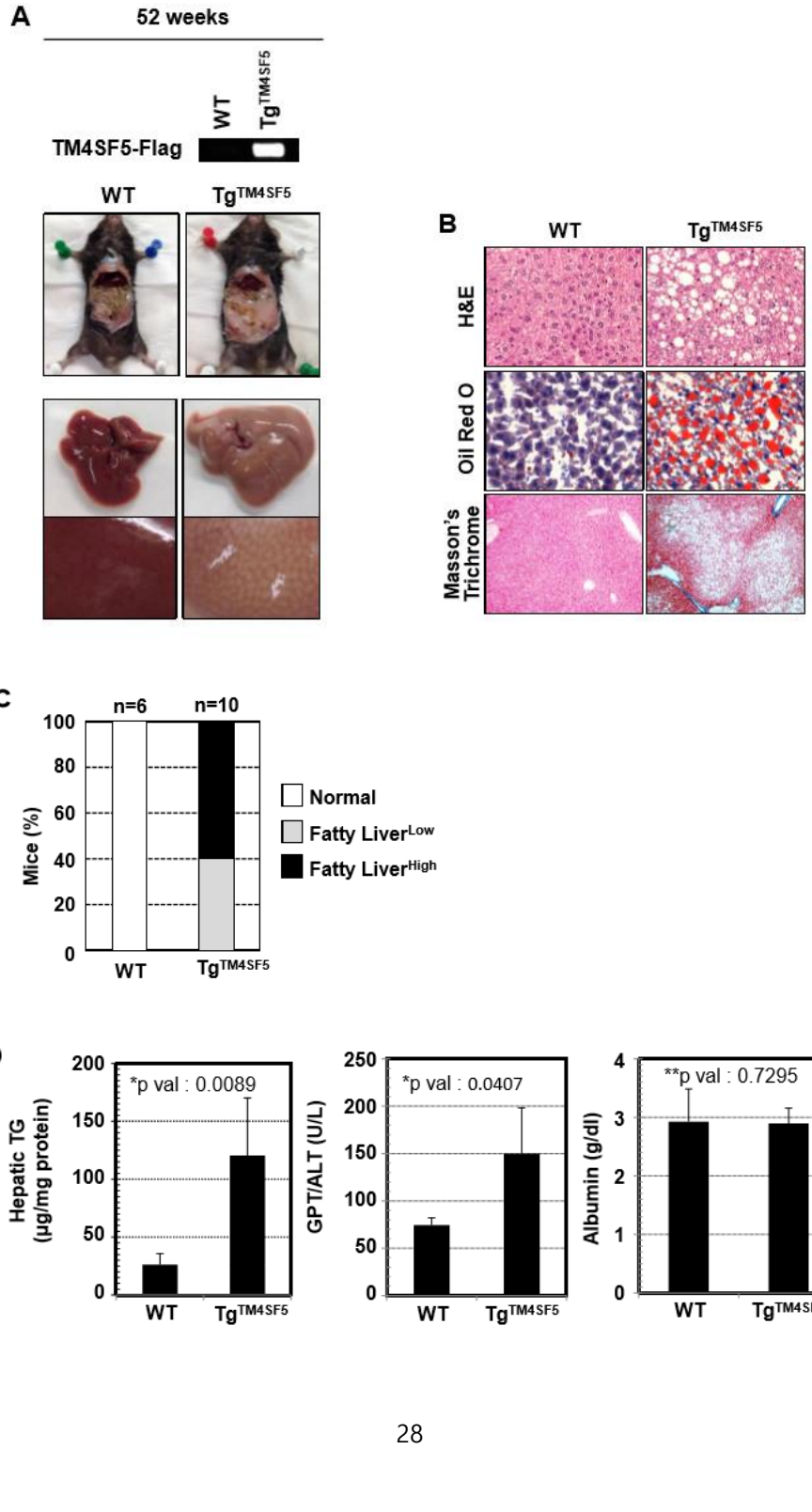
A
52 weeks
WT
Tg^TM4SF5
TM4SF5-Flag
WT
Tg^TM4SF5
B
WT
Tg^TM4SF5
H&E
Oil Red O
Masson's Trichrome
C
n=6
n=10
Mice (%)
100
80
60
40
20
0
WT
Tg^TM4SF5
Normal
Fatty Liver^Low
Fatty Liver^High
D
Hepatic TG (μg/mg protein)
*p val : 0.0089
GPT/ALT (U/L)
*p val : 0.0407
Albumin (g/dl)
**p val : 0.7295
WT
Tg^TM4SF5

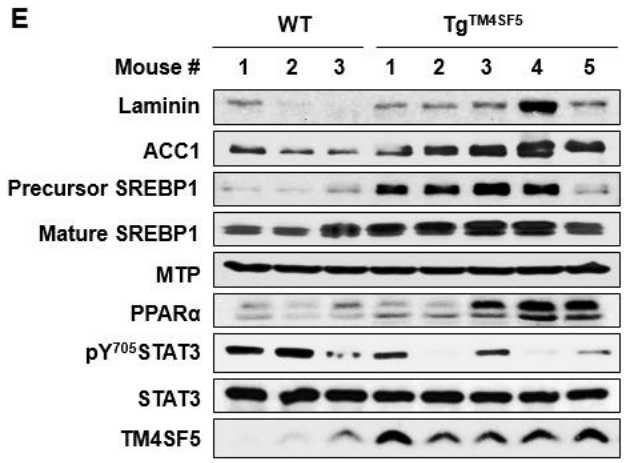
E
WT
Tg^TM4SF5
Mouse #
1 2 3 1 2 3 4 5
Laminin
ACC1
Precursor SREBP1
Mature SREBP1
MTP
PPARα
pY705STAT3
STAT3
TM4SF5

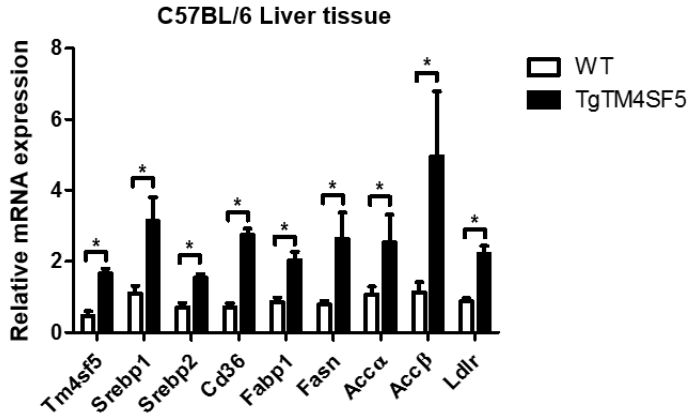
C57BL/6 Liver tissue
Relative mRNA expression
0
2
4
6
8
WT
TgTM4SF5
Tm4sf5
Srebp1
Srebp2
Cd36
Fabp1
Fasn
Accα
Accβ
Ldlr

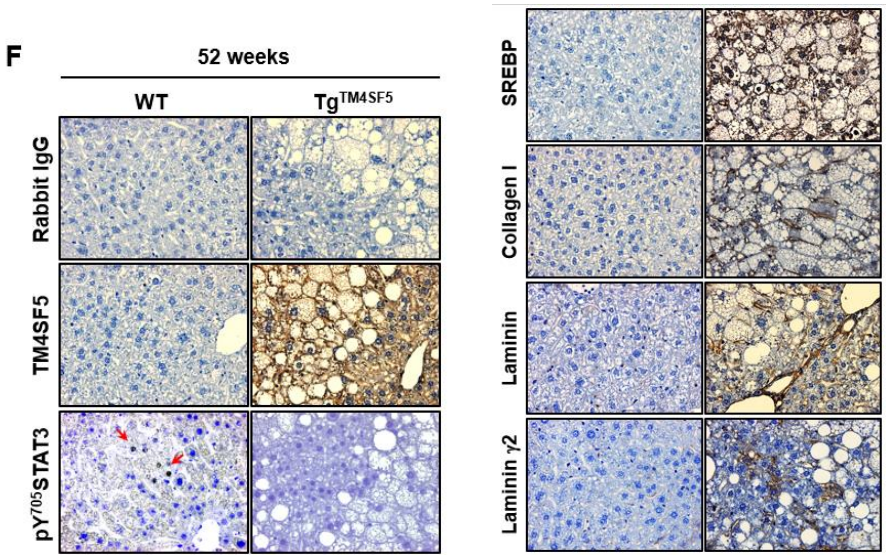
F
52 weeks
WT
Tg^TM4SF5
Rabbit IgG
TM4SF5
pY705STAT3
SREBP
Collagen I
Laminin
Laminin γ2

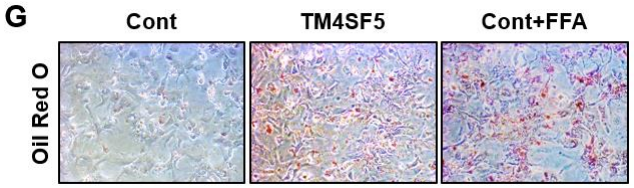
G
Cont
TM4SF5
Cont+FFA
Oil Red O

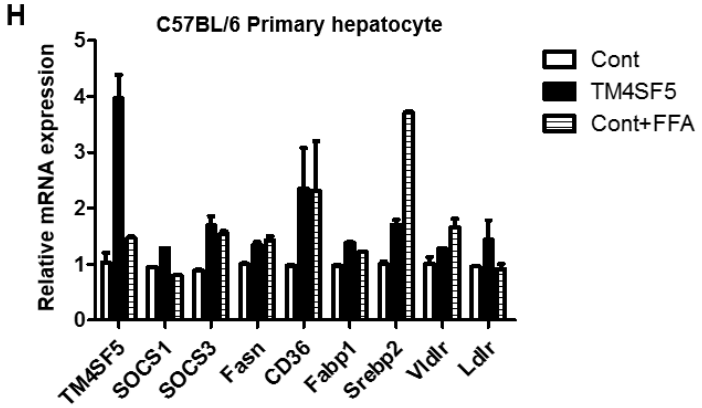
H
C57BL/6 Primary hepatocyte
Relative mRNA expression
0
1
2
3
4
5
TM4SF5
SOCS1
SOCS3
Fasn
CD36
Fabp1
Srebp2
Vldlr
Ldlr
Cont
TM4SF5
Cont+FFA

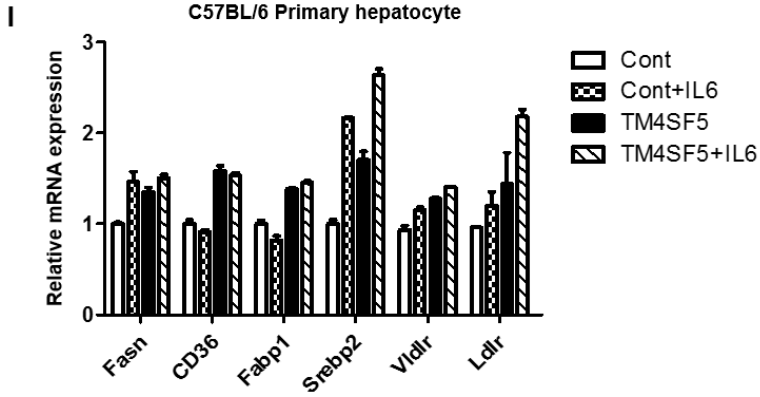
I
C57BL/6 Primary hepatocyte
Relative mRNA expression
3
2
1
0
Fasn
CD36
Fabp1
Srebp2
Vldlr
Ldlr
Cont
Cont+IL6
TM4SF5
TM4SF5+IL6

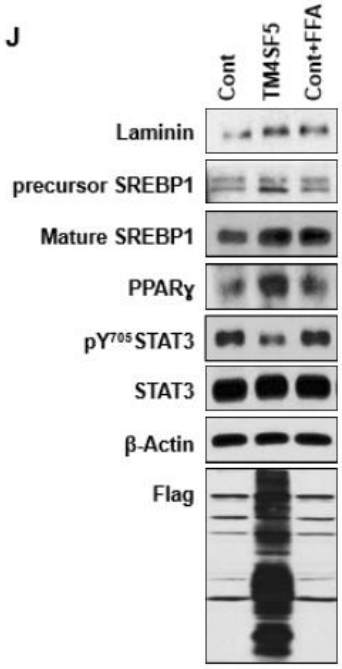
J
Cont
TM4SF5
Cont+FFA
Laminin
precursor SREBP1
Mature SREBP1
PPARγ
pY705STAT3
STAT3
β-Actin
Flag

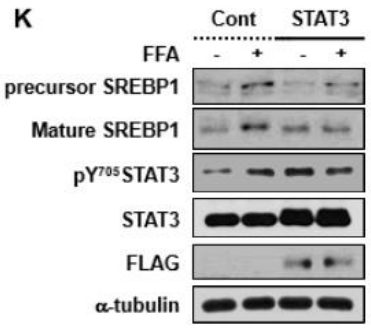
K
Cont
STAT3
FFA
- + - +
precursor SREBP1
Mature SREBP1
pY705STAT3
STAT3
FLAG
α-tubulin

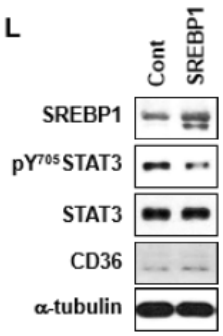
L
Cont
SREBP1
SREBP1
pY705STAT3
STAT3
CD36
α-tubulin

Fig. Ⅰ-1. TM4SF5 expression promoted nonalcoholic fatty liver disease (NAFLD). (A) Representative images of C57BL/6 WT and C57BL/6 Tg^{TM4SF5} mice in 52weeks. (B) H&E stained, Oil red O stained and Masson's trichrome stained liver sections from Tg^{TM4SF5} mice and WT mice ; n=5 WT group, n=10 Tg^{TM4SF5} group. (C) Phenotypes of fatty liver for mice from indicated groups. (D) The hepatic levels of triglyceride, ALT and albumin levels were determined. (E) Western blots and qRT-PCR analysis in the indicated tissues from 52weeks Tg^{TM4SF5} mice. (F) Representative TM4SF5, pY^{705}STAT3, SREBP1, Collagen Ⅰ, Laminin and Lamininγ2 immunohistochemical staining of paraffin embedded liver samples of WT and Tg^{TM4SF5} (G) Oil red O staining using primary hepatocytes. (H),(I) Primary hepatocytes were transfected with TM4SF5, treated FFA or IL-6 to identify mRNA levels. (J) Protein levels in primary hepatocytes transfected with TM4SF5 or treated FFA. (K) Protein levels in primary hepatocytes transfected with STAT3 or treated FFA. (L) Primary hepatocytes were transfected with SREBP1 were analyzed by western blotting.

2. TM4SF5-mediated lipid accumulation involved inactive STAT3 in hepatocytes.

Since adipocytes are involved in hepatic lipid metabolism, we checked how TM4SF5 expression affected lipid accumulation, STAT3 activity, and ECM production during adipocyte differentiation of 3T3-L1 cells. During differentiation of adipocyte 3T3-L1 cells, expression levels of TM4SF5, matured SREBP1, and laminin γ2 elevated gradually, whereas pY^{705}STAT3 and other ECMs including fibronectin, collagen I, and laminin increased and then gradually decreased as time passed after differentiation. During also adipocyte differentiation of the 3T3-L1 cells, STAT3 activity appeared positively-correlated with ECM expression but negatively-correlated with SREBP1 maturation, although laminin γ2 was different from the other ECMs. Suppression of TM4SF5 led to reduced lipid accumulation of the 3T3-L1 cells. Thus, TM4SF5 appeared to mediate lipid accumulation in adipocytes and hepatocytes.

Meanwhile, TM4SF5 overexpression in murine primary hepatocytes or AML12 hepatocytes led to increases in SOCS1 and SOCS3 expression levels (Fig.2A). Either TM4SF5 transfection without FFA treatment to primary hepatocytes elevated SOCS1 and SOCS3 levels, whereas TM4SF5 transfection to FFA-treated hepatocytes did not further increase them (Fig.2B). SREBP1 overexpression caused enhanced expression of SOCS1 and SOCS3

(Fig.2C). Thus, TM4SF5-mediated SREBP1 expression might be correlated with increased SOCSs levels. Further, exogenously TM4SF5-expressing murine AML12 hepatocytes showed a higher SOCS3 level than control AML12 cells, which was still maintained higher upon treatment with conditioned-media (CM) of differentiated 3T3-L1 cells (Fig.2D). Transfection of TM4SF5, treatment of FFA, or both to primary hepatocytes led to increase *SOCS3*, but TM4SF5 expression alone elevated *SOCS1* mRNA level (Fig.2B). And mRNA level of SOCS1, SOCS3 was higher in Tg^{TM4SF5} mice livers (Fig.2E). Among different SOCS isotypes, *SOCS1* and *SOCS3* were elevated in Tg^{TM4SF5} mice livers and their protein levels were confirmed by immunohistochemistry and western blots (Figs.2F and G). Thus, TM4SF5-mediated roles in lipid metabolism appeared to involve elevated SOCSs levels. Being consistent, TM4SF5-knockout (KO) mice showed lowered levels of SOCS1 and SOCS3 mRNA and protein (Fig.2H).

Since TM4SF5-KO mice showed reduced levels of SOCSs, it could be likely that TM4SF5-KO would lead to reduced fatty liver phenotypes. Thus, it was checked whether high fat diet (HFD) could lead to much less degree of fatty liver phenotypes in TM4SF5-KO mice livers, unlike greater fatty livers in normal wildtype mice with HFD. Following HFD (60 kCal% fat) for 5 weeks, wildtype male and female mice showed fatty liver phenotypes, whereas TM4SF5-KO mice revealed much reduced fatty phenotypes (Fig.2I). mRNAs of *PPARγ* and *SREBP-1C* (an isoform of *SREBP1*) in TM4SF5-KO mice

livers were less elevated by HFD than those in normal wildtype mice livers (Fig.2J). Therefore, during TM4SF5-mediated lipid accumulation, SREBP1 maturation correlated with enhanced SOCSs-mediated STAT3 inactivation might be involved in.

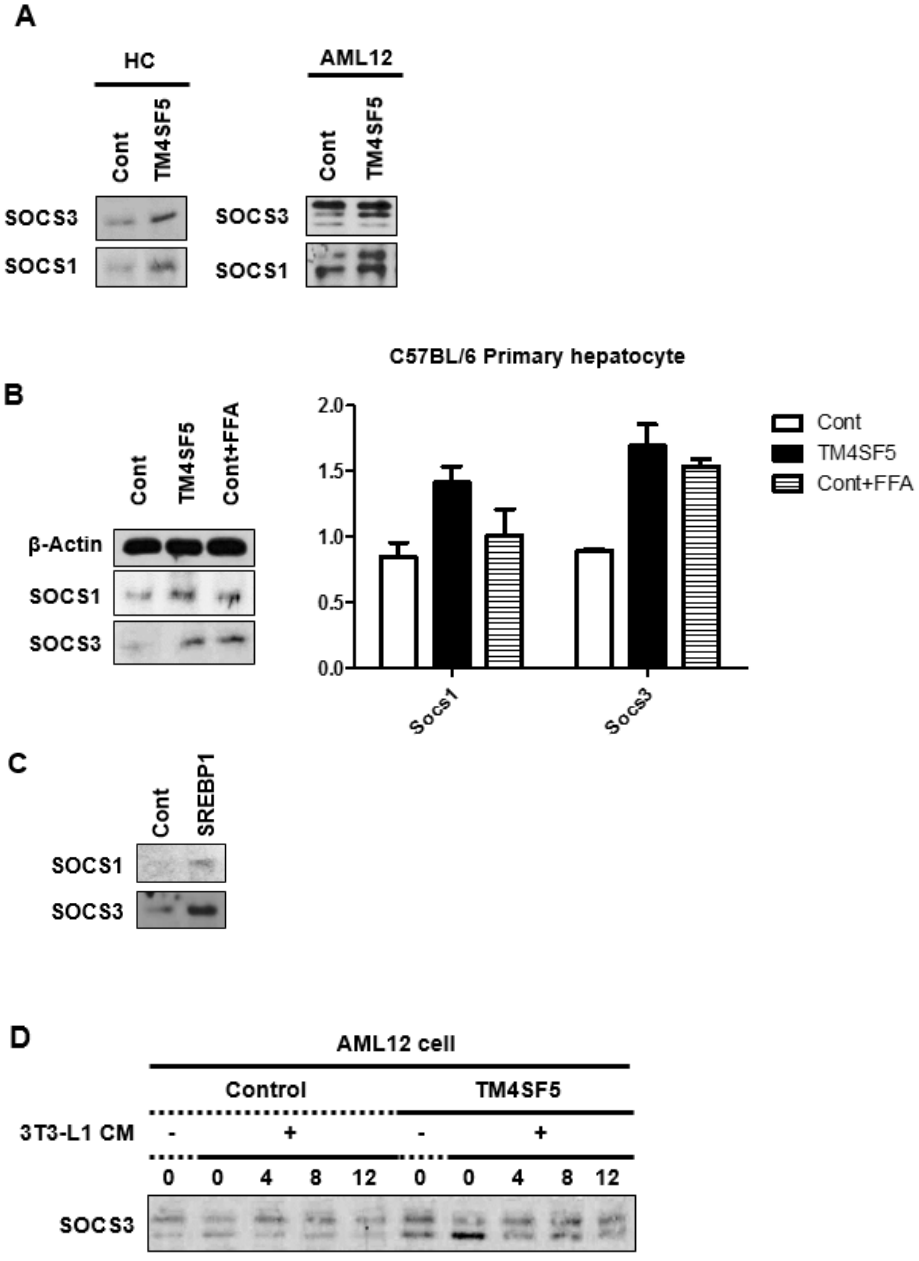
A
HC
AML12
Cont
TM4SF5
SOCS3
SOCS1
B
C57BL/6 Primary hepatocyte
Cont
TM4SF5
Cont+FFA
β-Actin
2.0
1.5
1.0
0.5
0.0
Socs1
Socs3
C
SREBP1
D
AML12 cell
Control
3T3-L1 CM
0 0 4 8 12 0 0 4 8 12

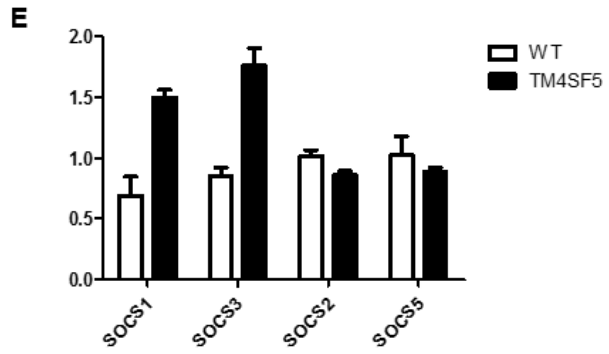
E
2.0
1.5
1.0
0.5
0.0
WT
TM4SF5
SOCS1
SOCS3
SOCS2
SOCS5

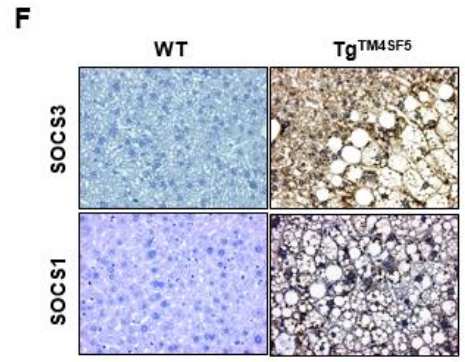
F
WT
Tg TM4SF5
SOCS3
SOCS1

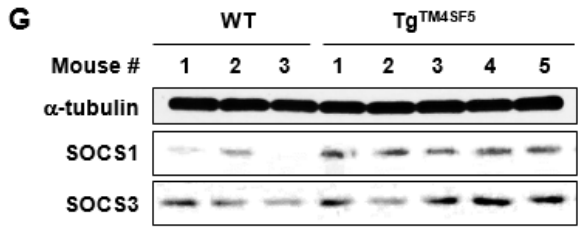
G
WT
Tg TM4SF5
Mouse #
1 2 3 1 2 3 4 5
α-tubulin
SOCS1
SOCS3

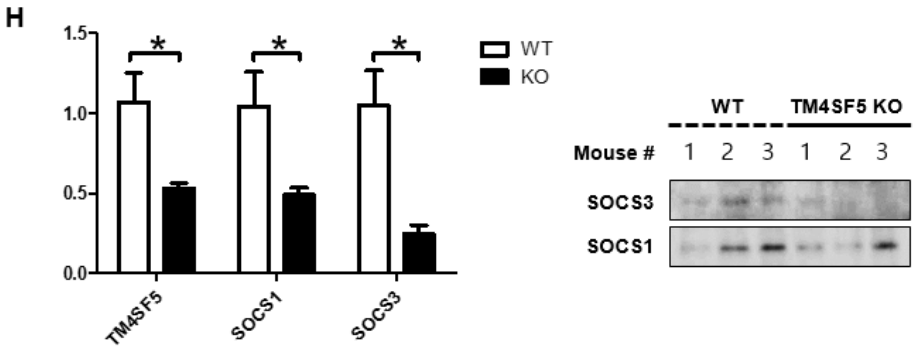
H
1.5
1.0
0.5
0.0
*
*
*
WT
KO
TM4SF5
SOCS1
SOCS3
WT
TM4SF5 KO
Mouse #
1 2 3 1 2 3
SOCS3
SOCS1

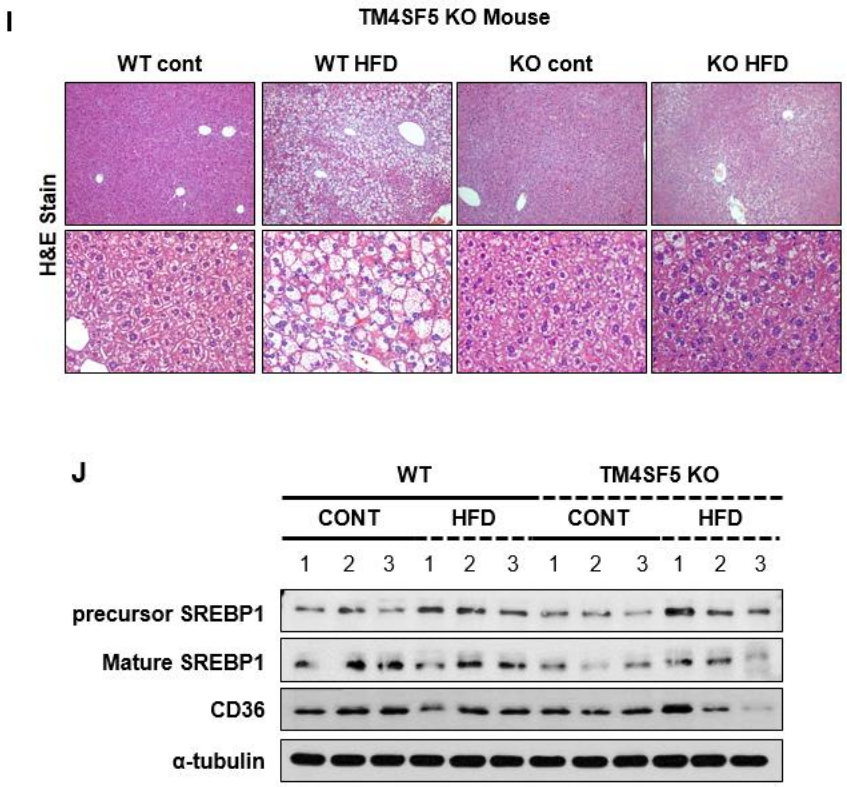
I
TM4SF5 KO Mouse
WT cont
WT HFD
KO cont
KO HFD
H&E Stain
J
WT
TM4SF5 KO
CONT
HFD
CONT
HFD
1 2 3 1 2 3 1 2 3 1 2 3
precursor SREBP1
Mature SREBP1
CD36
α-tubulin

Fig. Ⅰ-2. TM4SF5-mediated lipid accumulation involved inactive STAT3 in hepatocytes. (A) TM4SF5 was transfected into primary hepatocytes and AML12 cells to identify SOCS1,3 levels. (B) In addition, western blots and qRT-PCR were analyzed with FFA treated sample. (C) SREBP1 was transfected into primary hepatocytes to identify SOCS1,3 levels. (D) AML12 cells were transfected with TM4SF5 to treat 3T3-L1 conditioned medium. (E) SOCSs mRNA levels in WT and Tg^{TM4SF5} mice. (F) Representative SOCS1, and SOCS3 immunohistochemical staining of paraffin embedded liver samples of WT and Tg^{TM4SF5}. (G) Immunoblot of SOCS1 and SOCS3 in liver. (H) mRNA and protein levels in WT and TM4SF5-KO mice. (I) Representative images of H&E-stained liver sections from WT, HFD fed WT mice, HFD fed TM4SF5-KO mice or TM4SF5-KO mice. (J) Protein levels in WT, HFD fed WT, HFD fed TM4SF5-KO or TM4SF5-KO liver tissues.

3. TM4SF5-mediated fibrosis phenotypes involved STAT3 activation and laminin overexpression in hepatocytes.

Since one year (52 weeks) -old Tg^{TM4SF5} mice showed fatty livers, we rationalized that older aged-mice would show more malignant livers, such as fibrotic livers. Being consistent, one and a half year (78 weeks) -old mice showed fibrotic phenotypes with extramedullary hematopoiesis (Figs.3A and B), suggesting that the older Tg^{TM4SF5} is, the more malignant their livers are. Molecular analysis revealed a reduced level of matured SREBP1 and concomitantly elevated levels of pY^{705}STAT3, laminin, and TM4SF5 expression (Fig.3C). At the mRNA level, lipid-related genes appeared similar in Tg^{TM4SF5} mice or WT mice, whereas fibrosis related genes or hepatic inflammation related genes were higer in Tg^{TM4SF5} mice (Fig.3D). Immunohistochemistry study showed overexpression of laminin γ2 together with higher TM4SF5 and pY^{705}STAT3 levels in 78 week-old Tg^{TM4SF5} mouse livers, compared with normal wildtype mice livers (Fig.3E). Therefore, 78 week-old Tg^{TM4SF5} mice revealed fibrotic phenotypes with higher collagen I, laminin, and laminin γ2 expression and pY^{705}STAT3 levels. In addition to this genetically transgenic fibrosis model, CCl_4-induced fibrosis and cirrhosis models were mimicked via 4 weeks or 16 weeks treatments, respectively. Compared with normal control livers, CCl_4-treated mouse livers showed disturbed liver cell organization with collagen I deposition at the portal area

and slightly between the portal areas upon 4 weeks treatment (i.e., moderate fibrosis) and at the intensively bridging of portal areas upon 16 weeks treatment (incomplete cirrhosis or cirrhosis) (Fig.3F). In these fibrotic and/or cirrhotic livers, collagen I and laminin as well dramatically elevated in parallel to enhanced pY^{705}STAT3 level (Fig.3G). At the levels of mRNAs, *fibronectin* was not differential between untreated control or CCl_4treated mice livers (Fig.3H). However, in addition to *elastin, laminin* chains including α2, α3, α4, γ2, and γ3 were higher elevated in CCl_4-treated livers (Fig.3H). Immunohistochemistry revealed enhanced levels of TM4SF5, pY^{705}STAT3, α-smooth muscle actin (SMA), collagen I and IV, laminin, and laminin γ2 in CCl_4-treated livers, compared with untreated livers (Fig.3I). Interestingly, expression patterns of laminin and laminin γ2 were different from those of collagens and α-SMA mostly at the septa or bridging areas (Fig.3I), suggesting that the cell types might be differential for collagens and laminins. Nevertheless, TM4SF5-mediated induction of ECMs including laminins supported by STST3 activity could be involved in development of fibrosis/cirrhosis phenotypes.

Either suppression of TM4SF5 or STAT3 in primary hepatocytes prepared from the CCl_4 treated mice livers led to reduced expression of collagen I and laminins (Figs.3J and K). Suppression of endogenous TM4SF5 from Huh7 cells led to decrease in laminin together with pY^{705}STAT3 but not STAT1 or STAT5 phosphorylation. The elevated pY^{705}STAT3 was not correlated with

treatment of extracellular laminins or IL6 (Figs.3M and N), suggesting a ligand-independent and TM4SF5-dependent STAT3 activity. The pY^{705}STAT3 level to support laminin expression in the CCl_4-treated mouse liver depended on c-Src activity (Fig.3O), which depends on TM4SF5 expression [15].

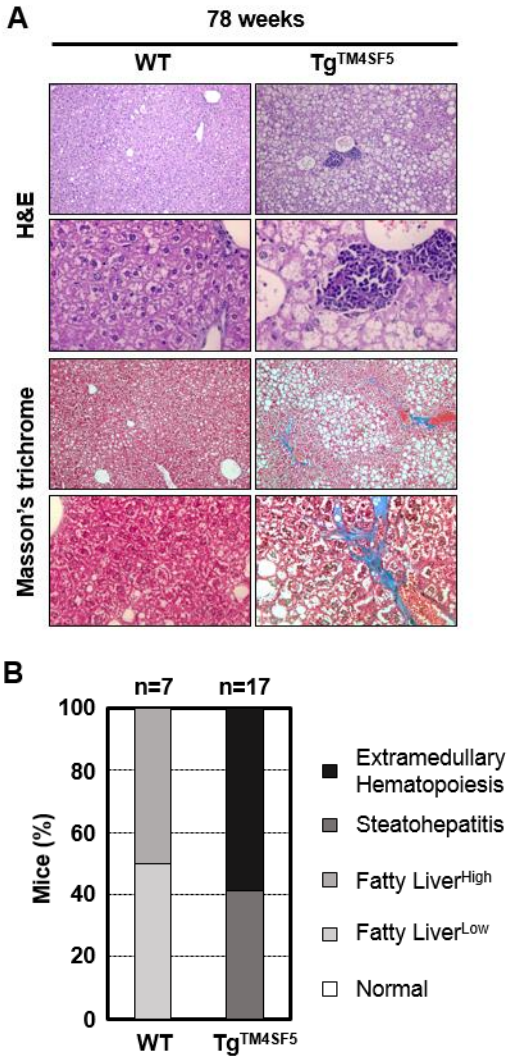
A
78 weeks
WT
Tg^TM4SF5
H&E
Masson's trichrome
B
n=7
n=17
100
80
60
40
20
0
Mice (%)
WT
Tg^TM4SF5
Extramedullary Hematopoiesis
Steatohepatitis
Fatty Liver^High
Fatty Liver^Low
Normal

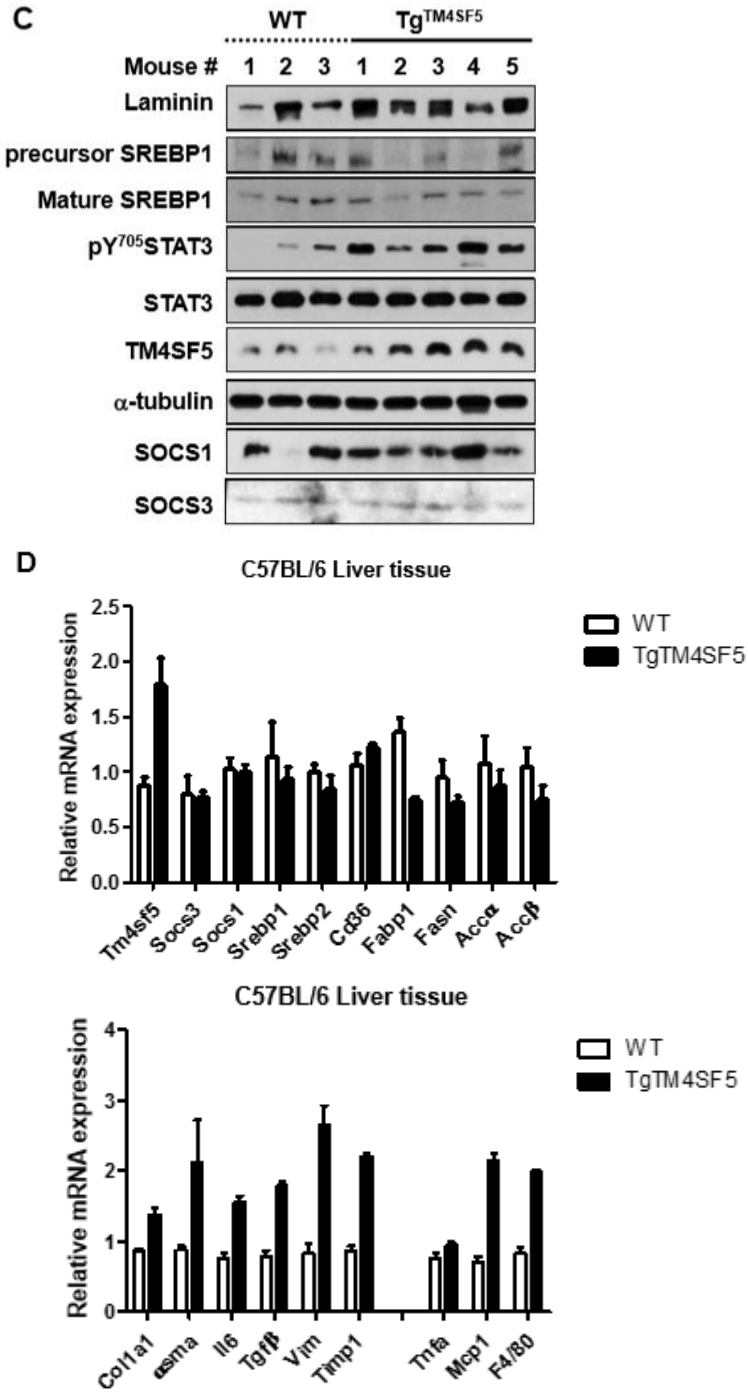
C
WT
Tg^TM4SF5
Mouse # 1 2 3 1 2 3 4 5
Laminin
precursor SREBP1
Mature SREBP1
pY705STAT3
STAT3
TM4SF5
α-tubulin
SOCS1
SOCS3
D
C57BL/6 Liver tissue
Relative mRNA expression
2.5
2.0
1.5
1.0
0.5
0.0
WT
TgTM4SF5
Tm4sf5
Socs3
Socs1
Srebp1
Srebp2
Cd36
Fabp1
Fasn
Accα
Accβ
C57BL/6 Liver tissue
Relative mRNA expression
4
3
2
1
0
WT
TgTM4SF5
Col1a1
αsma
Il6
Tgfβ
Vim
Timp1
Tnfa
Mcp1
F4/80

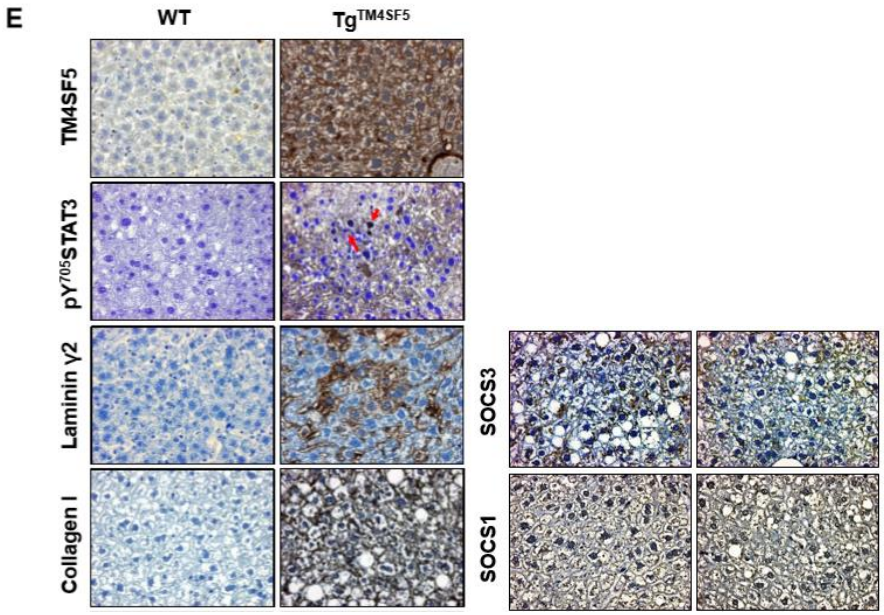
E
WT
Tg^TM4SF5
TM4SF5
pY^705STAT3
Laminin γ2
Collagen I
SOCS3
SOCS1

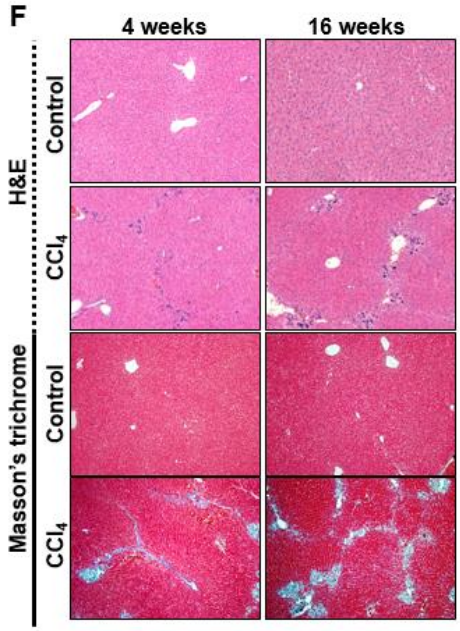
F
4 weeks
16 weeks
H&E
Control
CCl4
Masson's trichrome
Control
CCl4

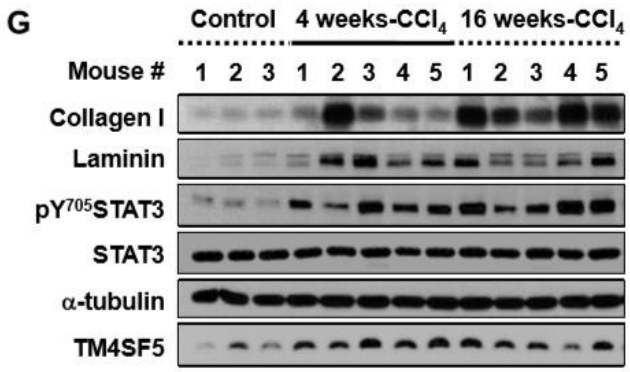
G
Control
4 weeks-CCl4
16 weeks-CCl4
Mouse # 1 2 3 1 2 3 4 5 1 2 3 4 5
Collagen I
Laminin
pY705STAT3
STAT3
α-tubulin
TM4SF5

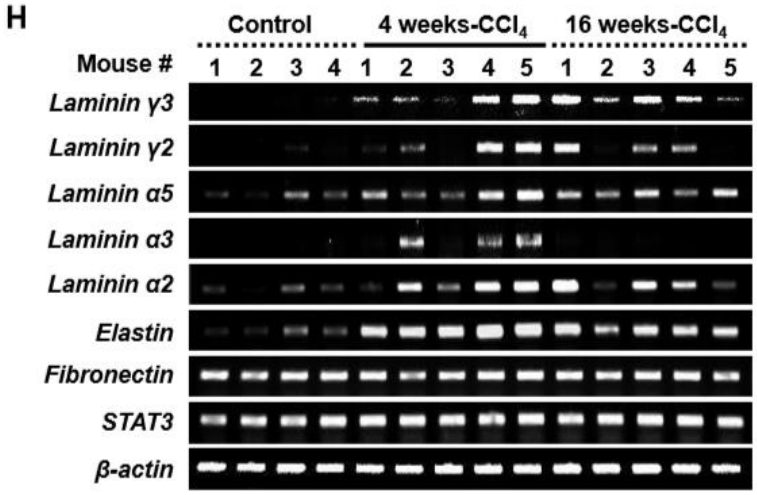
H
Control
4 weeks-CCl4
16 weeks-CCl4
Mouse # 1 2 3 4 1 2 3 4 5 1 2 3 4 5
Laminin γ3
Laminin γ2
Laminin α5
Laminin α3
Laminin α2
Elastin
Fibronectin
STAT3
β-actin

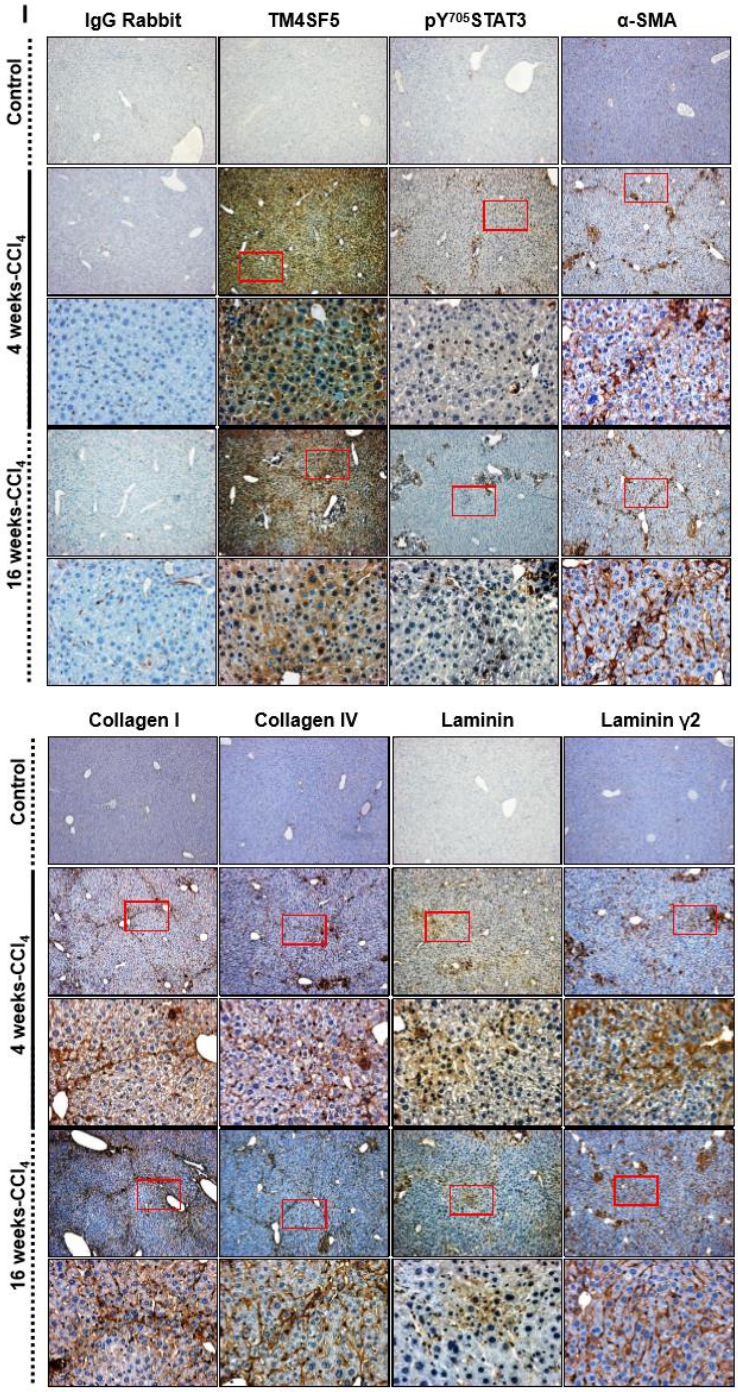
I
IgG Rabbit
TM4SF5
pY705STAT3
α-SMA
Control
4 weeks-CCl4
16 weeks-CCl4
Collagen I
Collagen IV
Laminin
Laminin γ2
Control
4 weeks-CCl4
16 weeks-CCl4

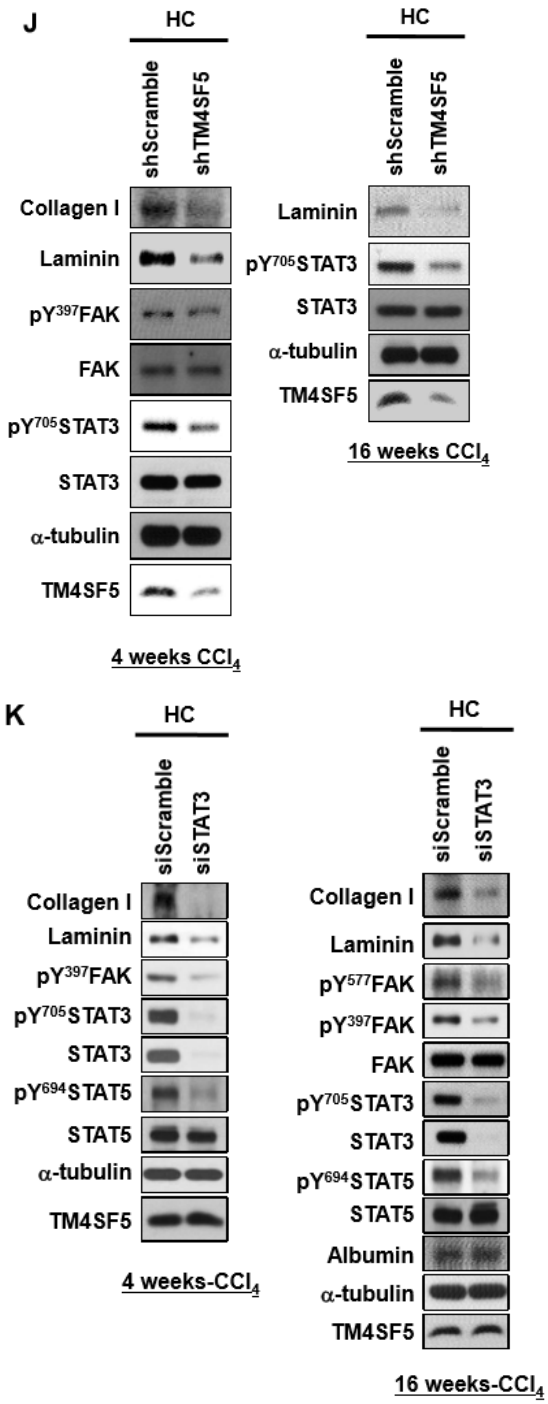
J
HC
shScramble
shTM4SF5
Collagen I
Laminin
pY397FAK
FAK
pY705STAT3
STAT3
α-tubulin
TM4SF5
4 weeks CCl4
HC
shScramble
shTM4SF5
Laminin
pY705STAT3
STAT3
α-tubulin
TM4SF5
16 weeks CCl4
K
HC
siScramble
siSTAT3
Collagen I
Laminin
pY397FAK
pY705STAT3
STAT3
pY694STAT5
STAT5
α-tubulin
TM4SF5
4 weeks-CCl4
HC
siScramble
siSTAT3
Collagen I
Laminin
pY577FAK
pY397FAK
FAK
pY705STAT3
STAT3
pY694STAT5
STAT5
Albumin
α-tubulin
TM4SF5
16 weeks-CCl4

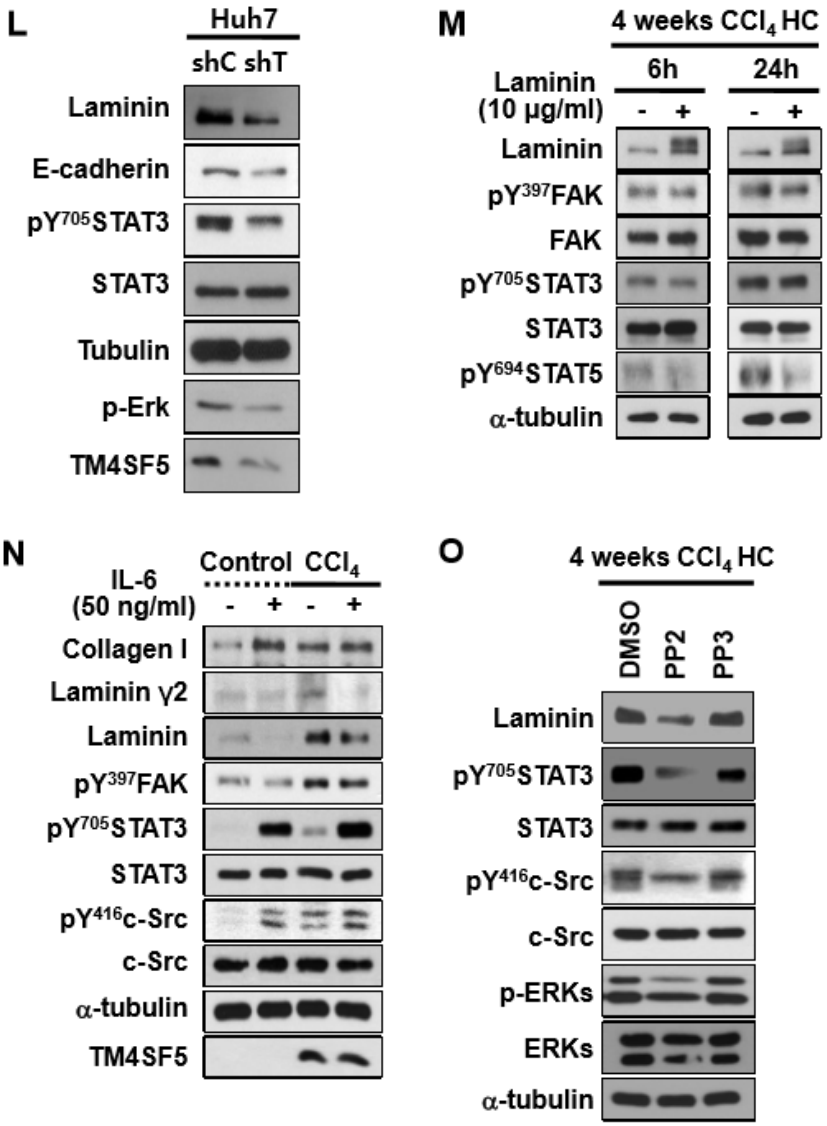
L
Huh7
shC shT
Laminin
E-cadherin
pY705STAT3
STAT3
Tubulin
p-Erk
TM4SF5
M
4 weeks CCl4 HC
6h
24h
Laminin (10 μg/ml)
- + - +
Laminin
pY397FAK
FAK
pY705STAT3
STAT3
pY694STAT5
α-tubulin
N
Control CCl4
IL-6 (50 ng/ml)
- + - +
Collagen I
Laminin γ2
Laminin
pY397FAK
pY705STAT3
STAT3
pY416c-Src
c-Src
α-tubulin
TM4SF5
O
4 weeks CCl4 HC
DMSO
PP2
PP3
Laminin
pY705STAT3
STAT3
pY416c-Src
c-Src
p-ERKs
ERKs
α-tubulin

Fig. Ⅰ-3. TM4SF5-mediated fibrosis phenotypes involved STAT3 activation and laminin overexpression in hepatocytes. (A) Representative H&E stained and Masson's trichrome stained sections of livers from C57BL/6 WT and C57BL/6 Tg^{TM4SF5} for 78weeks. (B) Phenotypes of steatohepatitis for mice from indicated groups. (C) Protein levels in WT and Tg^{TM4SF5} mice. (D) Hepatic gene expression patterns in WT and Tg^{TM4SF5} mice. (E) Representative TM4SF5, pY^{705}STAT3, Collagen Ⅰ, Lamininγ2, SOCS1 and SOCS3 immunohistochemical staining of paraffin embedded liver samples of WT and Tg^{TM4SF5} (F) Representative H&E stained and Masson's trichrome stained sections of livers from WT and CCl_4 treated mice. (G) Protein levels of Collagen Ⅰ, Laminin, pY^{705}STAT3, TM4SF5 in WT and CCl_4 treated mice. (H) mRNA levels of laminin chain in WT and CCl_4 treated mice. (I) Representative TM4SF5, pY^{705}STAT3, α-SMA, Collagen Ⅰ, CollagenⅣ, Laminin and Lamininγ2 immunohistochemical staining of paraffin embedded liver samples of WT and CCl_4 treated mice. (J) Primary hepatocytes prepared from the CCl_4 treated mice livers were transfected with shTM4SF5 to identify protein levels. (K) Primary hepatocytes prepared from the CCl_4 treated mice livers were transfected with siSTAT3. (L) Huh7 cells were transfected with shTM4SF5 to identify protein levels. (M) Primary hepatocytes prepared from the CCl_4 treated mice livers were treated with laminin for 6 hours or 24 hours. (N) Primary hepatocytes were treated with

IL-6. (O) Primary hepatocytes prepared from the CCl_4 treated mice livers were treated with Src inhibitor PP2 and negative control PP3.

4. Differential TM4SF5/STAT3-mediated ECM expression in hepatocytes and HSCs.

We next examined the promoter activities of *laminin γ2* (*Lamc2*) and *collagen I α1* (*Col1a1*) chain in hepatocytes to see whether they would be differential. Both promoter regions were constructed to have STAT3-binding elements upstream of the luciferase gene sequence (Fig.4A). Based on the luciferase assay using AML12 murine hepatocytes, TM4SF5 expression enhanced their promoter activities at approximately two folds, compared with mock control vectors, whereas STAT3 introduction caused much greater activation in case for *Lamc2* than for *Col1a1* (Fig.4B). Thus, TM4SF5/STAT3 signaling axis in hepatocytes might more greatly functional for the transcriptional activity for *Lamc2* than for *Col1a1*. Immunostaining of laminin of the animal liver tissues were overlapped in certain cell populations with TM4SF5-positive immunostains (Fig.4C). We then examined hepatic cells types to express each ECM during the CCl_4-induced fibrosis/cirrhosis. When CCl_4 was gradually treated for 1, 4, or 16 weeks to mice, collagen I expression was parallel with α-SMA expression to indicate activated HSCs but negatively parallel with albumin to depict the hepatocytes (Fig.4D). In case of laminin, it was opposite; laminin expression was parallel with albumin immunostains and inversely parallel with α-SMA (Fig.4E). Meanwhile, for a short CCl_4-treatment of 1 week, α-SMA immunostains were overlapped with

laminin stains, but later the overlapping was diminished and rather an overlapping between albumin and laminin stains would be obvious (Fig.4E). When the conditioned media (CM) collected from activated human HSCs (LX2 cells) cultures were treated to endogenously TM4SF5-expressing HepG2 cells with shRNA against a control sequence or a sequence in TM4SF5, laminin γ2 was not expressed upon TM4SF5 suppression, but collagen I was enhanced by the CM treatment nonetheless TM4SF5 expression (Fig.4F). Such no expression of laminin following TM4SF5 suppression was not recovered by the CM from even primary murine HSCs (Fig.4G). These data suggest that expression behaviors of laminins were different from those of collagen I during development of fibrosis/cirrhosis phenotypes, and that laminin or collagen I could be expressed mostly in hepatocytes and HSCs.

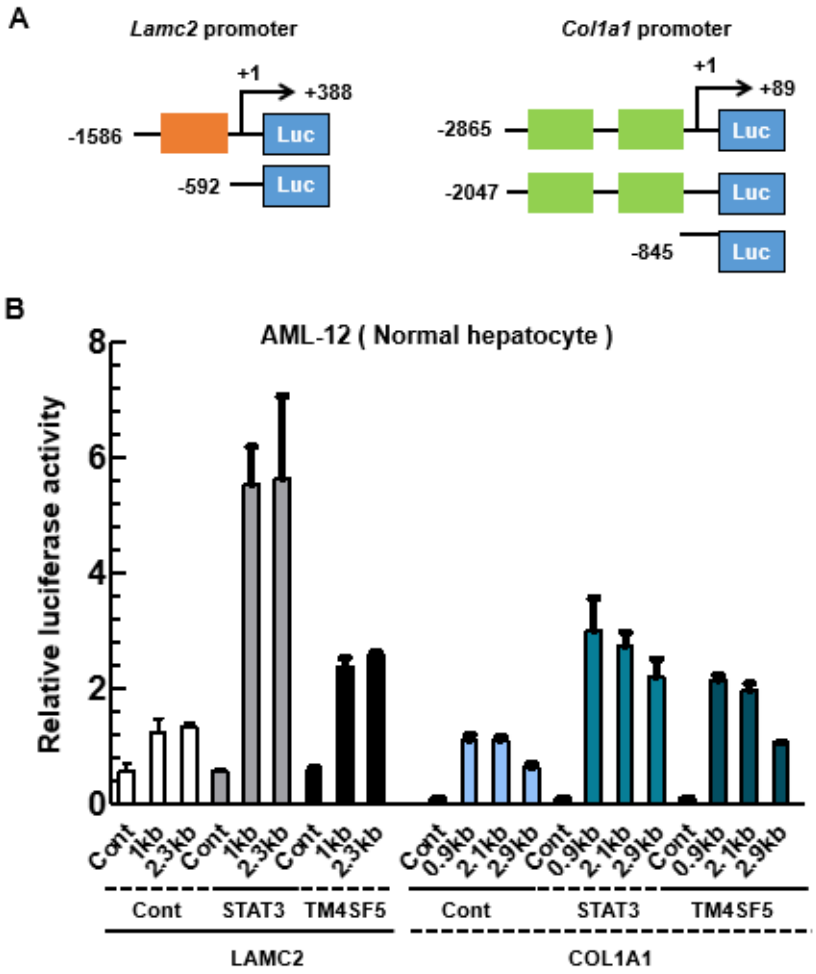
A
Lamc2 promoter
+1
+388
-1586
Luc
-592
Luc
Col1a1 promoter
+1
+89
-2865
Luc
-2047
Luc
-845
Luc
B
AML-12 (Normal hepatocyte)
Relative luciferase activity
0
2
4
6
8
Cont
1kb
2.3kb
Cont
1kb
2.3kb
Cont
1kb
2.3kb
Cont
0.9kb
2.1kb
2.9kb
Cont
0.9kb
2.1kb
2.9kb
Cont
0.9kb
2.1kb
2.9kb
Cont
STAT3
TM4SF5
Cont
STAT3
TM4SF5
LAMC2
COL1A1

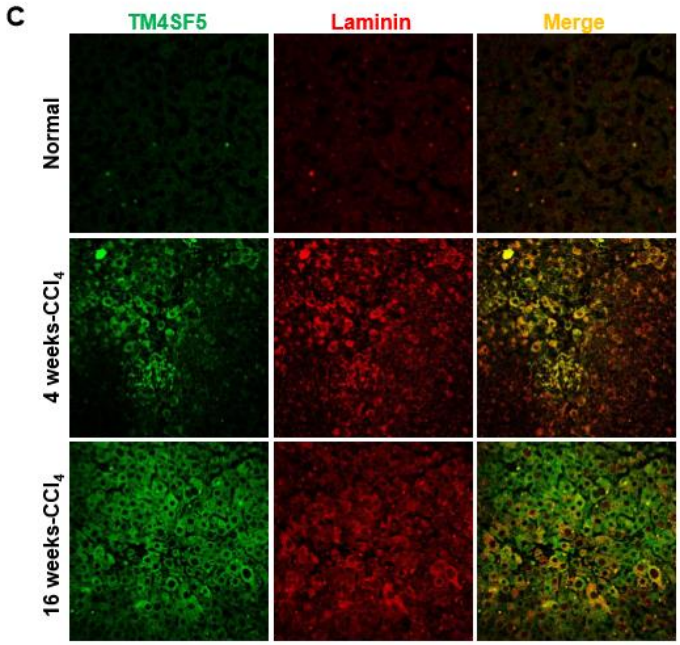
C
TM4SF5
Laminin
Merge
Normal
4 weeks-CCl4
16 weeks-CCl4

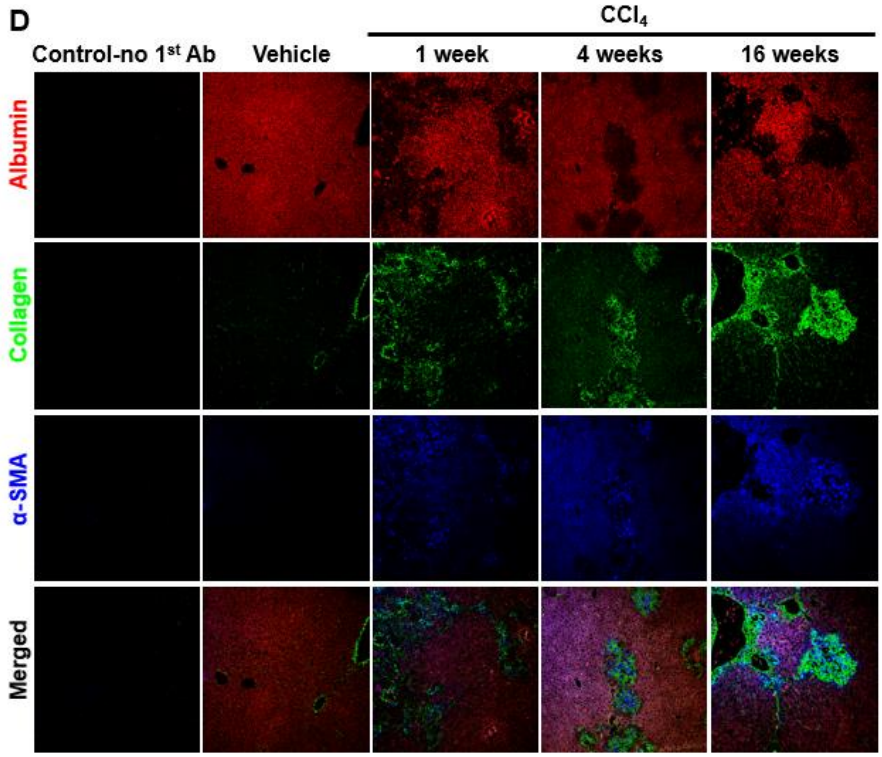
D
CCl4
Control-no 1st Ab
Vehicle
1 week
4 weeks
16 weeks
Albumin
Collagen
α-SMA
Merged

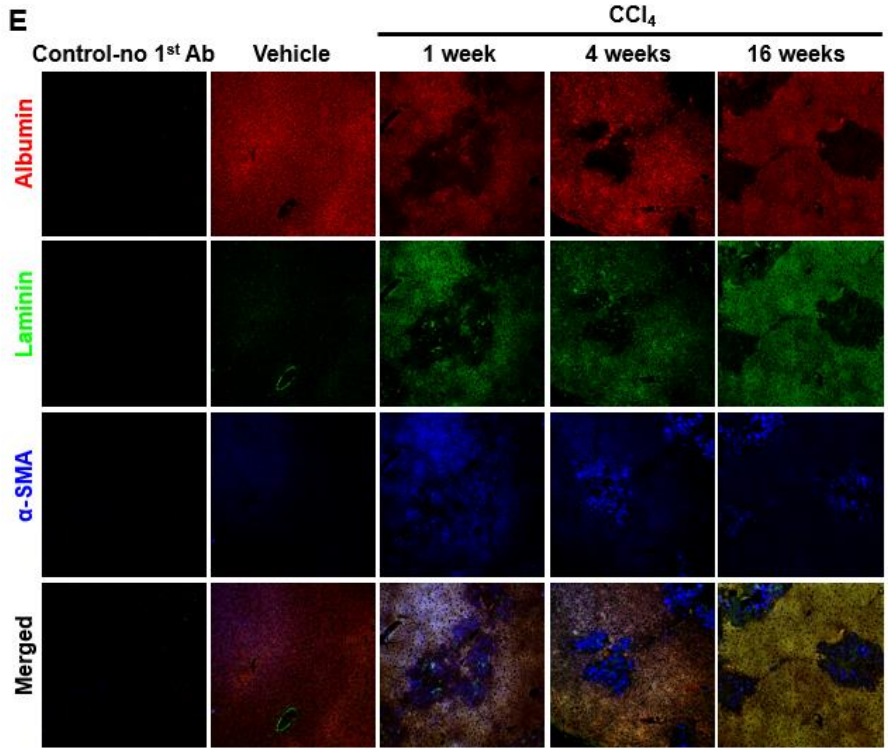
E
CCl4
Control-no 1st Ab
Vehicle
1 week
4 weeks
16 weeks
Albumin
Laminin
α-SMA
Merged

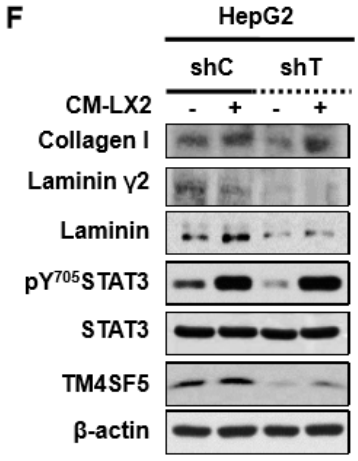
F
HepG2
shC
shT
CM-LX2
- + - +
Collagen I
Laminin γ2
Laminin
pY705STAT3
STAT3
TM4SF5
β-actin

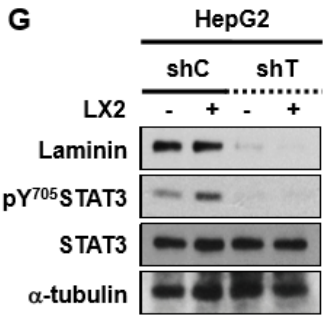
G
HepG2
shC
shT
LX2
- + - +
Laminin
pY705STAT3
STAT3
α-tubulin

Fig. Ⅰ-4. Differential TM4SF5/STAT3-mediated ECM expression in hepatocytes and HSCs. (A) Schematic representation of the mouse Lamc2 promoter and the mouse Col1a1 promoter. (B) AML12 cells were transfected with Lamc2 or Col1a1 promoter-Luc reporters with control, STAT3 or TM4SF5. (C) Mouse normal or CCl_4 treated liver tissues were processed for immunohistochemistry to identify TM4SF5 and Laminin. (D) Mouse normal or CCl_4 treated liver tissues were processed for immunohistochemistry to identify Albumin, collagen Ⅰ and α-SMA. (E) Mouse normal or CCl_4 treated liver tissues were processed for immunohistochemistry to identify Albumin, Laminin and α-SMA. (F) HepG2 cells were transfected with shTM4SF5 to treat the LX2 conditioned medium. (G) HepG2 cells were transfected with shTM4SF5 and co-cultured with LX2 cells.

5. TM4SF5-mediated laminin expression during hepatic carcinogenesis.

Since Tg^{TM4SF5} mice showed fatty and fibrotic livers, we wondered whether disease-prone mouse strain (i.e., FVB/N) to TM4SF5 overexpression might show cancerous phenotypes. Livers of one year-old FVB/N Tg^{TM4SF5} mice were thus analyzed. Expression of collagen I, α-SMA, laminin, and TM4SF5 were clearly elevated, and interestingly CD34 and α-fetoprotein (AFP), HCC markers [19,20], were dramatically expressed (Fig.5A). This observation support cancerous livers of the FVB/N Tg^{TM4SF5} mice. Further, hepatic mRNAs for *CD34*, *Hif1α*, *Ki67*, and *cyclin D1* of the FVB/N Tg^{TM4SF5} mice were higher than normal wildtype mice (Fig.5B). When laminin, pY^{705}STAT3, and p-ERKs were analyzed together in 54 or 78 weeks of C57BL/6-Tg^{TM4SF5} and 54 weeks of FVB/N-Tg^{TM4SF5} mice livers, there were highly maintained or gradually enhanced toward cancerous phenotypes (Fig.5C). This FVB/N-Tg^{TM4SF5} mice also showed higher AST, ALT, and LDL levels, compared with normal wildtype mice, but comparable levels for albumin and serum triacylglyceride (TG) similar to C57BL/6-Tg^{TM4SF5} mice (Fig.5D). Meanwhile, livers following diethylnitrosamine (DEN) treatment showed cancerous nodules (Fig.5E) with elevated TM4SF5 and laminin expression and enhanced pERKs and pY^{705}STAT3 (Fig.5F). Further, immunostainings of liver tissues from HCC patients for normal, tumor-near, and tumor regions revealed greatly elevated TM4SF5, laminin, collagen I, and pY^{705}STAT3 in tumor-near and

tumor regions, compared normal regions (Fig.5G). Interestingly, the immunostains for laminin appeared to be hepatocytes and different from those for collagen I (Fig.5G), suggesting a possible role of TM4SF5-mediated laminin expression in hepatocytes for hepatic carcinogenesis.

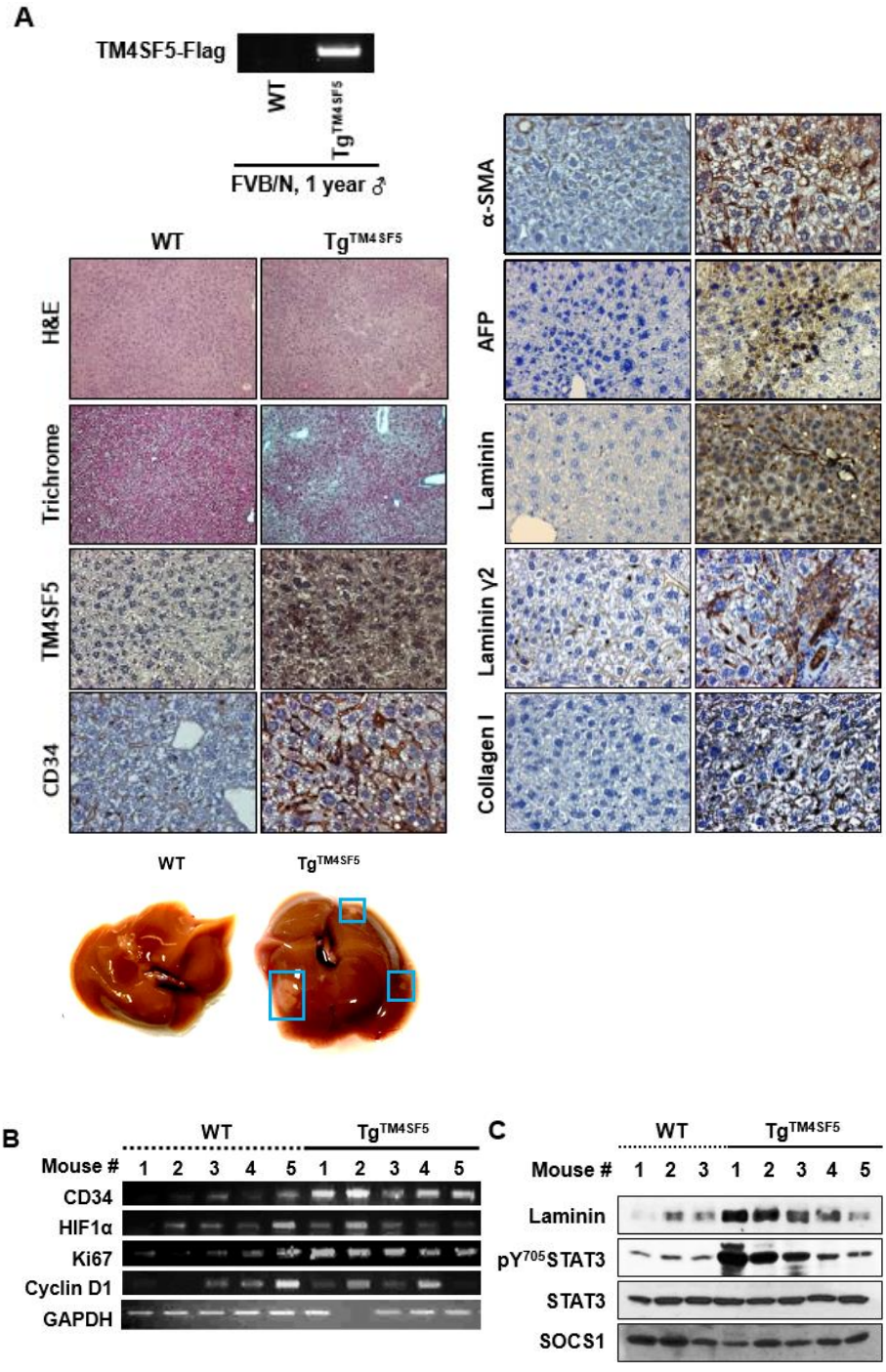
A
TM4SF5-Flag
WT
Tg^TM4SF5
FVB/N, 1 year ♂
WT
Tg^TM4SF5
H&E
Trichrome
TM4SF5
CD34
α-SMA
AFP
Laminin
Laminin γ2
Collagen I
WT
Tg^TM4SF5
B
WT
Tg^TM4SF5
Mouse # 1 2 3 4 5 1 2 3 4 5
CD34
HIF1α
Ki67
Cyclin D1
GAPDH
C
WT
Tg^TM4SF5
Mouse # 1 2 3 1 2 3 4 5
Laminin
pY705STAT3
STAT3
SOCS1

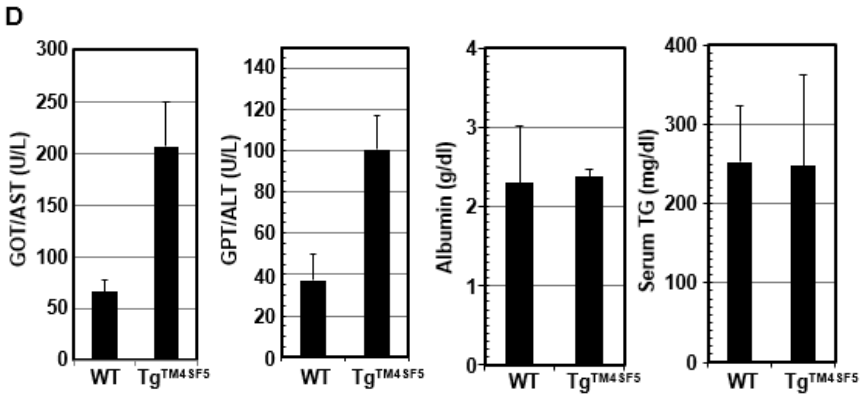
D
GOT/AST (U/L)
GPT/ALT (U/L)
Albumin (g/dl)
Serum TG (mg/dl)
WT
Tg^TM4SF5

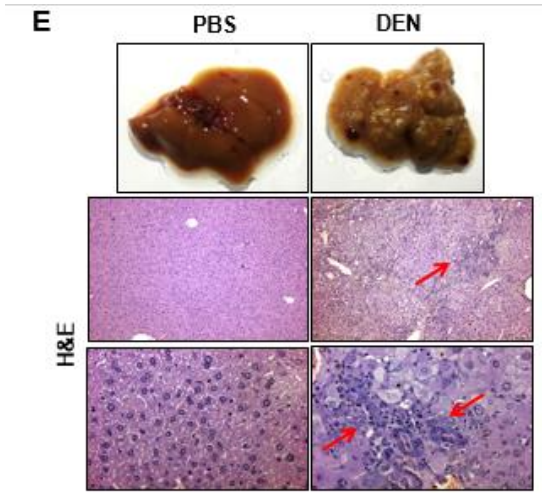
E
PBS
DEN
H&E

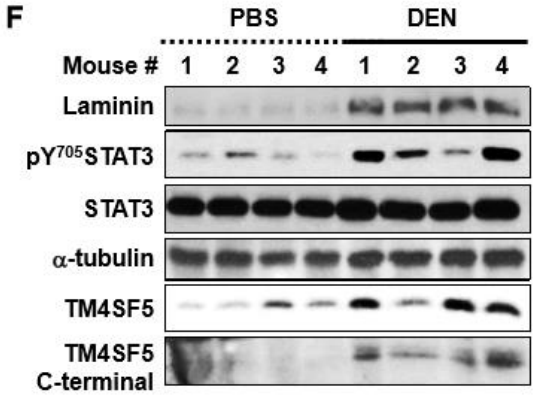
F
PBS
DEN
Mouse # 1 2 3 4 1 2 3 4
Laminin
pY705STAT3
STAT3
α-tubulin
TM4SF5
TM4SF5
C-terminal

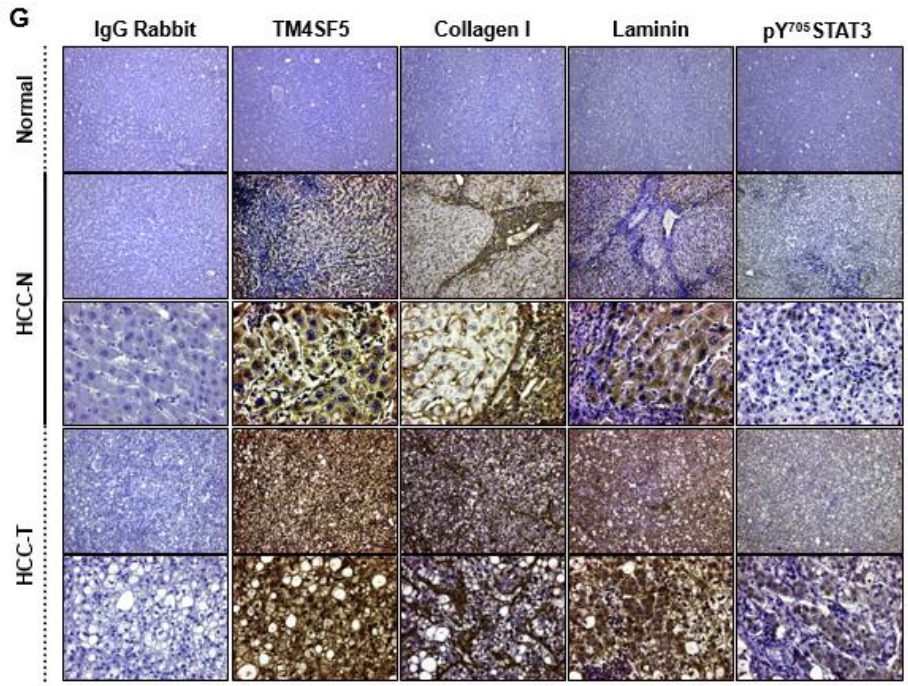
G
IgG Rabbit
TM4SF5
Collagen I
Laminin
pY705STAT3
Normal
HCC-N
HCC-T

Fig. Ⅰ-5. TM4SF5-mediated laminin expression during hepatic carcinogenesis. (A) Representative H&E stained and Masson's trichrome stained sections of livers from FVB/N WT and FVB/N Tg^{TM4SF5} for 52weeks. And liver tissues were processed for immunohistochemistry to identify TM4SF5, CD34, α-SMA, AFP, Laminin, Lamininγ2 and Collagen Ⅰ. (B) mRNA levels in WT and Tg^{TM4SF5}. (C) Protein levels in WT and Tg^{TM4SF5}. (D) AST, ALT, albumin and serum TG levels were determined. (E) Representative H&E stained sections of livers from WT and DEN treated mice. (F) Western blot analyses of WT and DEN treated liver tissues. (G) Liver tissues from HCC patients for normal, tumor-near, and tumor regions were processed for immunohistochemistry to identify TM4SF5, Collagen Ⅰ, Laminin and pY^{705}STAT3.

6. Anti-TM4SF5 reagents abolished TM4SF5-mediated fibrosis and carcinogenesis.

Anti-TM4SF5 reagents would be beneficial for the therapeutic purposes against liver diseases. A small compound of TSAHC and a chimeric anti-TM4SF5 antibody have been tested for the influence to block the TM4SF5-mediated fatty liver, fibrosis, and carcinogenesis. CCl_4-treated fibrotic livers with collagen I deposition were abolished with concomitant treatment of TSAHC but not of control vehicle (Fig.6A). During the TSAHC-mediated blocking of the TM4SF5-mediated fibrosis were paralleled also with decreases in CCl_4-treatment-induced collagen I and laminin expression and pY^{705}STAT3 levels (Fig.6B,C). Such CCl_4-mediated fibrotic phenotypes were also blocked by treatment of chimeric anti-TM4SF5 monoclonal antibodies (i.e., #27 and #79Ab) (Fig.6D). Consistently, the anti-TM4SF5 antibodies clocked the CCl_4-mediated collagen I and laminin expression and pY^{705}STAT3 levels, but not pERKs and TM4SF5 levels (Fig.6E). In case of DEN-mediated HCC models, TSAHC treatment inhibited the nodule formation in livers (Fig.6F) and supported longer survivals (Fig.6G). The anti-TM4SF5 antibodies (#27 and #79) also blocked tumor growth during the TM4SF5-mediated xenografts (Fig.6H). Thus, these observations indicated that blocking of TM4SF5 function or activity rather than expression could block the fibrosis and hepatic carcinogenesis presumably via abolishing the

TM4SF5-mediated activation of STAT3 activity and in turn collagen I and laminin expression. Laminin, collagen Ⅰ Lamininγ2 and pSTAT3 were decreased when DEN-induced HCC was treated with TSAHC in immunohistochemistry (Fig.6I).

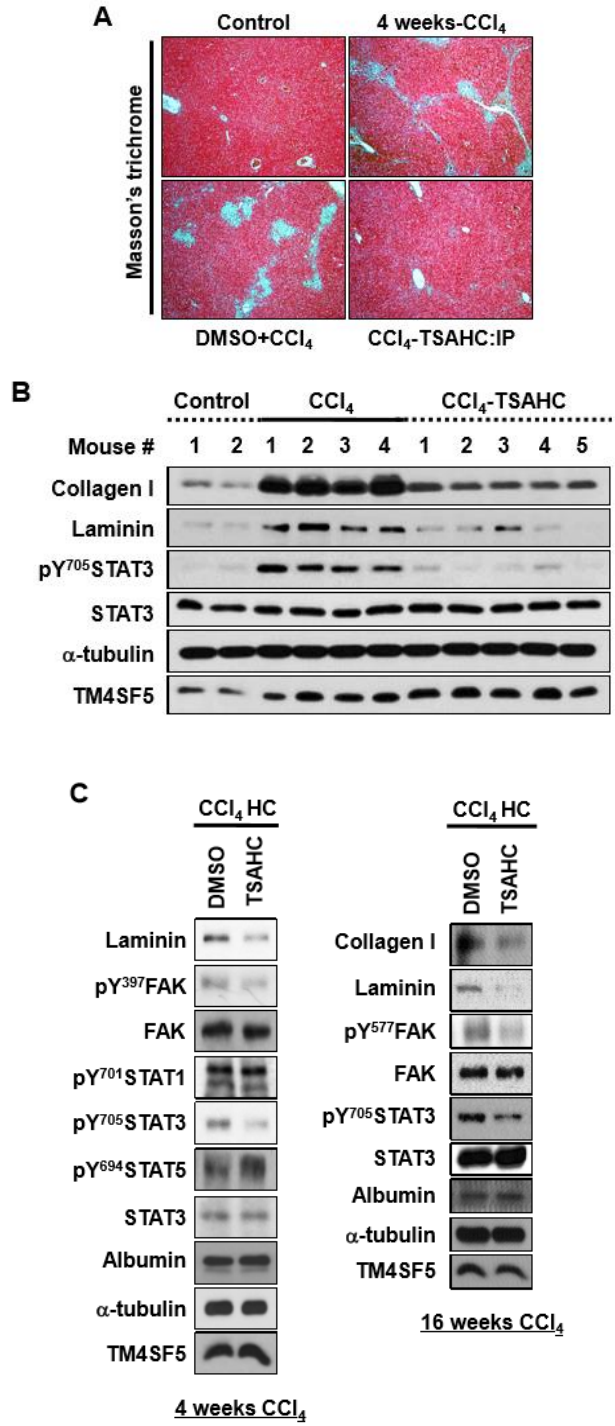
A
Control
4 weeks-CCl4
Masson's trichrome
DMSO+CCl4
CCl4-TSAHC:IP
B
Control
CCl4
CCl4-TSAHC
Mouse #
1 2 1 2 3 4 1 2 3 4 5
Collagen I
Laminin
pY705STAT3
STAT3
α-tubulin
TM4SF5
C
CCl4 HC
DMSO
TSAHC
Laminin
pY397FAK
FAK
pY701STAT1
pY705STAT3
pY694STAT5
STAT3
Albumin
α-tubulin
TM4SF5
4 weeks CCl4
CCl4 HC
DMSO
TSAHC
Collagen I
Laminin
pY577FAK
FAK
pY705STAT3
STAT3
Albumin
α-tubulin
TM4SF5
16 weeks CCl4

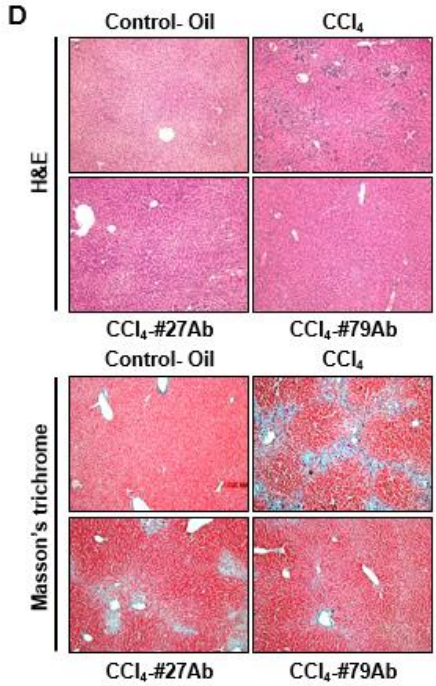
D
Control- Oil
CCl4
H&E
CCl4-#27Ab
CCl4-#79Ab
Control- Oil
CCl4
Masson's trichrome
CCl4-#27Ab
CCl4-#79Ab

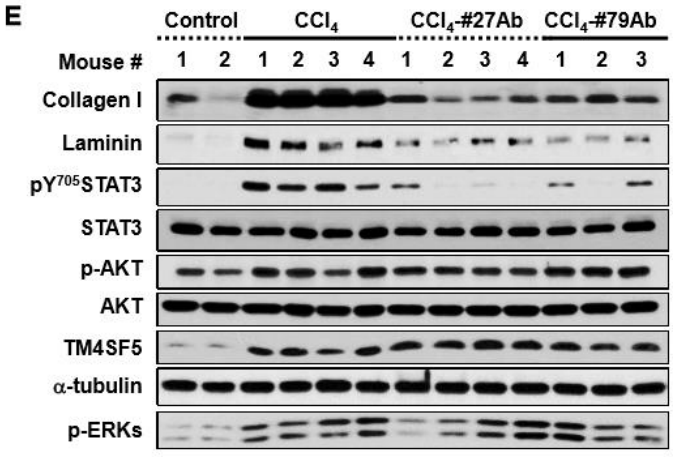
E
Control
CCl4
CCl4-#27Ab
CCl4-#79Ab
Mouse #
1 2 1 2 3 4 1 2 3 4 1 2 3
Collagen I
Laminin
pY705STAT3
STAT3
p-AKT
AKT
TM4SF5
α-tubulin
p-ERKs

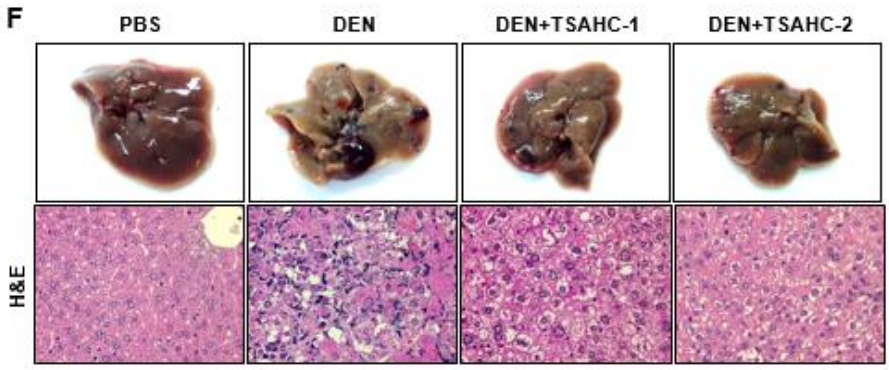
F
PBS
DEN
DEN+TSAHC-1
DEN+TSAHC-2
H&E

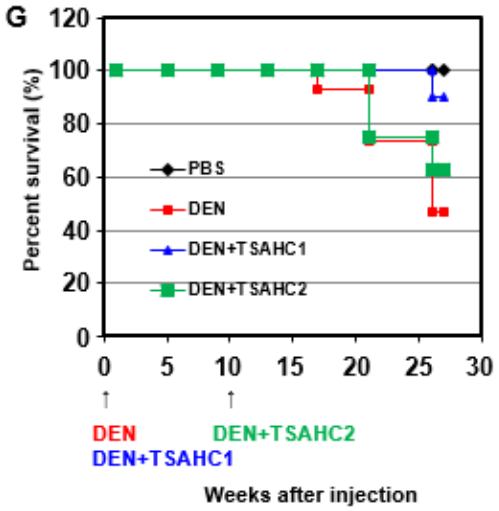
G
120
100
80
60
40
20
0
Percent survival (%)
PBS
DEN
DEN+TSAHC1
DEN+TSAHC2
0
5
10
15
20
25
30
DEN
DEN+TSAHC2
DEN+TSAHC1
Weeks after injection

H

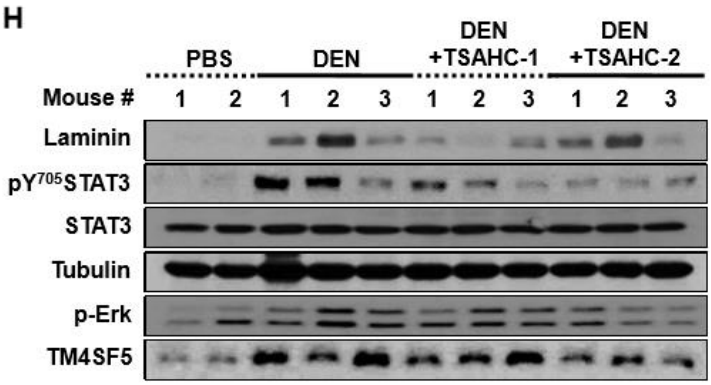
PBS
DEN
DEN +TSAHC-1
DEN +TSAHC-2
Mouse # 1 2 1 2 3 1 2 3 1 2 3
Laminin
pY705STAT3
STAT3
Tubulin
p-Erk
TM4SF5

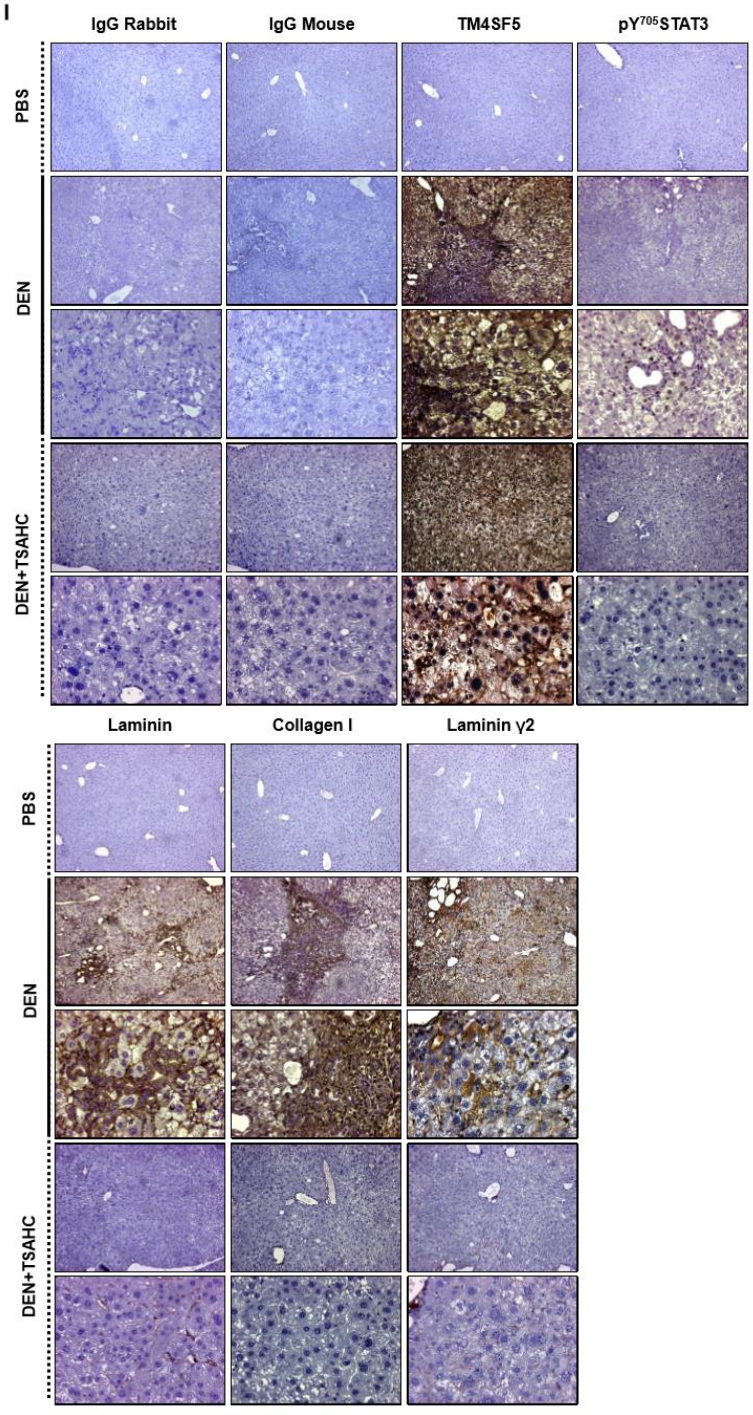
I
IgG Rabbit
IgG Mouse
TM4SF5
pY705STAT3
PBS
DEN
DEN+TSAHC
Laminin
Collagen I
Laminin γ2
PBS
DEN
DEN+TSAHC

Fig. Ⅰ-6. Anti-TM4SF5 reagents abolished TM4SF5-mediated fibrosis and carcinogenesis. (A) Representative Masson's trichrome stained sections of livers from Control, CCl_4 treated livers, and CCl_4-TSAHC treated livers for 4weeks. (B) Western blot analyses of Control, CCl_4 treated livers and CCl_4-TSAHC treated lives. (C) Primary hepatocytes prepared from the CCl_4 treated mice livers were treated with TSAHC to identify protein levels. (D) Representative H&E stained and Masson's trichrome stained sections of livers from Control, CCl_4 treated livers, and CCl_4-TM4SF5 Ab(#27,#79) treated livers for 4weeks. (E) Western blot analyses of Control, CCl_4 treated livers and CCl_4- TM4SF5 Ab(#27,#79) treated lives. (F) Representative H&E stained sections of livers from Control, DEN treated livers, and DEN-TSAHC treated livers for 28weeks. (G) Survival curves of BALB/C male mice injected with DEN or DEN-TSAHC. (H) Protein levels in Control, DEN treated livers and DEN-TSAHC treated livers. (I) Mouse normal, DEN treated liver tissues or DEN-TSAHC treated liver tissues were processed for immunohistochemistry to identify TM4SF5, pY^{705}STAT3, Laminin, Collagen Ⅰ and Lamininγ2.

4. Discussion

This study evidences that TM4SF5-overexpressing transgenic (Tg^{TM4SF5}) mice revealed phenotypes from fatty liver to fibrosis or from fibrosis to cancer depending on ages or disease-proneness, respectively. During TM4SF5-mediated phenotypes of such liver diseases, STAT3 phosphorylation at Tyr 705 residue could play a turning-point factor from fatty to fibrotic liver; SOCS1/3 expression was highly kept for lower STAT3 activity leading to fatty liver phenotypes in 1 year-old C57BL/6-Tg^{TM4SF5} mice, and during further aggravation toward fibrosis, SOCS1/3 decreased for elevated STAT3 leading to ECM production 1.5 year-old C57BL/6-Tg^{TM4SF5}. TM4SF5 activated ligand-independently STAT3, which could in turn trigger transcription of collagen Ⅰ in HSCs and laminins (especially laminin γ2) in hepatocytes, during developments of fibrotic/cirrhotic phenotypes animals following treatment with CCl_4 for 4 or 16 weeks. Such TM4SF5/STAT3-mediated ECM expression including laminin γ2 in hepatocytes was involved in the hepatic fibrosis/cirrhosis and carcinogenesis in 1 year-old disease-prone FVB/N-Tg^{TM4SF5}. These observations on SOSCs/STAT3 as a turning-point factor(s) from fatty to fibrotic liver phenotypes and laminins (including laminin γ2 chain) expression in hepatocytes during hepatic fibrosis/cirrhosis and carcinogenesis could be confirmed in not only *in vitro* cell but also *in vivo* transgenic/knock-out mice and clinical tissue systems. Furthermore, anti-

TM4SF5 small compound or chimeric antibody could abolish such TM4SF5-mediated phenotypes in cells and animal systems. Therefore, TM4SF5-mediated STAT3 signaling activity could be modulated to drive the chronic processes from inflammatory/fatty, fibrotic/cirrhotic, and cancerous liver, suggesting that TM4SF5 can be a promising target therapeutic against liver diseases.

Liver diseases are chronically aggravated via severe inflammation, metabolic dysfunctions, and abnormal ECM production, regeneration, cell proliferation leading to cancer, which involve diverse cellular activities and functions. Although different studies using diverse models or systems have been reported, most of them have focused on limited aspects or categories of the diseases. The factors to drive chronically step-wise processes of the liver diseases have rarely been studied. Although one single molecule might not be reasonably considered to contribute to the complicated processes with different cellular functions, cross-talks between pathways emanated from the molecule(s) may be importantly involved in the chronical processes. Thus, TM4SF5-mediated such a signaling hub may play roles in different disease steps.

On cell surface, there are certain domains where a specifically categorized membrane proteins or receptors to assign certain signaling pathways; they include focal adhesion, lipid raft, caveolae, and tetraspanin-enriched microdomain (TERM). Like the focal adhesion with integrin/ECM

engagement and lipid rafts/caveolae with glycosylphosphatidylinisotol (GPI)-linked proteins [21,22], TERM would form massive protein-protein complexes involving the tetraspanins, integrins, growth factor receptors, and so on [23]. TM4SF5, as a member of transmembrane 4 L six family similar to the tetraspanins or TM4SFs [24], binds to integrins α2 [25], α5 [26], EGFR [27], CD44 [13], and CD151 [28]. Recently, TM4SF5 is shown to associate with EGFR and integrin α5 depending on cellular level of cholesterol and post-translational modification of TM4SF5, which coordinated modulation of their association and trafficking can lead to spatiotemporal migration properties [27]. Further, TM4SF5 interacts with IL6R via its extracellular loop 2 (EC2) that has N138 and N155 of *N*-glycosylation residues and leads to STAT3 activation in hepatic cancer cells even without a sufficient IL6 ligand expression [16]. Indeed, IL6 and IL22 are known to activate STAT3 in HCC growth [29]. However, 60% of inflammatory hepatocellular adenomas harbor small in-frame deletion around the binding site of gp130 for IL-6 and expression of such mutants in hepatocytes leads to activation of STAT3 and induction of its downstream targets even without ligand binding [30]. Thus, ligand-independent STAT3 signaling may play roles in malignant conversion from adenomas to carcinomas. Similarly, TM4SF5 may mediate ligand-independently STAT3 activation through cooperation between TM4SF5 and integrins for FAK/JAK2 activation [31] or between TM4SF5 and EGFR in hepatocytes [32]. In addition, TM4SF5 directly binds to c-Src [15], which is

an upstream of STAT3 [33], so that TM4SF5-mediated c-Src/STAT3 activation can be possible. Therefore, TM4SF5 expression and cooperation with other receptors in hepatocytes can lead to STAT3 activation even without ligand engagement, playing as an important component of a signaling platform or hub, T_5ERM, during malignant aggravation of hepatic cancer from fibrosis, following fatty liver.

Interestingly, this study also reveals that during the aggravation from fatty to fibrotic liver phenotypes, STAT3 activity appeared to be a turning-point factor; a lower activity of STAT3 is kept during fatty liver, but its activity is elevated as fibrotic phenotypes follows. This turnover of the STAT3 activity was correlated with expression levels of SOCSs, which is a negative regulator [34]. In case of fatty liver, TM4SF5 expression was correlated with elevated expression of certain mRNAs and proteins related to lipid/fatty synthesis and accumulation. Among them**,** sterol regulatory element binding proteins **(**SREBPs) are clearly enhanced in parallel with TM4SF5 expression. Among the three SREBP isoforms, SREBP-1a and SREBP-1c functions in FFA synthesis and SREBP-2 in cholesterol synthesis.[34] Tg^{TM4SF5} mouse liver showed higher TG and SREBP-1 and SREBP-2 mRNA and/or protein levels and TM4SF5 transfection into primary hepatocytes resulted in elevated *SREBP-1* mRNA level. Thus, FFA synthesis and uptakes in hepatocytes could be by TM4SF5 expression. Meanwhile, during the fatty acid synthesis and accumulation leading to fatty liver, TM4SF5 expression reduced STAT3

phosphorylation. Thus, during fatty liver, TM4SF5-mediated SREBPs expression was inversely correlated with STAT3 phosphorylation (and activity); Lower STAT3 phosphorylation was correlated with higher expression of SOCS1/3. Then, TM4SF5-mediated STAT3 activation was followed during fibrotic/cirrhotic ECM production, with concomitantly reduced SOCSs levels in TM4SF5-positive cells. Activated STAT3 could transcriptionally induce ECMs; *laminin γ2* transcriptional activation was more obvious in hepatocytes, compared with *collagen α1*. TM4SF5-mediated transcriptional activation for *laminin γ2* and *collagen αI* were comparable, but STAT3 expression-mediated transcriptional activation for laminin γ2 was more dramatically elevated in hepatocytes than for *collagen α1*. Thus, in hepatocytes, TM4SF5/STAT3 signaling activity was more effective for *laminin γ2* rather than *collagen α1*. Such a preferential expression of laminin γ2 in hepatocytes was also shown in liver tissues of mice treated with CCl_4 or human liver disease patients. Therefore, it is quite interesting that laminin expression in hepatocytes is involved in the processes for fibrosis/cirrhosis and hepatic carcinogenesis. Such chronically-injured hepatocytes appeared to induce laminin γ2 and/or laminins for the processes toward fibrosis and carcinogenesis, being importantly additional to HSCs-mediated collagen I expression [35]. Being consistently, laminin γ2 is highly immunostained in cytoplasm of hepatic carcinoma cells at invasive front of a tumor [36]. Very recently it is shown that serum monomeric laminin γ2 is a novel biomarker for

HCC [37]. Thus, our FVB/N-Tg^{TM4SF5} cancerous mice showed hepatic carcinoma biomarkers of CD34 [19], α-FTP [38], and laminin γ2 [37], in addition to HIF-1α [39,40]. Beyond the chemical-induced fatty, fibrotic and/or cancerous liver models of mice, these genetic Tg^{TM4SF5} mice models would be very beneficial for the mechanistic studies for the liver diseases and pharmaceutical screening of anti-liver diseases reagents. Indeed, TM4SF5$^{-/+}$ or TM4SF5$^{-/-}$ knockout mice showed abnormal metabolic phenotypes, although their studies are going currently on, which is consistent with the fact that dysregulated metabolic activities would be importantly involved in the aggravation of the liver diseases.

Altogether, we found that TM4SF5 could be involved in the aggravation of chronically complicated processes of liver diseases, via modulation of TM4SF5-mediated SOCSs/STAT3 signaling activity to convert NAFLD to fibrosis and TM4SF5-mediated laminin γ2 induction in hepatocytes during fibrosis and carcinogenesis. Thus, TM4SF5 is a promising target candidate for the liver diseases, and therapeutic reagents to block TM4SF5-mediated cellular signaling and functions [18,41] would be pharmaceutically and clinically beneficial.

5. Reference

1. Tu, T., Calabro, S.R., Lee, A., Maczurek, A.E., Budzinska, M.A., Warner, F.J., McLennan, S.V., and Shackel, N.A. (2015). Hepatocytes in liver injury: Victim, bystander, or accomplice in progressive fibrosis? J Gastroenterol Hepatol *30*, 1696-1704.
2. Guicciardi, M.E., Malhi, H., Mott, J.L., and Gores, G.J. (2013). Apoptosis and necrosis in the liver. Compr Physiol *3*, 977-1010.
3. Bonnans, C., Chou, J., and Werb, Z. (2014). Remodelling the extracellular matrix in development and disease. Nat Rev Mol Cell Biol *15*, 786-801
4. Gressner, A.M., and Weiskirchen, R. (2006). Modern pathogenetic concepts of liver fibrosis suggest stellate cells and TGF-beta as major players and therapeutic targets. J Cell Mol Med *10*, 76-99.
5. Maher, J.J., and McGuire, R.F. (1990). Extracellular matrix gene expression increases preferentially in rat lipocytes and sinusoidal endothelial cells during hepatic fibrosis in vivo. J Clin Invest *86*, 1641-1648.
6. Biancheri, P., Giuffrida, P., Docena, G.H., MacDonald, T.T., Corazza, G.R., and Di Sabatino, A. (2014). The role of transforming growth factor (TGF)-beta in modulating the immune response and

fibrogenesis in the gut. Cytokine Growth Factor Rev *25*, 45-55.

7. Clarke, D.L., Carruthers, A.M., Mustelin, T., and Murray, L.A. (2013). Matrix regulation of idiopathic pulmonary fibrosis: the role of enzymes. Fibrogenesis Tissue Repair *6*, 20.
8. Hynes, R.O., and Naba, A. (2012). Overview of the matrisome--an inventory of extracellular matrix constituents and functions. Cold Spring Harb Perspect Biol *4*, a004903.
9. Kang, M., Choi, S., Jeong, S.J., Lee, S.A., Kwak, T.K., Kim, H., Jung, O., Lee, M.S., Ko, Y., Ryu, J., *et al.* (2012a). Cross-talk between TGFbeta1 and EGFR signalling pathways induces TM4SF5 expression and epithelial-mesenchymal transition. Biochem J *443*, 691-700.
10. Kang, M., Jeong, S.J., Park, S.Y., Lee, H.J., Kim, H.J., Park, K.H., Ye, S.K., Kim, S.H., and Lee, J.W. (2012b). Antagonistic regulation of transmembrane 4 L6 family member 5 attenuates fibrotic phenotypes in CCl(4) -treated mice. FEBS J *279*, 625-635.
11. Muller-Pillasch, F., Wallrapp, C., Lacher, U., Friess, H., Buchler, M., Adler, G., and Gress, T.M. (1998). Identification of a new tumour-associated antigen TM4SF5 and its expression in human cancer. Gene *208*, 25-30.
12. Lee, S.A., Lee, S.Y., Cho, I.H., Oh, M.A., Kang, E.S., Kim, Y.B., Seo, W.D., Choi, S., Nam, J.O., Tamamori-Adachi, M., *et al.* (2008).

Tetraspanin TM4SF5 mediates loss of contact inhibition through epithelial-mesenchymal transition in human hepatocarcinoma. J Clin Invest *118*, 1354-1366.

13. Lee, D., Na, J., Ryu, J., Kim, H.J., Nam, S.H., Kang, M., Jung, J.W., Lee, M.S., Song, H.E., and Choi, J. (2015). Interaction of tetraspan (in) TM4SF5 with CD44 promotes self-renewal and circulating capacities of hepatocarcinoma cells. Hepatology *61*, 1978-1997.
14. Jung, O., Choi, S., Jang, S.B., Lee, S.A., Lim, S.T., Choi, Y.J., Kim, H.J., Kim, D.H., Kwak, T.K., Kim, H., *et al.* (2012). Tetraspan TM4SF5-dependent direct activation of FAK and metastatic potential of hepatocarcinoma cells. J Cell Sci *125*, 5960-5973.
15. Jung, O., Choi, Y.J., Kwak, T.K., Kang, M., Lee, M.S., Ryu, J., Kim, H.J., and Lee, J.W. (2013). The COOH-terminus of TM4SF5 in hepatoma cell lines regulates c-Src to form invasive protrusions via EGFR Tyr845 phosphorylation. Biochim Biophys Acta *1833*, 629-642.
16. J Ryu, M Kang, M-S Lee, H-J Kim, SH Nam, HE Song, D Lee, and Lee JW., et al.(2014) Cross-talk between the TM4SF5/FAK and the IL6/STAT3 pathways controls invasion and immune escape. Molecular and Cellular Biology. 34(16):2946-2960.
17. Zhong, W., Shen, W.F., Ning, B.F., Hu, P.F., Lin, Y., Yue, H.Y., Yin,

C., Hou, J.L., Chen, Y.X., Zhang, J.P., *et al.* (2009). Inhibition of extracellular signal-regulated kinase 1 by adenovirus mediated small interfering RNA attenuates hepatic fibrosis in rats. Hepatology *50*, 1524-1536.

18. Lee, S.A., Kim, Y.M., Kwak, T.K., Kim, H.J., Kim, S., Kim, S.H., Park, K.H., Cho, M., and Lee, J.W. (2009a). The extracellular loop 2 of TM4SF5 inhibits integrin {alpha}2 on hepatocytes under collagen type I environment. Carcinogenesis *30*, 1872-1879.
19. Dai, L., Peng, X.X., Tan, E.M., and Zhang, J.Y. (2016). Tumor-associated antigen CAPERalpha and microvessel density in hepatocellular carcinoma. Oncotarget *7*, 16985-16995.
20. Zhao, Y.J., Ju, Q., and Li, G.C. (2013). Tumor markers for hepatocellular carcinoma. Mol Clin Oncol *1*, 593-598.
21. Eke, I., and Cordes, N. (2015). Focal adhesion signaling and therapy resistance in cancer. Semin Cancer Biol *31*, 65-75.
22. Sezgin, E., Levental, I., Mayor, S., and Eggeling, C. (2017). The mystery of membrane organization: composition, regulation and roles of lipid rafts. Nat Rev Mol Cell Biol *18*, 361-374.
23. Lee, J.W. (2014). TM4SF5-mediated protein-protein networks and tumorigenic roles. BMB Rep *47*, 483-487.
24. Wright, M.D., Ni, J., and Rudy, G.B. (2000). The L6 membrane

proteins--a new four-transmembrane superfamily. Protein Sci *9*, 1594-1600.

25. Lee, S.A., Ryu, H.W., Kim, Y.M., Choi, S., Lee, M.J., Kwak, T.K., Kim, H.J., Cho, M., Park, K.H., and Lee, J.W. (2009b). Blockade of four-transmembrane L6 family member 5 (TM4SF5)-mediated tumorigenicity in hepatocytes by a synthetic chalcone derivative. Hepatology *49*, 1316-1325.
26. Lee, S.A., Kim, T.Y., Kwak, T.K., Kim, H., Kim, S., Lee, H.J., Kim, S.H., Park, K.H., Kim, H.J., Cho, M., *et al.* (2010). Transmembrane 4 L six family member 5 (TM4SF5) enhances migration and invasion of hepatocytes for effective metastasis. J Cell Biochem *111*, 59-66.
27. Kim, H.J., Kwon, S., Nam, S.H., Jung, J.W., Kang, M., Ryu, J., Kim, J.E., Cheong, J.G., Cho, C.Y., Kim, S., *et al.* (2017). Dynamic and coordinated single-molecular interactions at TM4SF5-enriched microdomains guide invasive behaviors in 2- and 3-dimensional environments. FASEB J *31*, 1461-1481.
28. Kang, M., Ryu, J., Lee, D., Lee, M.-S., Kim, H.-J., Nam, S.H., Song, H.E., Choi, J., Lee, G.-H., and Kim, T.Y. (2014). Correlations between Transmembrane 4 L6 family member 5 (TM4SF5), CD151, and CD63 in liver fibrotic phenotypes and hepatic migration and invasive capacities. PloS one *9*, e102817.
29. Wang, H., Lafdil, F., Kong, X., and Gao, B. (2011). Signal transducer

and activator of transcription 3 in liver diseases: a novel therapeutic target. Int J Biol Sci *7*, 536-550.

30. Rebouissou S, Amessou M, Couchy G, Poussin K, Imbeaud S, Pilati C, Izard T, Balabaud C, Bioulac-Sage P, Zucman-Rossi J.(2009). Frequent in-frame somatic deletions activate gp130 in inflammatory hepatocellular tumours. *Nature* 457, 200-204
31. Balanis, N., Wendt, M.K., Schiemann, B.J., Wang, Z., Schiemann, W.P., and Carlin, C.R. (2013). Epithelial to Mesenchymal Transition Promotes Breast Cancer Progression via a Fibronectin-dependent STAT3 Signaling Pathway. J Biol Chem *288*, 17954-17967.
32. Guren, T.K., Abrahamsen, H., Thoresen, G.H., Babaie, E., Berg, T., and Christoffersen, T. (1999). EGF-induced activation of Stat1, Stat3, and Stat5b is unrelated to the stimulation of DNA synthesis in cultured hepatocytes. Biochem Biophys Res Commun *258*, 565-571.
33. Jung, J.E., Lee, H.G., Cho, I.H., Chung, D.H., Yoon, S.H., Yang, Y.M., Lee, J.W., Choi, S., Park, J.W., Ye, S.K., *et al.* (2005). STAT3 is a potential modulator of HIF-1-mediated VEGF expression in human renal carcinoma cells. Faseb J *19*, 1296-1298.
34. Yin, Y., Liu, W., and Dai, Y. (2015). SOCS3 and its role in associated diseases. Hum Immunol *76*, 775-780.

Ⅱ. Chapter 2.

Cross Talk between the TM4SF5/Focal Adhesion Kinase and the Interleukin-6/STAT3 Pathways Promotes Immune Escape of Human Liver Cancer Cells

ABSTRACT

TM4SF5 overexpressed in hepatocellular carcinoma activates focal adhesion kinase (FAK) during tumor cell migration. However, it remains unknown how TM4SF5 in hepatocellular carcinoma cells compromises with immune actions initiated by extracellular cytokines. Normal and cancerous hepatocytes with or without TM4SF5 expression were analyzed for the effects of cytokine signaling activity on TM4SF5/FAK signaling and metastatic potential. We found that interleukin-6(IL-6 was differentially expressed in hepatocytes depending on cancerous malignancy and TM4SF5 expression. IL-6 treatment activated FAK and STAT3 and enhanced focal adhesion(FA) formation in TM4SF5-nullcells, but it decreased TM4SF5-dependent FAK activity and FA formation in SNU761-TM4SF5 cells. STAT3 suppression abolished the IL-6-mediated effects in normal Chang cells, but it did not recover the TM4SF5-dependent FAK activity that was inhibited by IL-6 treatment in cancerous SNU761-TM4SF5 cells. In addition, modulation of FAK activity did not change the IL-6-mediated STAT3 activity in either the Chang or SNU761 cell system. TM4SF5 expression in SNU761 cells caused invasive extracellular matrix degradation negatively depending on IL-6/IL-6 receptor (IL-6R) signaling. Thus, it is likely that hepatic cancer cells adopt TM4SF5-dependent FAK activation and metastatic potential by lowering IL-6 expression and avoiding its immunological action through the IL-6-STAT3 pathway.

Keywords : Hepatocellular carcinoma, Collagen I, TM4SF5, STAT3, FAK, IL-6, IL-6R

Student Number : 2011-21717

1.Introduction

Cell migration and invasion are critical for the homeostatic maintenance of multicellular organisms as well as for cancer metastasis [1], which involves highly complex processes regulated by coordinated signaling pathways responding to extracellular matrix (ECM) or soluble factors [2]. As one of the most important signaling molecules activated by cell adhesion, focal adhesion kinase (FAK) plays critical roles in cell migration and invasion [3]. FAK is overexpressed in a diverse set of primary and metastatic tumor tissues including hepatocellular carcinoma (HCC), supporting its pro-tumorigenic and -metastatic roles [4-6].

Tetraspanins (TM4SFs) collaborate with integrins during cell adhesion and migration [7]. Similar to tetraspanins, transmembrane 4 L six family member 5 (TM4SF5) is a membrane glycoprotein with four transmembrane domains whose intracellular loop and NH_2- and COOH-terminal tails are oriented toward the cytosol [8,9]. TM4SF5 is overexpressed in a diverse set of cancers, and its overexpression in hepatocytes enhances their tumorigenic proliferation, migration, and invasion [8]. TM4SF5 binds and activates FAK thereby directing motility, and this interaction can be the basis for adhesion-dependent FAK activation by TM4SF5 [10]. Therefore, TM4SF5 causes abnormal cell growth and enhances the metastatic potential of liver cancer cells [8,9].

Tumor progression is often driven by inflammatory cells, which produce cytokines that influence the growth and survival of malignant cells. The identifications of these cytokines and their mechanisms of action are important because the inhibition of protumorigenic cytokine actions or the enhancement of anti-tumorigenic cytokine actions may allow therapeutic strategies [11]. Immune cells that often infiltrate tumors produce various cytokines, which propagate a localized inflammatory response and also regulate the growth/survival of premalignant cells [12]. IL6 is a multifunctional cytokine that is important for immune responses, cell fate, and proliferation [13]. IL6 is produced by immune cells and tumor cells [14].

IL6 signaling requires the membrane-bound IL6-receptor α subunit (mIL-6R, CD126) of the IL6 receptor and glycoprotein 130 (gp130) on target cells, and the expression of these proteins is limited to hepatocytes and certain leukocytes [15], suggesting possible autocrine effects by IL6 on hepatocellular carcinoma cells. By binding to its gp130-associated receptor, IL-6 transduces the signaling pathway that activates JAK1/2-STAT3 [13]. The binding of IL6 to the receptor complex activates the protein tyrosine kinases JAKs, leading to the phosphorylation of IL6R and the recruitment and activation of STAT3. The IL6/JAKs/STAT3 signaling pathway can be negatively regulated by the actions of the SOCS3 and PIAS proteins [16]. The activation of STAT3 induces a diverse group of target genes in diverse tumor

types, including HCC [16]. In addition, IL-6-independent STAT3 activation [17] or somatic mutation mediated activation of STAT3 [18] has been reported in hepatocellular tumors. The effect of IL6-mediated JAKs/STAT3 signaling on breast cancer proliferation can be either inhibitory or stimulatory [19].

We were interested in understanding how TM4SF5-mediated migration/invasion may interact with the cytokine-mediated immune responses. In particular, we examined how TM4SF5/FAK-based signaling, which promotes invasion, might be influenced by IL6/STAT3 signaling, which could be effective in an autocrine manner. We found that the cross-talk between FAK and STAT3 depended on TM4SF5 expression in both normal and cancerous hepatocytes; IL6/STAT3 signaling activity in Chang cells promoted TM4SF5/FAK activity, whereas IL6/STAT3 signaling in SNUU761 cells appeared to block TM4SF5/FAK activity. Owing to reduced IL6 expression, TM4SF5 expression in cancerous cells appears to increase FAK activity, thus avoiding IL6/STAT3-mediated inhibition.

2.Material and Methods

1. Cell culture

Control (normal hepatocyte AML12, Chang, hepatocarcinoma SNU449, or SNU761, Huh7-shTM4SF5, non-small-cell lung cancer [NSCLC] HCC827) or TM4SF5 WT-expressing (Chang-TM4SF5, Huh7-shControl, SNU449-TM4SF5, SNU761-TM4SF5, or HCC827-TM4SF5) cells have been described previously [20] or were prepared by G418 (A.G. Scientifics, San Diego, CA) selection following transfection of FLAG-mock or FLAG-TM4SF5 wild type (WT) into the parental cells. Stable cells were maintained in RPMI 1640 (WelGene, Daegu, South Korea) containing 10% fetal bovine serum (FBS), G418 (250 μg/ml), and antibiotics (Invitrogen, Grand Island, NY).

2. Extract preparation and Western blotting

Subconfluent cells in normal culture medium or cells transiently transfected with short interfering RNA (siRNA; control or siRNA against STAT3,termed siSTAT3) for 48h were either kept in suspension or reseeded onto collagen I-, laminin I-, or fibronectin (10 μg/ml; BD Biosciences, San Jose, CA)-precoated dishes with or without IL-6 (50 ng/ml) and/or dimethylsulfoxide (DMSO; vehicle) or diverse pharmacological inhibitors for the indicated periods, as previously explained [10]. PF271 (1.0 μM), specifically against FAK [21], and AG490 (100 μM), specifically against

JAK2 (LC Laboratories, Woburn, MA), were added in the middle of rocking prior to replating. Cells were either kept in suspension or replated on different extracellular matrix (ECM;10 μg/ml)-precoated culture dishes for the indicated times. Normal human or cancer liver or colon tissues were obtained after informed consent from each patient according to institutional review board (IRB)-approved methods of the Institute of Laboratory Animal Resources, Seoul National University (ILARSNU). The whole-tissue extracts were prepared as explained previously [20]. Whole-cell lysates were prepared with a lysis buffer (1% Brij58, 0.1% SDS, 150 mM NaCl, 20 mM HEPES, pH7.4, 2mM MgCl2, 2mM CaCl2, and protease inhibitors). The primary antibodies included anti-pY^{397}FAK (Abcam, Cambridge, United Kingdom), anti-pY^{416} Src, anti-FLAG, anti-Akt, anti-pY^{165} p130Cas, anti-phospho-extracellular signal-regulated kinases (anti-p-ERKs), anti-ERKs (Cell Signaling Technology, Danvers, MA), anti-pY^{705} STAT3, anti-pY^{486} cortactin (Millipore, Billerica, MA), anti-tubulin, anti-FLAG (Sigma, St. Louis, MO), anti-c-Src, anti-pY^{577} FAK, anti-pY^{118} paxillin, anti-PIAS3, anti-SOCS3, anti-IL-6R, anti-pS^{473} Akt (Santa Cruz Biotech, Santa Cruz, CA), anti-paxillin, anti-FAK (BD Transduction Laboratory, Bedford, MA), and anti-STAT3 (Millipore, Solna, Sweden).

3. Cytokine antibody array

Cytokine analysis using whole-cell extracts from the subconfluent cells was

performed using RayBio human cytokine antibody array 3 by following the manufacturer's protocols (RayBiotech Inc., Norcross, GA).

4. Coimmunoprecipitation

Cells were subjected to mock transfection or were transiently transfected with TM4SF5 WT or the TM4SF5 N138A/ N155Q (NANQ) mutant (of N-glycosylation residues) together with or without the extracellular domain of human IL-6R [amino acids 1 to 365; pTarget-hIL-6R (ECD); a kind gift from Soohyun Kim, Medical Immunology Center, KonKuk University, Seoul, South Korea] for 48 h, and whole-cell lysates were prepared as described above. Whole-cell extracts prepared as described above were immunoprecipitated with biotin-precoated beads for 2 h (IBA, Germany) prior to immunoblotting for the indicated molecules.

5. Indirect immunofluorescence

Cells under normal culture conditions on glass coverslips or transiently transfected for 48 h with siRNA against a control scramble sequence (siControl) or siSTAT3 (Dharmacon, Pittsburgh, PA), together with green fluorescent protein (GFP)-conjugated control siRNA, were immunostained using antibody against pY^{397} FAK or pY^{705} STAT3 and subjected to 4',6-diamidino-2-phenylindole (DAPI) staining for DNA. Immunofluorescent images were acquired on a microscope (BX51TR; Olympus, Japan).

Randomly saved images for 10 fields in each experimental condition were visually counted by two independent individuals. Cells with at least similar or increased spreading area and FA numbers upon IL-6 treatment were counted, and the mean ± standard deviation values are presented as a graph.

6. Transwell migration assay

Cells were analyzed for migration using Transwell chambers with 8-μm pores (Corning Inc., Corning, NY). The assay was performed with or without IL-6 treatment (50 ng/ml) for 5 h (Chang cells), 7 h (HCC827 cells), or 12 h (SNU761 cells) with serum-free medium containing 10 μg/ml collagen I (Sigma) in the lower chambers. In the case of antibody blocking, anti-IL-6R antibody (20 μg/ml; US Biological, Salem, MA) was incubated with the cells before loading into the chambers. More than at least 5 random images of migrated cells were saved for each experimental condition. After independent visual counts of cells in each image, mean values ± standard deviations were graphed.

7. ECM degradation analysis

Cells were transiently transfected with siControl or siSTAT3 (Dharmacon) for 48 h or were treated with DMSO or 1.0 μM PF271 [21] for 1 day. ECM degradation by cells on Oregon Green 488-conjugated gelatin (Invitrogen), with or without IL-6 treatment (50 ng/ml) for 4 h, were analyzed as described

previously [22]. Antibody neutralizing was performed by a preincubation of the cells using anti-IL-6R antibody (20 μg/ml; US Biological).

8. Immunohistochemistry

Immunohistochemistry of human liver tissues was performed with primary antibodies for normal rabbit IgG, TM4SF5 [20], pY^{397} FAK (Abcam, Cambridge, United Kingdom), or pY^{705} STAT3 (Millipore, Solna, Sweden)

9. Statistical methods

Student's *t* tests were performed for comparisons of mean values to determine statistical significance. A *P* value of less than 0.05 was considered statistically significant.

3. Results

1. Differential expression of IL-6 in normal and cancerous cells depends on TM4SF5 expression.

The autocrine effects of cytokines on TM4SF5-mediated tumorigenic functions were studied in normal and cancerous epithelial cells with or without TM4SF5 expression by using an antibody array. Whole-cell lysates from normal Chang hepatocytes, HCC827 lung cancer cells, and SNU449 and SNU761 hepatocellular carcinoma cells lacking or overexpressing TM4SF5 were processed for the array analyses. Interestingly, IL-6 was expressed at higher levels in the Chang TM4SF5 cells than in parental Chang cells (Fig.1A, left). However, for the cancer cells, parental TM4SF5-negative cells showed higher IL-6 expression than the TM4SF5-expressing cells (Fig.1A, right, white boxes). Meanwhile, another cytokine, IL-12 (p40 and p70), which was located 4 rows directly below the IL-6 spots, showed a similar expression pattern, although its intensity was less than that of IL-6 (Fig. 1A). Although IL-12 and other cytokines not tested in this study might be similarly differential in the cellular systems with or without TM4SF5 expression, we focused on IL-6 for further experiments. In contrast, the SNU761 cancer cells and the Chang hepatocytes with or without TM4SF5 expression showed similar IL6R mRNA levels (Fig.1B). Further, quantitative PCR analyses of

downstream target genes in the cells, such as CCL2 (chemokine[C-C motif] ligand 2) and MCL1 (myeloid cell leukemia sequence 1) [23, 24], showed no significant differences in their mRNA levels (Fig. 1B, C, and D). These observations indicated that signaling activities for gene expression by IL-6/IL-6R were comparable between TM4SF5-null and -expressing cells. Thus, the differential effects of IL-6 on TM4SF5-mediated cellular function may be attributed to tumorigenic malignancy. Normal liver or colon tissues were compared to their counterpart cancer tissues for levels of TM4SF5 expression, FAK Tyr397 phosphorylation, or STAT3 Tyr705 phosphorylation. Cancer tissues clearly showed higher levels than those seen in normal tissues for 6 out of 7 TM4SF5-positive tumors (Fig. 1E). Immunohistochemistry analysis of tumor liver tissues resulted in higher TM4SF5, pY^{397} FAK, and pY^{705} STAT3 levels (Fig. 1F) than those in normal tissues, indicating that these factors are correlated with liver tumorigenesis. Throughout Western blotting and immunohistochemistry using limited sample numbers, TM4SF5-positive liver or colon cancer cells were highly correlated with increased FAK and STAT3 phosphorylation (6/6 and 3/4, respectively) (Fig. 1E and F).

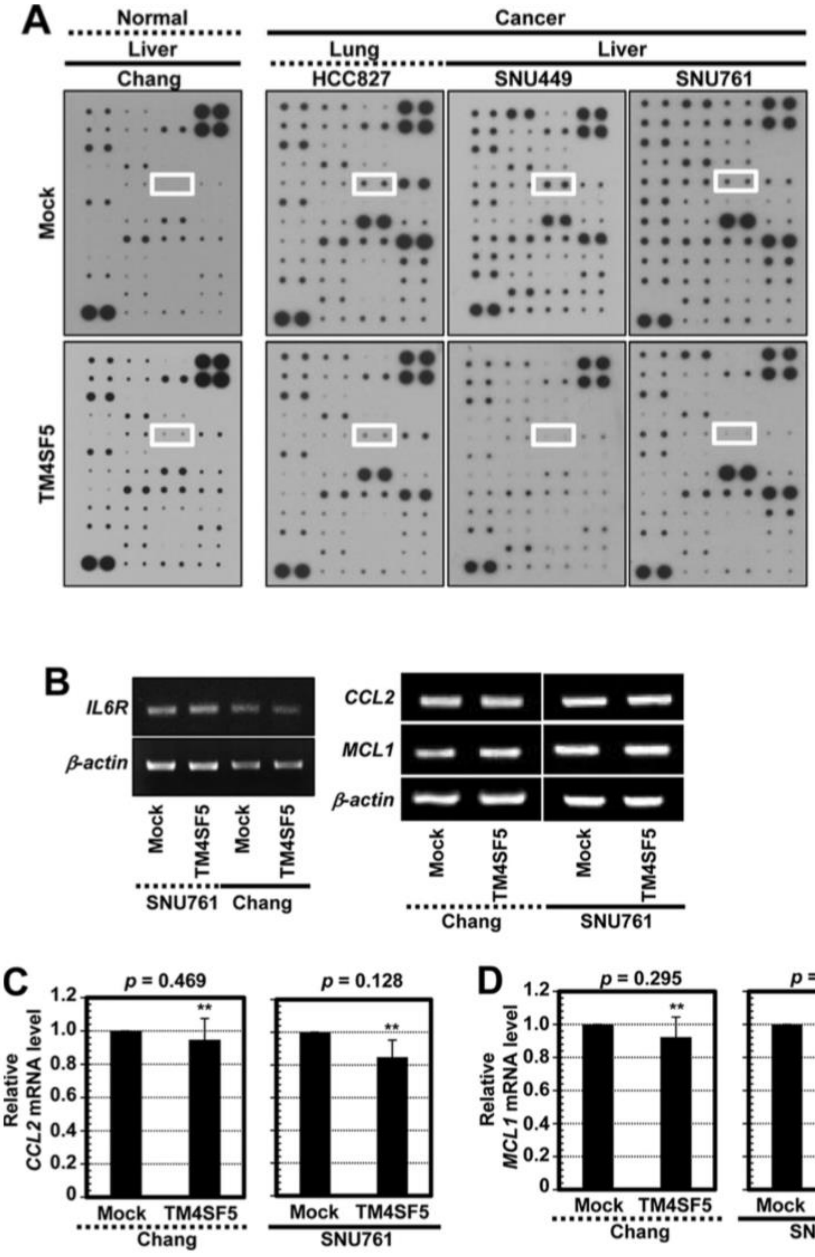
A
Normal
Cancer
Liver
Lung
Liver
Chang
HCC827
SNU449
SNU761
Mock
TM4SF5
B
IL6R
β-actin
Mock
TM4SF5
Mock
TM4SF5
SNU761
Chang
CCL2
MCL1
β-actin
Mock
TM4SF5
Mock
TM4SF5
Chang
SNU761
C
p = 0.469
p = 0.128
Relative CCL2 mRNA level
1.2
1.0
0.8
0.6
0.4
0.2
0
**
**
Mock
TM4SF5
Mock
TM4SF5
Chang
SNU761
D
p = 0.295
p = 0.894
Relative MCL1 mRNA level
1.2
1.0
0.8
0.6
0.4
0.2
0
**
**
Mock
TM4SF5
Mock
TM4SF5
Chang
SNU761

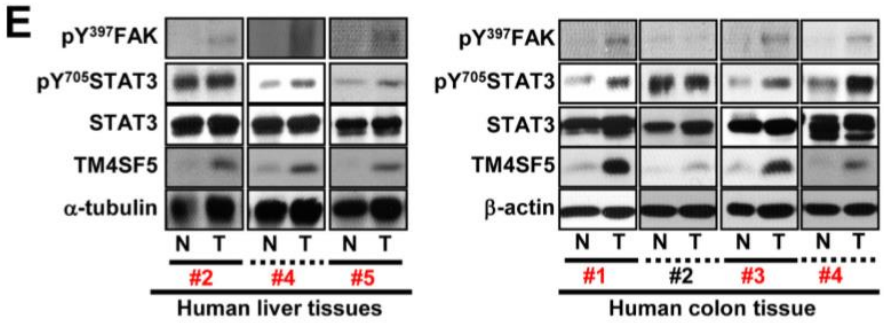
E
pY397FAK
pY705STAT3
STAT3
TM4SF5
α-tubulin
N T N T N T
#2 #4 #5
Human liver tissues
pY397FAK
pY705STAT3
STAT3
TM4SF5
β-actin
N T N T N T N T
#1 #2 #3 #4
Human colon tissue

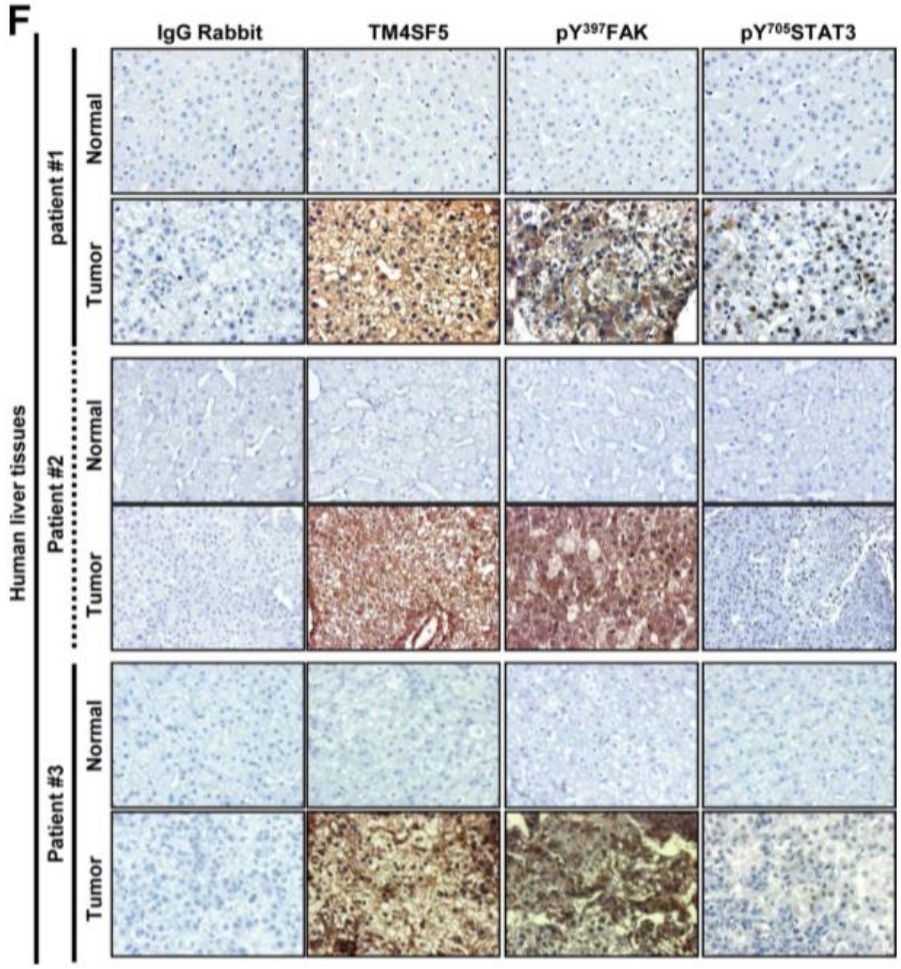
F
IgG Rabbit
TM4SF5
pY397FAK
pY705STAT3
Human liver tissues
patient #1
Normal
Tumor
Patient #2
Normal
Tumor
Patient #3
Normal
Tumor

Fig. Ⅱ-1. Differential expression of IL-6 between normal and cancer cells depending on TM4SF5 expression. (A) Cytokine antibody array using whole-cell lysates from diverse mock- or TM4SF5-expressing cells showed differential expression levels of IL-6 (white boxes). (B) Equal expression levels of IL6R mRNA (left) or of certain genes downstream of IL-6/IL-6R (right) in normal Chang and SNU761 cancerous hepatocytes with or without TM4SF5 expression were confirmed by RT-PCR. (C and D) Quantitative real-time PCR analyses for CCL2 (C) or MCL1 (D) were performed using normal Chang and SNU761 cancerous hepatocytes with or without TM4SF5 expression. *P* values larger than 0.05(**) depict statistically insignificant differences. (E) Whole extracts prepared from normal (N) or cancer (T) tissues of liver or colon cancer patients were immunoblotted for the indicated molecules. Patient case numbers in red showed a positive relationship among TM4SF5 expression, FAK Tyr397 phosphorylation, and STAT3 Tyr705 phosphorylation. (F) Immunohistochemistry of human liver tissues shows increased TM4SF5, pY^{397} FAK, or pY^{705} STAT3 in tumor tissues compared to levels in normal tissues. The data represent three independent experiments

2. TM4SF5-mediated FAK phosphorylation and focal adhesion formation were maintained or enhanced upon IL-6 treatment of Chang cells but abolished by IL-6 treatment of SNU761 cells.

To understand the TM4SF5 dependency of the adhesion-related signaling activities, the cells were reseeded onto a variety of ECM proteins before being analyzed by immunoblotting. Chang cells that were grown on collagen I for 30 min but not 60 min showed obvious TM4SF5-dependent enhancements of the adhesion-related signaling activities compared to cells grown on fibronectin or laminin I (Fig. 2A). Therefore, the cells were analyzed 15 or 30 min after being suspended or reseeded onto collagen I with or without IL-6 treatment. In either the mock-transfected or TM4SF5-expressing cells, the adhesion onto collagen I increased the phosphorylation levels of FAK and paxillin (Pax); this increase was more obvious in cells expressing TM4SF5 than in TM4SF5 null mock-transfected cells (Fig.2B and C, lanes 1 to 3 and 7 to 9). IL-6 treatment was functional because it increased the Tyr705 phosphorylation of STAT3 (i.e., pY^{705} STAT3) (Fig. 2B and C). Chang and SNU761 mock-treated cells maintained or increased adhesion-dependent FAK and paxillin phosphorylation upon IL-6 treatment, whereas these phosphorylation levels decreased in the SNU761-TM4SF5 cells; the Chang-TM4SF5 cells maintained the phosphorylation levels (Fig. 2B and C, lanes 4 to 6 and 10 to 12). Thus, IL-6 signaling seemed to negatively affect TM4SF5

dependent FAK activity in SNU761 cancer cells. Such differential TM4SF5-dependent effects on FAK and paxillin phosphorylation following IL-6 treatment also were observed in NSCLC HCC827 cells replated on collagen I (Fig.2D) and in SNU761 cells replated on fibronectin (Fig.2E). This point is interesting because the IL-6 levels in TM4SF5-positive cancer cells were lower than those in the TM4SF5-null tumor cells (Fig. 1), which suggests that there was no effective inhibition of TM4SF5 activity by IL-6 signaling in the cancerous cells. Although normal Chang hepatocytes showed IL-6-dependent pY^{705} STAT3 levels (Fig. 2A, B, and C), pY^{705} STAT3, even without IL-6 treatment (i.e., IL-6-independent pY^{705} STAT3), might be a characteristic of liver cancer cells. The IL-6-dependent pY^{705} STAT3 level in Chang cells or in SNU761 mock-treated cells was increased or sustained following cell adhesion, whereas IL-6 independent pY^{705} STAT3 in SNU761-TM4SF5 cells declined after cell adhesion (Fig.2C and E, lanes 7 to 9). However, in the case of NSCLC HCC7827, IL-6-independent pY^{705} STAT3 was observed even without TM4SF5 (Fig.2D), indicating the presence of tissue-specific IL-6-independent pY^{705} STAT3 in TM4SF5-positive cells. The effects of IL-6 treatment on FA formation were examined. TM4SF5 expression in Chang or SNU761 cells resulted in obvious pY^{397} FAK-enriched FA formation (Fig. 2F, left). Although the mock-transfected Chang (Chang-mock) cells had enhanced FA formation following IL-6 treatment, IL-6-treated Chang-TM4SF5 cells maintained their ability to form FAs and formed more than did the mock cells

(Fig. 2F, upper). In addition, SNU761-mock cells showed an IL-6-mediated increase in FA formation similar to that of the Chang cells, but the TM4SF5-dependent FA formation in SNU761-TM4SF5 cells was lost following IL-6 treatment (Fig. 2F, lower). Such observations showing unchanged phospho Tyr397 FAK-enriched FA formation or decreased FA formation upon IL-6 treatment to TM4SF5-expressing cells also were valid in normal mouse hepatocyte AML12 or NSCLC HCC827 cells that were transiently or stably transfected with TM4SF5, respectively (Fig.2G). Furthermore, IL-6 treatment enhanced the nuclear translocation of pY^{705} STAT3, indicating IL-6-mediated STAT3 activation (Fig.2H). Interestingly, SNU761-mock cells showed obvious localization of pY^{705} STAT3 at the cellular periphery after IL-6 treatment; it is currently not clear how this occurred (Fig.2H).

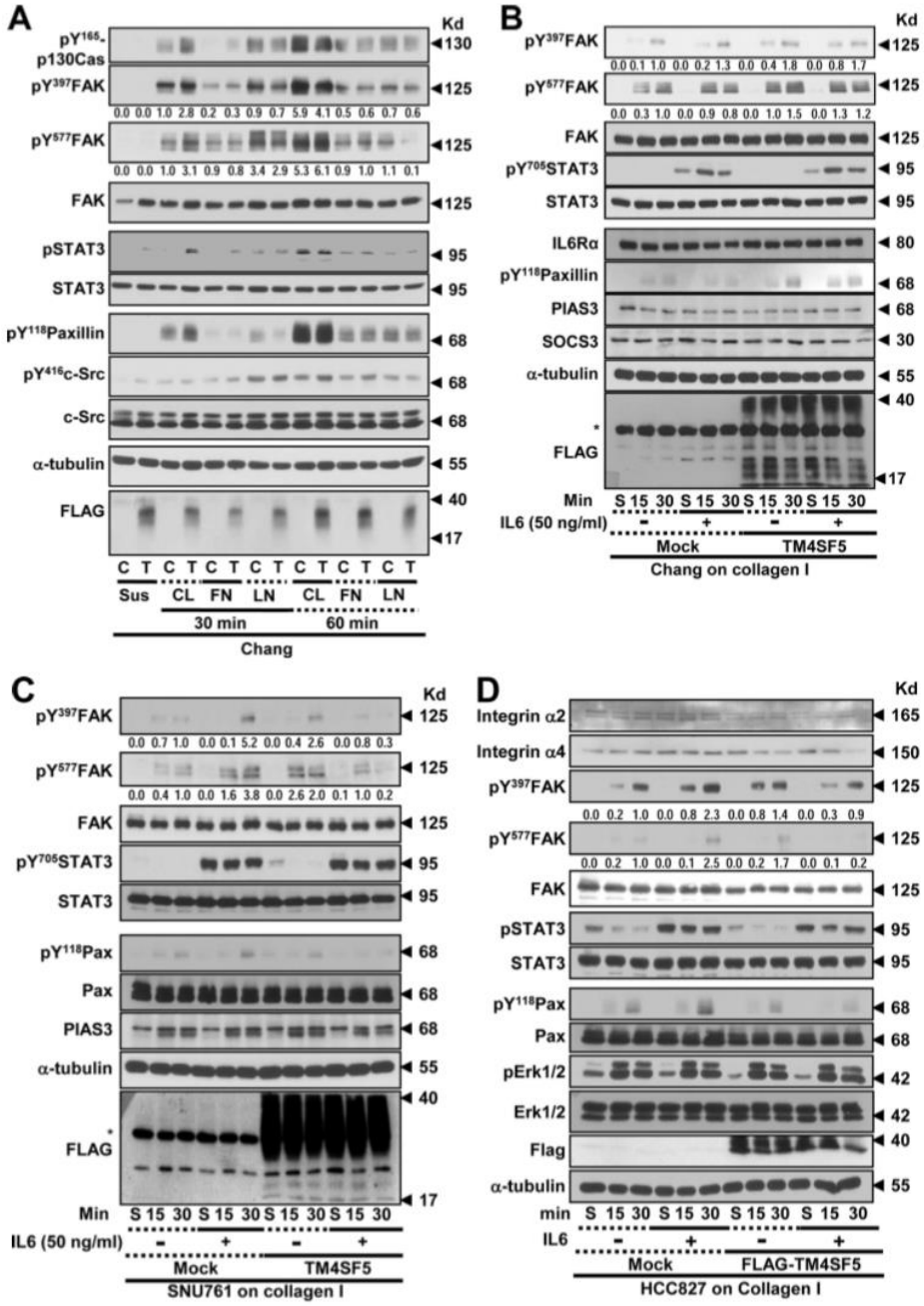
A
Kd
pY165-p130Cas
130
pY397FAK
125
0.0 0.0 1.0 2.8 0.2 0.3 0.9 0.7 5.9 4.1 0.5 0.6 0.7 0.6
pY577FAK
125
0.0 0.0 1.0 3.1 0.9 0.8 3.4 2.9 5.3 6.1 0.9 1.0 1.1 0.1
FAK
125
pSTAT3
95
STAT3
95
pY118Paxillin
68
pY416c-Src
68
c-Src
68
α-tubulin
55
FLAG
40
17
C T C T C T C T C T C T C T
Sus CL FN LN CL FN LN
30 min 60 min
Chang
B
Kd
pY397FAK
125
0.0 0.1 1.0 0.0 0.2 1.3 0.0 0.4 1.8 0.0 0.8 1.7
pY577FAK
125
0.0 0.3 1.0 0.0 0.9 0.8 0.0 1.0 1.5 0.0 1.3 1.2
FAK
125
pY705STAT3
95
STAT3
95
IL6Rα
80
pY118Paxillin
68
PIAS3
68
SOCS3
30
α-tubulin
55
40
*
FLAG
17
Min S 15 30 S 15 30 S 15 30 S 15 30
IL6 (50 ng/ml) - + - +
Mock TM4SF5
Chang on collagen I
C
Kd
pY397FAK
125
0.0 0.7 1.0 0.0 0.1 5.2 0.0 0.4 2.6 0.0 0.8 0.3
pY577FAK
125
0.0 0.4 1.0 0.0 1.6 3.8 0.0 2.6 2.0 0.1 1.0 0.2
FAK
125
pY705STAT3
95
STAT3
95
pY118Pax
68
Pax
68
PIAS3
68
α-tubulin
55
40
*
FLAG
17
Min S 15 30 S 15 30 S 15 30 S 15 30
IL6 (50 ng/ml) - + - +
Mock TM4SF5
SNU761 on collagen I
D
Kd
Integrin α2
165
Integrin α4
150
pY397FAK
125
0.0 0.2 1.0 0.0 0.8 2.3 0.0 0.8 1.4 0.0 0.3 0.9
pY577FAK
125
0.0 0.2 1.0 0.0 0.1 2.5 0.0 0.2 1.7 0.0 0.1 0.2
FAK
125
pSTAT3
95
STAT3
95
pY118Pax
68
Pax
68
pErk1/2
42
Erk1/2
42
Flag
40
α-tubulin
55
min S 15 30 S 15 30 S 15 30 S 15 30
IL6 - + - +
Mock FLAG-TM4SF5
HCC827 on Collagen I

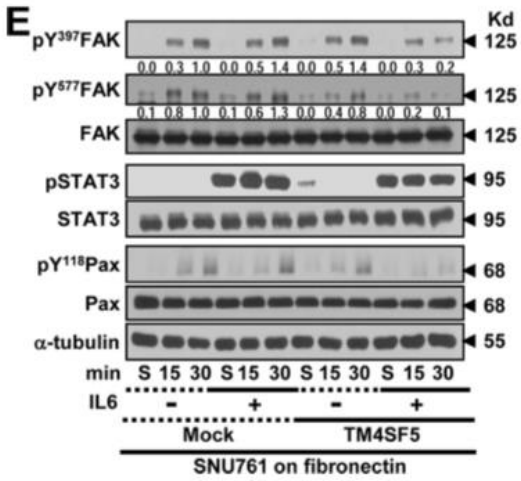
E
pY397FAK
Kd
125
0.0 0.3 1.0 0.0 0.5 1.4 0.0 0.5 1.4 0.0 0.3 0.2
pY577FAK
125
0.1 0.8 1.0 0.1 0.6 1.3 0.0 0.4 0.8 0.0 0.2 0.1
FAK
125
pSTAT3
95
STAT3
95
pY118Pax
68
Pax
68
α-tubulin
55
min S 15 30 S 15 30 S 15 30 S 15 30
IL6 - + - +
Mock
TM4SF5
SNU761 on fibronectin

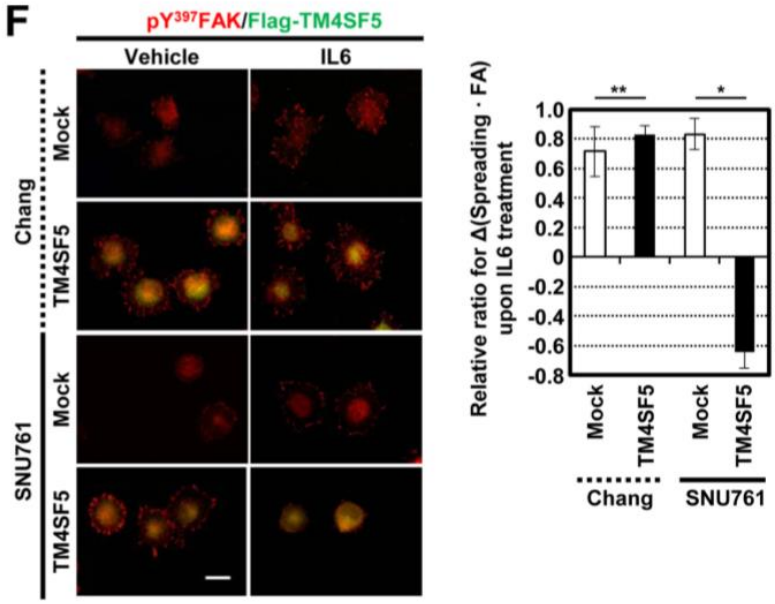
F
pY397FAK/Flag-TM4SF5
Vehicle
IL6
Chang
Mock
TM4SF5
SNU761
Mock
TM4SF5
Relative ratio for Δ(Spreading · FA) upon IL6 treatment
**
*
1.0
0.8
0.6
0.4
0.2
0
-0.2
-0.4
-0.6
-0.8
Mock
TM4SF5
Mock
TM4SF5
Chang
SNU761

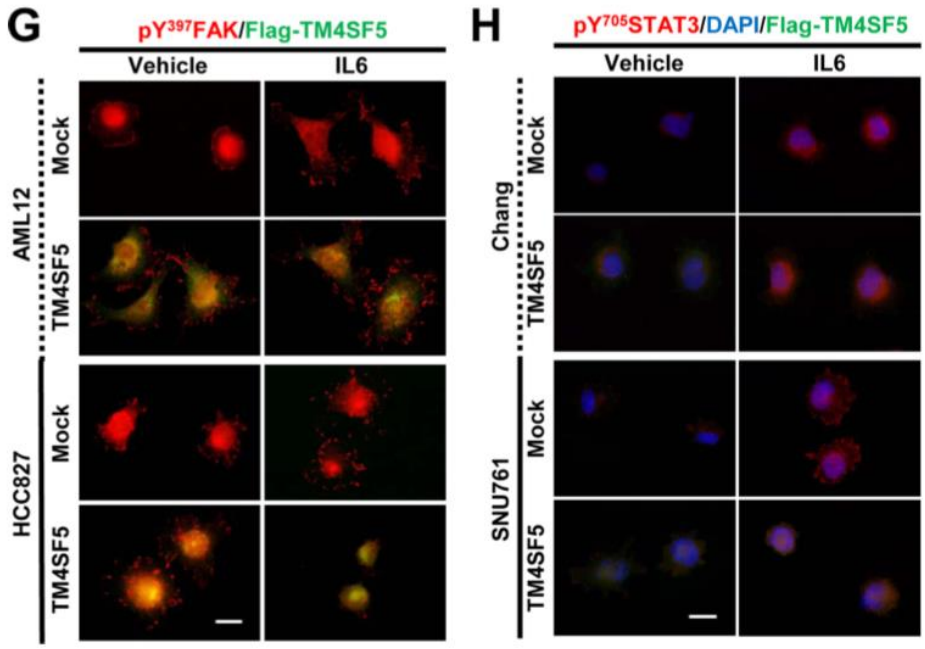
G
pY397FAK/Flag-TM4SF5
Vehicle
IL6
AML12
Mock
TM4SF5
HCC827
Mock
TM4SF5
H
pY705STAT3/DAPI/Flag-TM4SF5
Vehicle
IL6
Chang
Mock
TM4SF5
SNU761
Mock
TM4SF5

Fig. Ⅱ-2. **TM4SF5-mediated FAK phosphorylation and focal adhesion formation were maintained upon IL-6 treatment of Chang cells but was abolished upon IL-6 treatment of SNU761 cells.** (A) Chang cells without (C) or with (T) TM4SF5 expression were trypsinized, washed in serum-free medium with 1% bovine serum albumin (BSA), and kept rolling for 1 h prior to being kept in suspension (Sus) for 60 min or reseeding onto collagen I (CL)-, fibronectin (FN)-, or laminin I (LN)-precoated (10 μg/ml) dishes for 30 or 60 min prior to whole-cell lysate preparation. The indicated molecules were immunoblotted using the lysates.(B to H) Chang (B, F, and H), SNU761 (C, F, and H), HCC827 (D and G), or AML12 (G) cells lacking FLAG-TM4SF5 (mock) or overexpressing FLAG-TM4SF5 (TM4SF5) were kept in suspension (S) or were reseeded onto collagen I-or fibronectin (10 μg/ml)-precoated dishes (E) for the indicated times (min) or on cover glasses for 30 min. Vehicle or IL-6 was added as cells were reseeded. The cells were harvested prior to immunoblotting using antibodies against the indicated molecules (B to E) or processed for immunostaining for pY^{397} FAK (F and G) or pY^{705} STAT3 in addition to DAPI staining for the nucleus (H). (F) Randomly saved images for 10 fields in each experimental condition were visually counted by two independent individuals. Cells with at least similar or increased spreading areas and FA numbers upon IL-6 treatment were counted, and their mean ± standard deviation values were graphed. Positive y values depict relative

ratios of cells with at least similar or increased spreading areas and FA numbers upon IL-6 treatment, and negative y values depict decreased spreading and FA numbers upon IL-6 treatment. Asterisks in panels B and C denote nonspecific bands by the anti-FLAG antibody. One or two asterisks in panel F depict statistically significant or insignificant differences, respectively. The data represent three different experiments.

3. SNU761 cells differentially regulated migration and invasive ECM degradation in a TM4SF5-dependent manner after IL-6 treatment.

We next examined how IL-6 treatment affected the TM4SF5-mediated migration and invasive ECM degradation. IL-6 treatment or TM4SF5 expression in Chang cells each increased the migration of the cells, but treating Chang-TM4SF5 cells with IL-6 did not enhance the TM4SF5-mediated migration (Fig.3A); instead, the migration rate was maintained. In addition, treatment of SNU761-TM4SF5 cells with IL-6 decreased their migration compared to that of untreated SNU761-TM4SF5 cells; however, IL-6 treatment and TM4SF5 expression in SNU761 cells each increased cellular migration (Fig.3B). Interestingly, preincubation of cells with anti-IL-6R antibody reduced migration of TM4SF5-null SNU761 cells but did not decrease that of SNU761 TM4SF5 cells (Fig. 3B, right, 2nd and 5th bars), supporting endogenous IL-6 expression in SNU761-mock cells but not IL-6 expression in SNU761-TM4SF5 cells (Fig. 1A). Such IL-6 treatment-mediated decreases in migration of TM4SF5-positive cells but increases in TM4SF5-negative cells compared to levels in untreated cells also were valid in NSCLC HCC827 cells (Fig. 3C). We next examined invasive ECM degradation by culturing cells on OG^{488}-gelatin-precoated cover glasses. Chang hepatocytes did not exhibit ECM degradation under our experimental conditions (Fig.3D). However, SNU761 cells treated with IL-6 or

overexpressing TM4SF5 both exhibited enhanced ECM degradation. Interestingly, treating SNU761-TM4SF5 cells with IL-6 abolished the TM4SF5-enhanced ECM degradation (Fig.3E). Consistent with these findings, MMP2 activity in the culture medium was not observed in the Chang cells, but the TM4SF5-mediated MMP2 activity of the SNU761-TM4SF5 cells was slightly reduced following IL-6 treatment (Fig. 3F). Neutralization of the SNU761-TM4SF5 cells with an anti-IL-6R antibody was performed to examine whether IL-6R is critically involved in ECM degradation. Preincubation of the SNU761-mock cells with the anti-IL-6R antibody abolished both basal and IL-6-enhanced ECM degradation, whereas preincubation with the antibody recovered the IL-6-suppressed ECM degradation of the SNU761-TM4SF5 cells to the level of TM4SF5 mediated ECM degradation (Fig. 3G). Again, preincubation of SNU761-mock, but not SNU761-TM4SF5, cells with anti-IL-6R antibody decreased ECM degradation (Fig.3G), supporting the roles of endogenous IL-6 expression in TM4SF5-negative cells. Further, the IL-6 treatment-mediated decrease in ECM degradation by TM4SF5 positive cancer cells also was observed with Huh7 cells (Fig.3H). We then tested whether IL-6R could associate with TM4SF5. Streptavidin (Strep)-tagged TM4SF5 coimmunoprecipitated IL-6R in both Chang and SNU761 cell systems (Fig. 3I). Interestingly, a mutant of TM4SF5 where the N-glycosylation residues were mutated (i.e., NANQ for N138A and N155Q) did not bind to IL-6R (Fig. 3J, 3rd lane in each IP

sample). The ectopic extracellular domain of IL-6R (amino acids 1 to 365) resulted in binding to TM4SF5 WT but not to the NANQ mutant (Fig.3J, 4th and 5th lanes in each IP sample), indicating that their extracellular domains were important for the interaction. Thus, IL-6/IL-6R may differentially regulate adhesion-related signaling and cellular functions of TM4SF5-expressing cells depending on the degree of their malignancy, possibly via extracellular association(s) between IL-6R and TM4SF5.

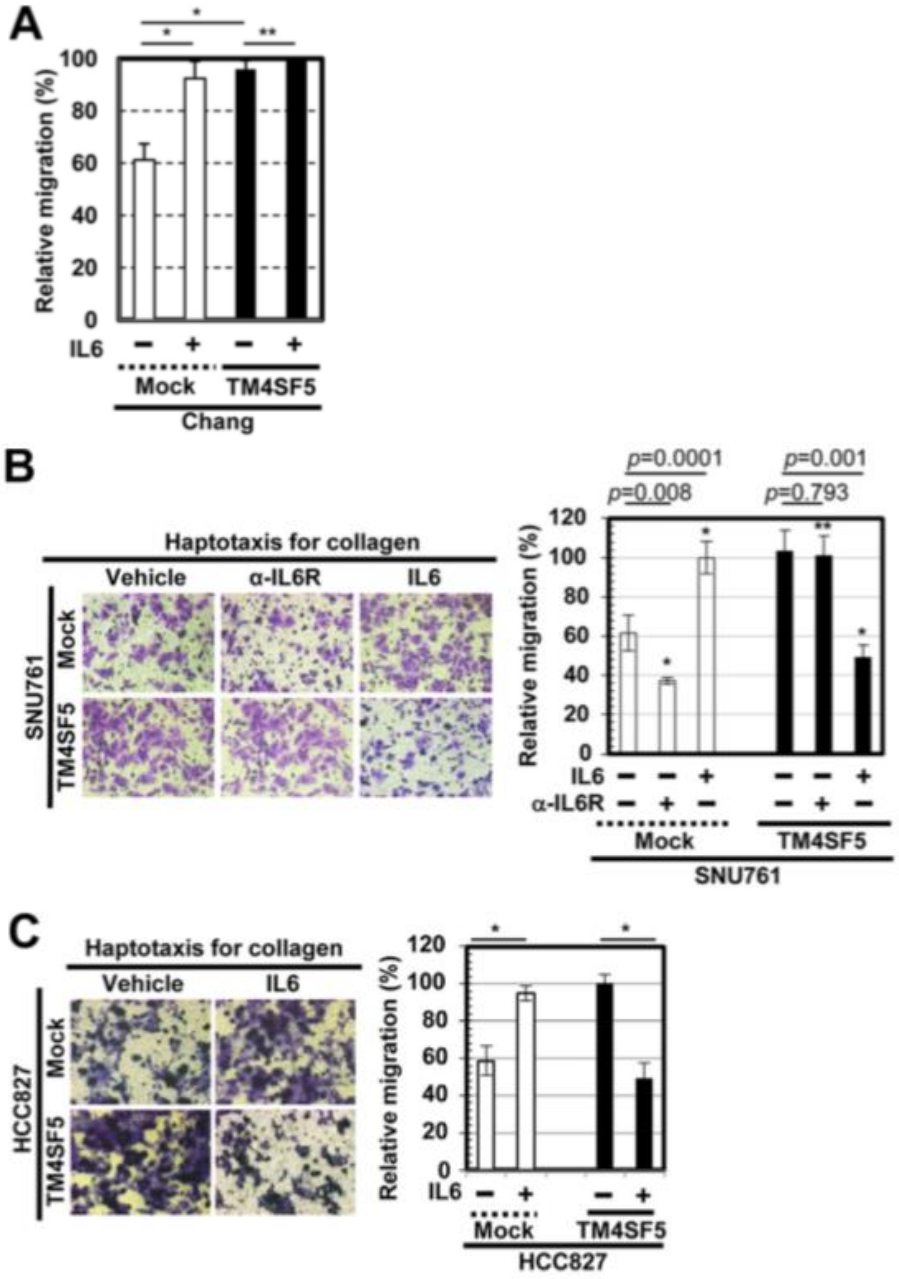
A
Relative migration (%)
IL6
Mock
TM4SF5
Chang
B
Haptotaxis for collagen
Vehicle
α-IL6R
IL6
SNU761
Mock
TM4SF5
p=0.0001
p=0.008
p=0.001
p=0.793
Relative migration (%)
IL6
α-IL6R
Mock
TM4SF5
SNU761
C
Haptotaxis for collagen
Vehicle
IL6
HCC827
Mock
TM4SF5
Relative migration (%)
IL6
Mock
TM4SF5
HCC827

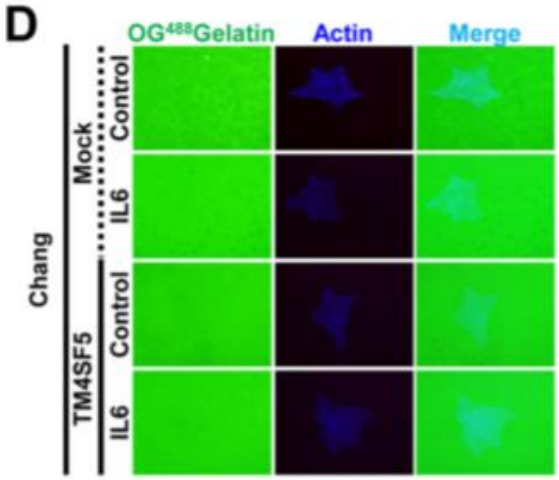
D
OG488Gelatin
Actin
Merge
Chang
Mock
TM4SF5
Control
IL6
Control
IL6

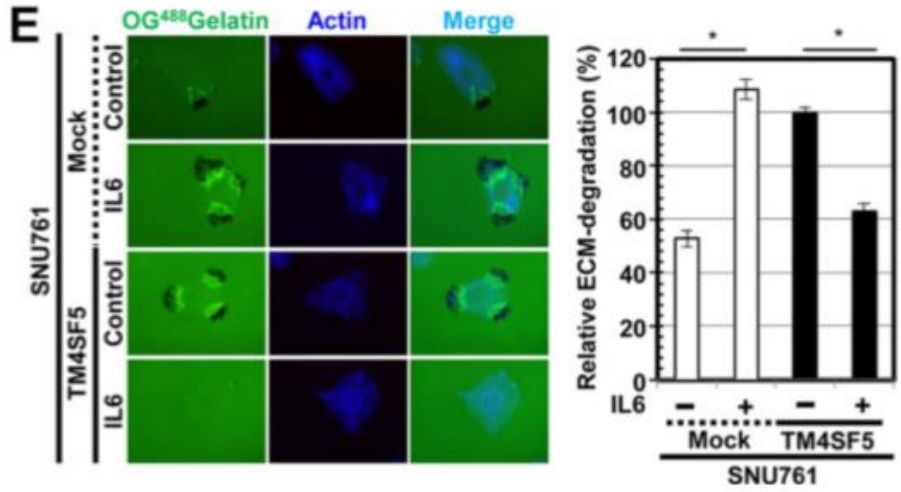
E
OG488Gelatin
Actin
Merge
SNU761
Mock
TM4SF5
Control
IL6
Control
IL6
Relative ECM-degradation (%)
120
100
80
60
40
20
0
*
*
IL6
−
+
−
+
Mock
TM4SF5
SNU761

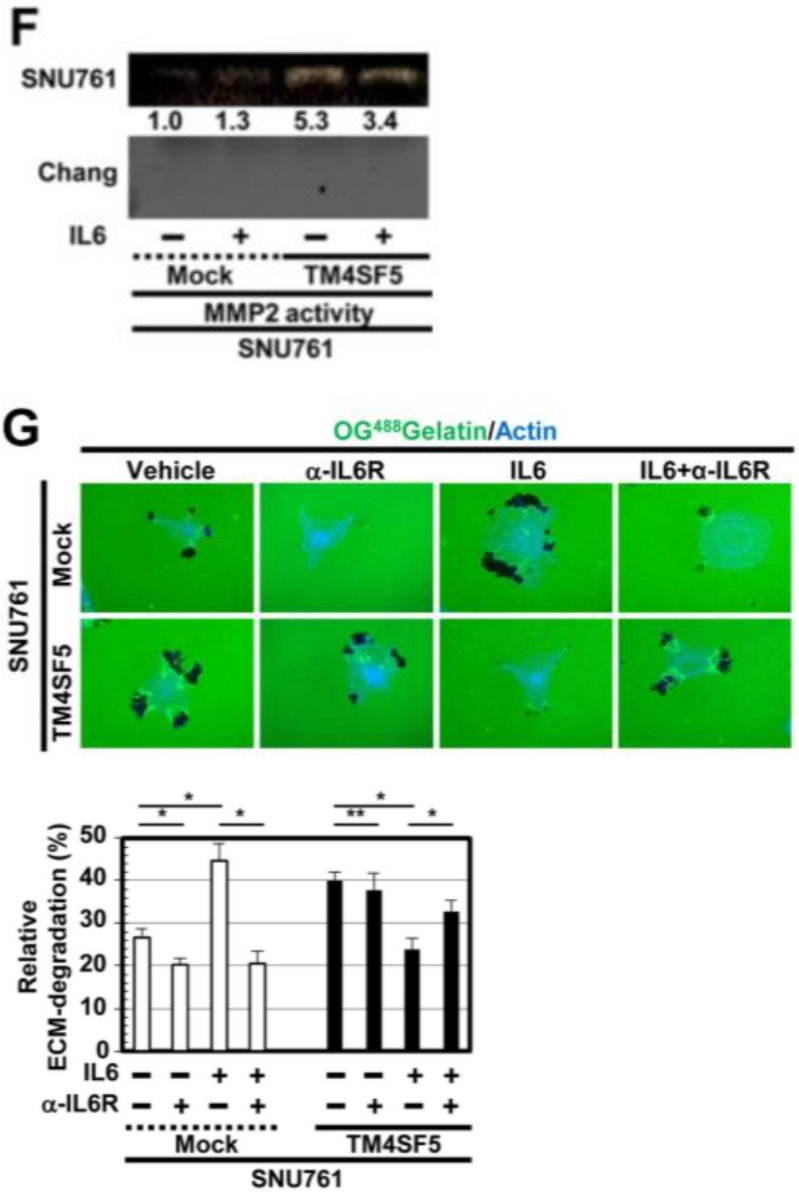
F
SNU761
1.0 1.3 5.3 3.4
Chang
IL6
– + – +
Mock
TM4SF5
MMP2 activity
SNU761
G
OG488Gelatin/Actin
Vehicle
α-IL6R
IL6
IL6+α-IL6R
SNU761
Mock
TM4SF5
Relative ECM-degradation (%)
50
40
30
20
10
0
IL6 – – + + – – + +
α-IL6R – + – + – + – +
Mock
TM4SF5
SNU761

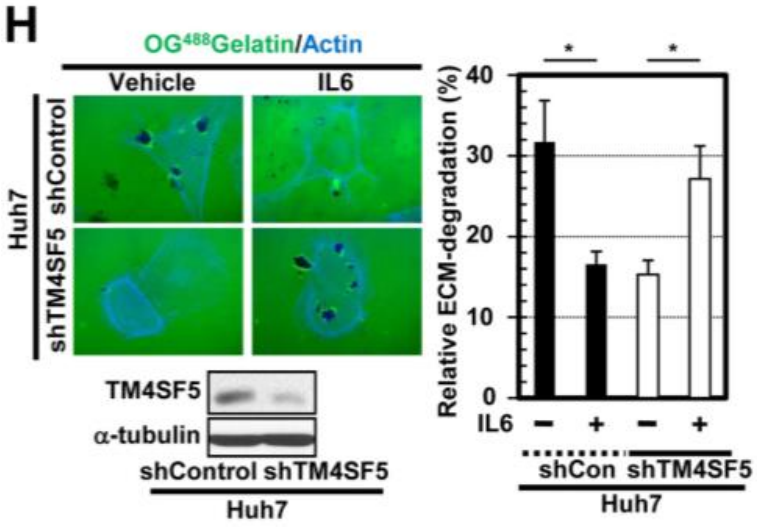
H
OG488Gelatin/Actin
Vehicle
IL6
Huh7
shControl
shTM4SF5
TM4SF5
α-tubulin
shControl shTM4SF5
Huh7
Relative ECM-degradation (%)
40
30
20
10
0
*
*
IL6 − + − +
shCon shTM4SF5
Huh7

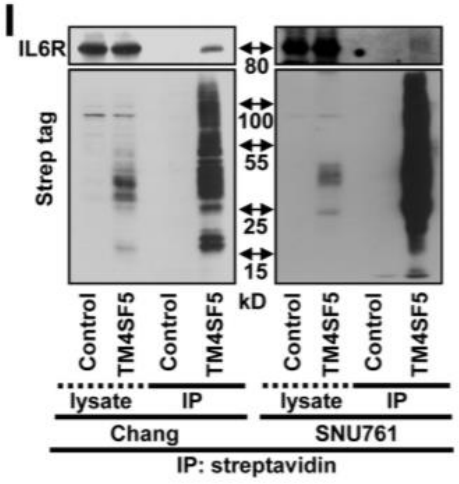
I
IL6R
Strep tag
80
100
55
25
15
kD
Control
TM4SF5
Control
TM4SF5
Control
TM4SF5
Control
TM4SF5
lysate
IP
lysate
IP
Chang
SNU761
IP: streptavidin

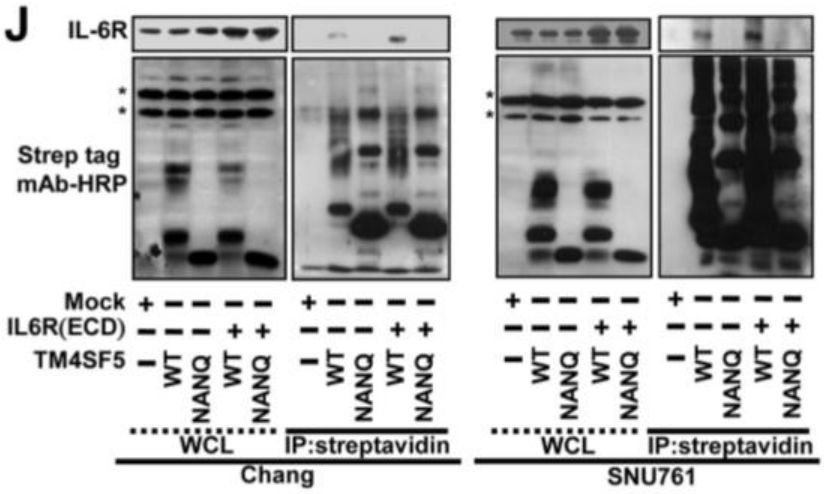
J
IL-6R
Strep tag
mAb-HRP
Mock
IL6R(ECD)
TM4SF5
WT
NANQ
WT
NANQ
WCL
IP:streptavidin
Chang
SNU761

Fig. Ⅱ-3. **IL-6 treatment of cells differentially regulates migration and invasive ECM degradation depending on TM4SF5 expression.** (A to C) The migrations of Chang (A) and SNU761 (B) cells preincubated without or with anti-IL-6R antibody (α-IL-6R; 20 μg/ml) in suspension at 37℃ for 1 h or of HCC827 cells (C) stably expressing TM4SF5 or mock transfected were analyzed using Transwell chambers in the presence or absence of IL-6. (D to H) Cells were cultured on cover glasses precoated with Oregon Green 488-conjugated gelatin and were treated with either vehicle or 50 ng/ml IL-6 for 4h prior to fluorescence imaging. The dark spots indicate ECM degradation, and 10 random regions were imaged under each set of experimental conditions; the means ± standard deviations for the relative ECM degradation are shown in percentages. (E) Conditioned media from the cultures of cells lacking (mock) or ectopically expressing FLAG-TM4SF5 (TM4SF5) in the absence(-) or presence(+) of IL-6 (10 μg/ml) were collected and concentrated before analysis of MMP2 activity by gelatin zymography. (G) Neutralizing anti-IL-6R antibody (20 μg/ml) was added to the cells before analysis. In panels A to D and E to H, one or two asterisks depict statistically significant or insignificant differences, respectively. (I and J) Whole-cell lysates prepared from cells transfected with control-Strep (Control), TM4SF5 WT-Strep (TM4SF5 WT), or TM4SF5 N138A/N155Q-Strep (NANQ) mutant with or without cotransfection of IL-6R (ECD) for 48h were immunoprecipitated (IP)

with streptavidin before immunoblotting using the anti-Strep-tag monoclonal antibody (MAb) conjugated to horse radish peroxidase or an anti-IL-6R antibody. The asterisks in panel J denote nonspecific bands by the anti-Strep tag MAb–horseradish peroxidase (HRP) antibody. The data represent three isolated experiments. shControl, short hairpin control RNA; shTM4SF5, short hairpin TM4SF5 RNA; WCL, whole-cell lysate.

4. Suppression of JAK/STAT3 signaling inhibited IL-6-mediated FAK phosphorylation in Chang-TM4SF5 cells, but it did not recover the IL-6-suppressed FAK phosphorylation in SNU761-TM4SF5 cells.

We next explored whether the suppression or inhibition of JAK/STAT3 signaling affected the TM4SF5 dependent FAK phosphorylation. STAT3 suppression, through introduction of siSTAT3, did not significantly alter the FAK activity in the Chang-mock cells compared to that of the nonsuppressed cells (Fig. 4A, lanes 1 to 3 and 7 to 9). However, STAT3 suppression in the Chang-TM4SF5 cells abolished IL-6-mediated enhancement of FAK activity (Fig.4A, lane 6 versus 12); the IL-6/STAT3 signaling pathway did not affect the basal FAK activity (TM4SF5 independent) of the Chang-mock cells but enhanced the TM4SF5-dependent FAK activity of the Chang-TM4SF5 cells. Additionally, pharmacological inhibition of JAK2 using the AG490 inhibitor blocked the IL-6-mediated FAK activity in both the Chang-mock and Chang-TM4SF5 cell lines (Fig.4B, lanes3, 6, 7, 10, 13, and 14). This discrepancy in FAK activities between IL-6-treated Chang-mock cells following STAT3 suppression (Fig. 4A lane 9) and IL-6-treated Chang-mock cells following JAK2 inhibition (Fig.4B. lane7) may reflect nonspecific effects of AG490 on FAK activity, in contrast to the effects observed after siRNA-based specific suppression of STAT3. Furthermore, STAT3 suppression or AG490 treatment in the SNU761-TM4SF5 cells did not recover the FAK activity that was

inhibited by IL-6 treatment (Fig. 4C and D). IL-6-independent pY^{705} STAT3 was undetectable in the SNU761-TM4SF5 cells kept in suspension after STAT3 suppression or AG490 treatment (Fig. 4C and D, lanes 1 and 4), indicating that the IL-6-independent STAT3 activity in the SNU761 cancer cells was obvious, dependent on STAT3 level and JAK2 activity, and presumably competitive with adhesion dependent TM4SF5/FAK activity.

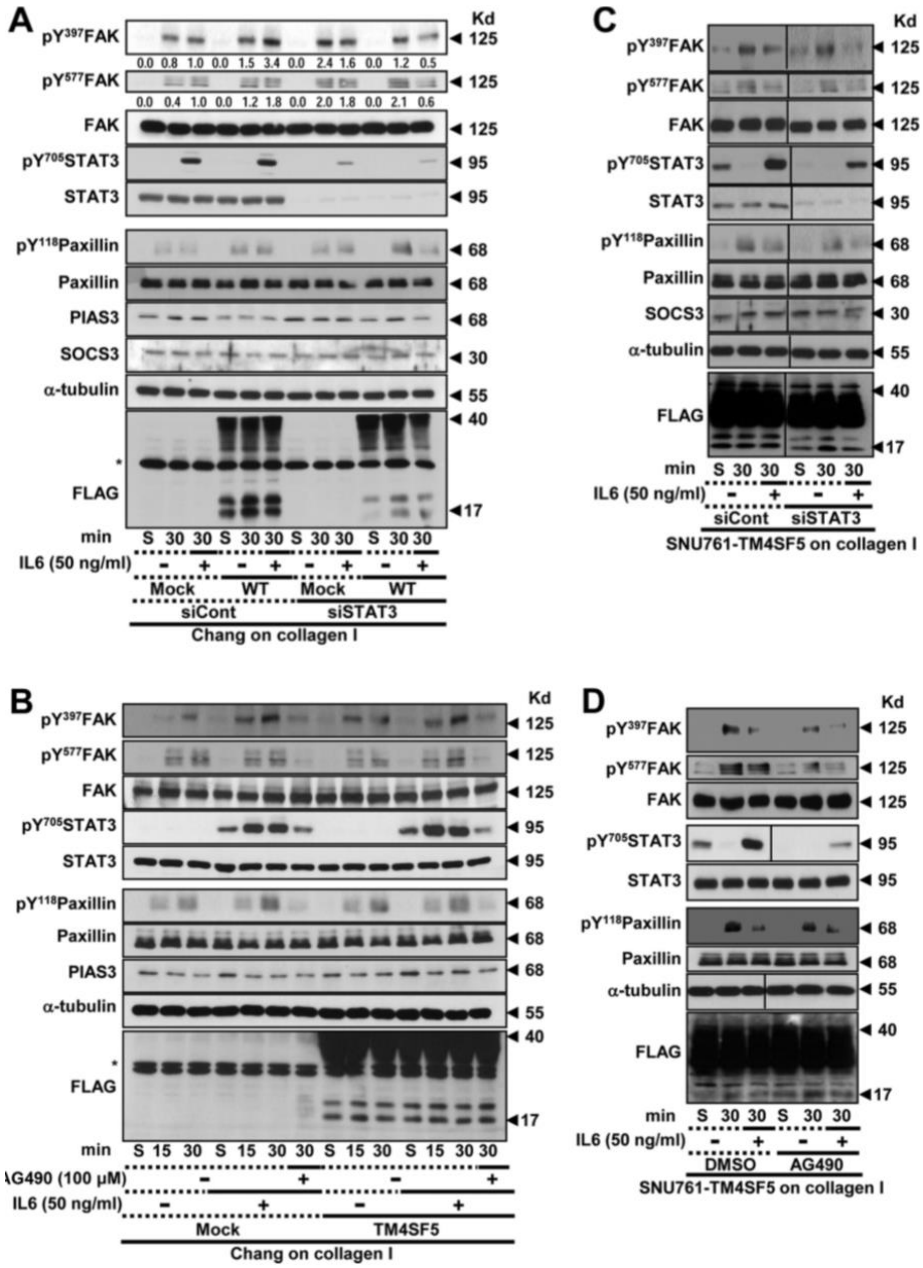
A
pY397FAK
pY577FAK
FAK
pY705STAT3
STAT3
pY118Paxillin
Paxillin
PIAS3
SOCS3
α-tubulin
FLAG
Kd
125
95
68
55
40
30
17
min
IL6 (50 ng/ml)
Mock
WT
siCont
siSTAT3
Chang on collagen I
B
AG490 (100 μM)
TM4SF5
C
SNU761-TM4SF5 on collagen I
D
DMSO
AG490

Fig Ⅱ-4. Suppression of STAT3/JAK signaling inhibited IL-6-mediated FAK phosphorylation of Chang-TM4SF5 cells but did not recover IL-6-suppressed FAK phosphorylation of SNU761-TM4SF5 cells. Cells were manipulated, as explained in the legend to Fig. 2, after transfection of siRNA against control sequence (siCont) or siSTAT3 for 48 h or after AG490 (a specific JAK2 inhibitor) treatment in the middle of the rolling step. The asterisks in panels A and C depict nonspecific bands to anti-FLAG antibody. S, suspension. Data represent three independent experiments.

5. STAT3 suppression inhibited IL-6-mediated FA formation by Chang-TM4SF5 cells but did not recover the IL-6-suppressed FA formation and ECM degradation by SNU761-TM4SF5 cells.

The effects of STAT3 suppression on FA formation and ECM degradation were examined next. To mark the siSTAT3-transfected cells, siSTAT3 was cotransfected with a GFP-conjugated siRNA control that forms foci in perinuclear regions [25]. Transfection of Chang cells with siControl did not alter FA formation, regardless of IL-6 treatment, compared to FA formation by untransfected cells (Fig. 5A, upper), and the Chang-mock cells after STAT3 suppression did not alter FA formation regardless of IL-6 treatment (Fig. 5A, lower). However, STAT3 suppression in the Chang-TM4SF5 cells decreased FA formation upon IL-6 treatment (Fig. 5A, lower, cells marked by an arrow), although the siSTAT3-untransfected Chang-TM4SF5 cells showed an obvious increaseinTM4SF5-mediated FA formation upon IL-6 treatment (Fig. 5A, lower, cells without an arrow). In addition, SNU761-mock cells that were transfected with siControl still exhibited enhanced FA formation in response to IL-6 treatment, whereas siControl-transfected SNU761-TM4SF5 cells exhibited reduced FA formation upon IL-6 treatment (Fig. 5B, upper), as shown in Fig. 2F. STAT3 suppression in the SNU761 mock cells did not alter IL-6-mediated FA formation compared with FA formation by nonsuppressed cells (Fig. 5B, 3rd row). STAT3 suppression in SNU761-TM4SF5 cells did

not alter the IL-6-mediated decrease in FA formation; in other words, IL-6 treatment also decreased FA formation in the cells in which STAT3 had been suppressed (Fig. 5B, lower right, arrow), similar to nonsuppressed cells (Fig. 5B, lower, no arrow). Statistically, STAT3 silencing in Chang-TM4SF5 blocked and decreased spreading and FA formation upon IL-6 treatment (Fig.5C, upper, bars 7 and 8), but STAT3 silencing in SNU761-TM4SF5 did not change the IL-6-mediated decrease in spreading and FA formation (Fig. 5C, lower, bars 7 and 8). The importance of STAT3 for the IL-6-mediated FA formation in normal hepatocytes was confirmed with mouse normal AML12 hepatocytes (Fig.5D), whereas a STAT3-independent decrease in FA formation upon IL-6 treatment of TM4SF5-expressing cancer cells also was verified with NSCLC HCC827 cells stably expressing TM4SF5 (Fig. 5E). Furthermore, STAT3 suppression in the SNU761-TM4SF5 cells resulted in no ECM degradation following IL-6 treatment, again similar to the behavior of nonsuppressed cells (Fig. 5F).

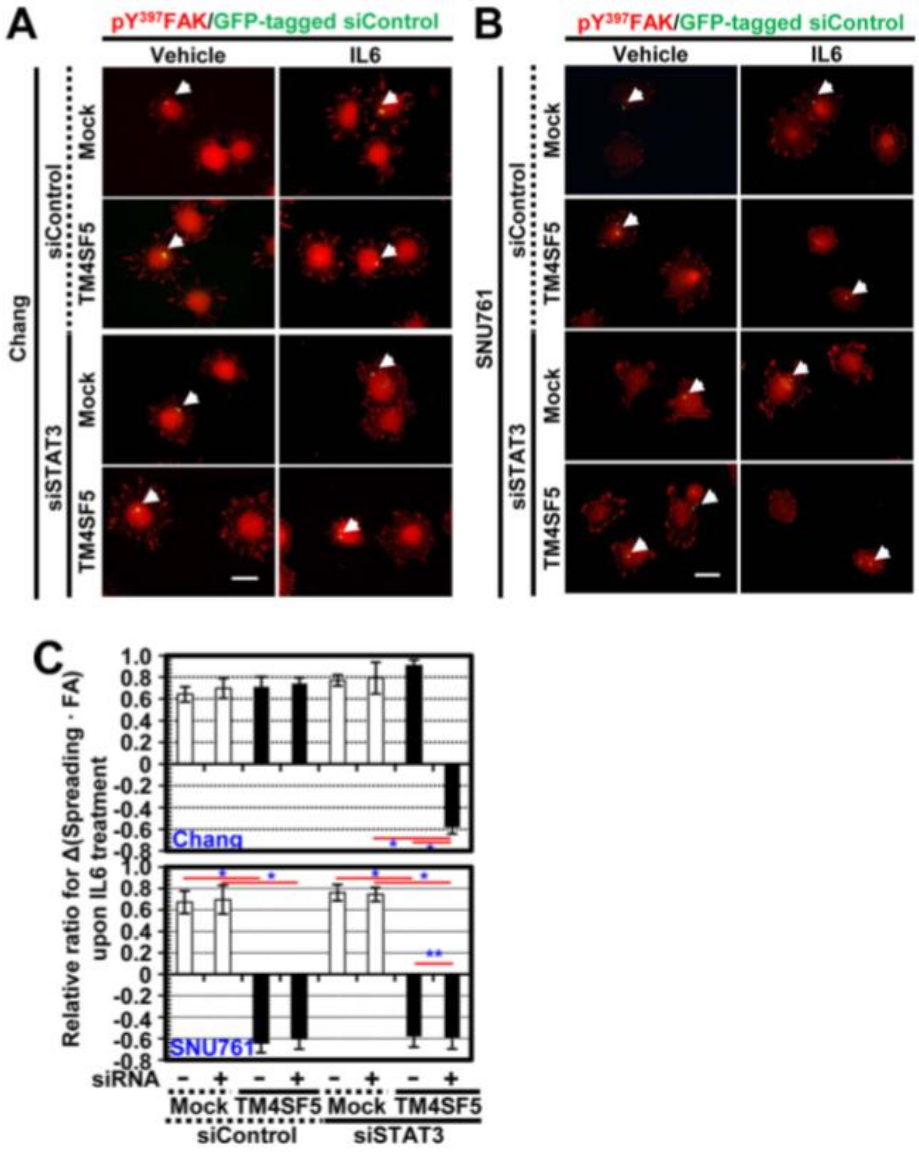
A
pY397FAK/GFP-tagged siControl
Vehicle
IL6
Chang
siControl
siSTAT3
Mock
TM4SF5
Mock
TM4SF5
B
pY397FAK/GFP-tagged siControl
Vehicle
IL6
SNU761
siControl
siSTAT3
Mock
TM4SF5
Mock
TM4SF5
C
Relative ratio for Δ(Spreading · FA) upon IL6 treatment
1.0
0.8
0.6
0.4
0.2
0
-0.2
-0.4
-0.6
-0.8
Chang
SNU761
siRNA
- + - + - + - +
Mock TM4SF5 Mock TM4SF5
siControl
siSTAT3

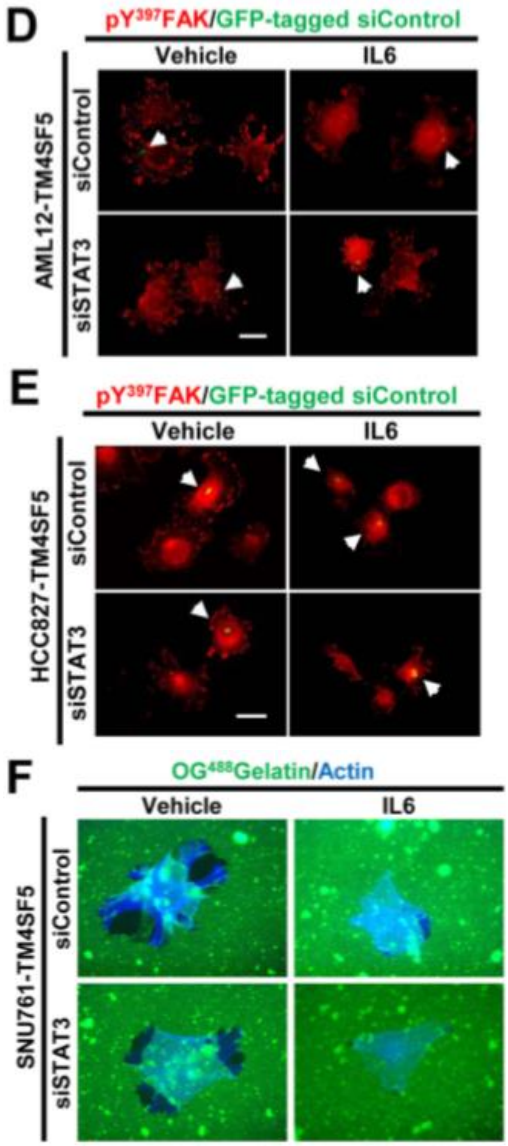
D
pY397FAK/GFP-tagged siControl
Vehicle
IL6
AML12-TM4SF5
siControl
siSTAT3
E
pY397FAK/GFP-tagged siControl
Vehicle
IL6
HCC827-TM4SF5
siControl
siSTAT3
F
OG488Gelatin/Actin
Vehicle
IL6
SNU761-TM4SF5
siControl
siSTAT3

Fig Ⅱ-5. STAT3 suppression inhibited IL-6-mediated FA formation by Chang-TM4SF5 cells but did not recover the IL-6-suppressed FA formation and ECM degradation by SNU761-TM4SF5 cells. (A to E) Normal Chang (A and C), AML12-TM4SF5 (D), cancerous SNU761 (B and C), or HCC827-TM4SF5 (E) cells transiently transfected with siRNAs (either siControl or siSTAT3 together with the GFP-tagged siControl) were immunostained for pY^{397} FAK (red) following treatment with vehicle or IL-6, as explained in the legend to Fig.2. The arrowheads indicate the GFP-tagged siRNA cotransfected with siControl or siSTAT3. (C) Randomly saved images for 10 fields in each experimental condition were quantitated as explained in the legend to Fig.2E. One or two asterisks depict statistically significant or insignificant differences, respectively. (F) SNU761-TM4SF5 cells transfected with siControl or siSTAT3 were analyzed for ECM degradation following vehicle or IL-6 treatment for 4 h, as explained in the legend to Fig. 3. The data shown represent three different experiments.

6. Inhibition of FAK activity did not alter IL-6-mediated pY^{705} STAT3 in Chang or SNU761 cells.

We next wondered whether FAK affected STAT3 phosphorylation. To test this, we used the specific FAK inhibitor PF271 [10]. FAK inhibition in Chang cells did not alter pY^{705} STAT3 or its translocation into the nucleus under any circumstances, although FAK activity and FA formation were decreased (Fig. 6A and B). Furthermore, the SNU761 TM4SF5 cells did not show any change in pY^{705} STAT3 levels or nuclear localization, even after FAK inhibition; however, FAK activity, FA formation, and ECM degradation were diminished after treatment with the inhibitor (Fig. 6C, D, and E). These data support the hypothesis that FAK does not function in the regulation of IL-6/STAT3 signaling.

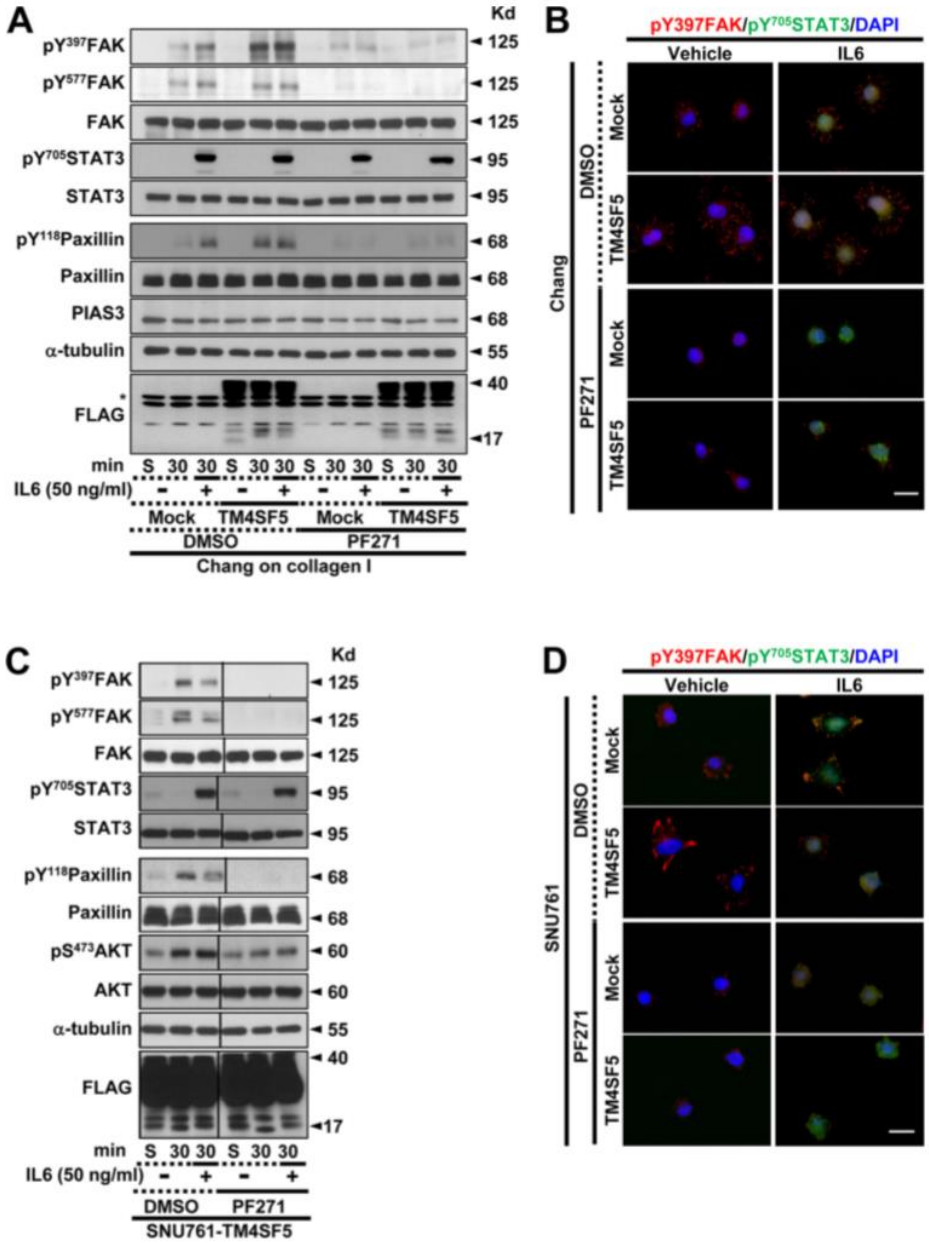
A
Kd
pY397FAK
pY577FAK
FAK
pY705STAT3
STAT3
pY118Paxillin
Paxillin
PIAS3
α-tubulin
FLAG
125
125
125
95
95
68
68
68
55
40
17
min S 30 30 S 30 30 S 30 30 S 30 30
IL6 (50 ng/ml) - + - + - + - +
Mock TM4SF5 Mock TM4SF5
DMSO PF271
Chang on collagen I
B
pY397FAK/pY705STAT3/DAPI
Vehicle
IL6
Chang
DMSO
PF271
Mock
TM4SF5
Mock
TM4SF5
C
Kd
pY397FAK
pY577FAK
FAK
pY705STAT3
STAT3
pY118Paxillin
Paxillin
pS473AKT
AKT
α-tubulin
FLAG
125
125
125
95
95
68
68
60
60
55
40
17
min S 30 30 S 30 30
IL6 (50 ng/ml) - + - +
DMSO PF271
SNU761-TM4SF5
D
pY397FAK/pY705STAT3/DAPI
Vehicle
IL6
SNU761
DMSO
PF271
Mock
TM4SF5
Mock
TM4SF5

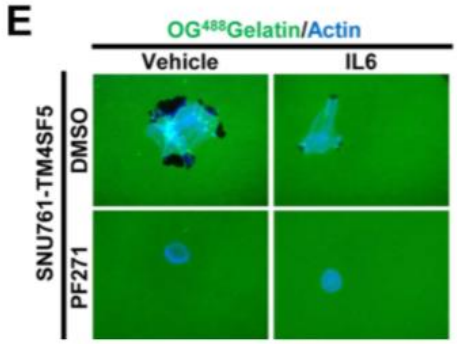
E
OG488Gelatin/Actin
Vehicle
IL6
SNU761-TM4SF5
DMSO
PF271

Fig. Ⅱ-6. Inhibition of FAK activity did not alter IL-6-mediated pY^{705} STAT3 in Chang or SNU761 cells.

The cells were manipulated as explained in the legend to Fig.2 and were treated with or without PF271 (a specific FAK inhibitor) prior to being kept in suspension(S) or reseeding onto collagen I-precoated dishes. The cells were treated with IL-6 when they were reseeded. The cells were harvested for immunoblot analysis (A and C) or were immunostained for pY^{397} FAK (red) and pY^{705} STAT3 (green); the nuclei were counterstained with DAPI (blue) (B and D). The asterisk in panel A denotes nonspecific bands by the anti-FLAG antibody. (E) SNU761-TM4SF5 cells were cultured on OG^{488}-conjugated gelatin for 4 h in the presence or absence of DMSO or PF271 together with vehicle or IL-6. Visualization of ECM-degraded black spots around cells (stained with actin; blue) using an immunofluorescence microscope then was performed to save at least 10 independent images for each experimental condition. Representative images are shown. The data shown represent three independent experiments.

4. Discussion

This study shows that forced expression of TM4SF5 reduced expression of the cytokine IL-6 in cancerous hepatocytes compared to TM4SF5-null cancer cells but increased IL-6 expression in normal Chang hepatocytes. IL-6/STAT3 signaling activity appeared to promote FAK activity in Chang or AML12 normal cells but blocked FAK activity in SNU761, Huh7, and HCC827 cancer cells. Furthermore, TM4SF5 expression in cancer cells but not in normal cells caused an increase in IL-6-independent pY^{705} STAT3 under suspended conditions which declined following cell adhesion to ECM, indicating TM4SF5-mediated aberrant STAT3 activation that is competitive with adhesion-dependent FAK activity. However, in both the Chang and SNU761 cell lines, FAK activity did not affect IL-6-dependent pY^{705} STAT3. The enhanced IL-6 expression in the Chang cells might regulate homeostatic cell functions, such as migration, whereas reduced IL-6 expression and enhanced FAK activity upon TM4SF5 expression in the SNU761 cancer cells might allow the cells to escape from IL-6/ STAT3-mediated immune activity. Thus, in cancer cells, TM4SF5 plays a tumorigenic role by promoting immune escape (Fig. 7). TM4SF5, a member of the tetraspan(in) family [9], is overexpressed in various cancers, including liver cancers [20]. TM4SF5 can localize to tetraspanin-enriched microdomains (TEMs) [26], where tetraspan(in)s form complexes with other tetraspan(in)s, integrins, or growth

factor receptors [27] and transduce signals that lead to a diverse set of cellular functions. TM4SF5 collaborates with integrins and regulates cell migration and invasion [28]. In addition, the cytosolic region of TM4SF5 interacts with and activates FAK and c-Src, promoting directional migration and invasive protrusions [10, 29]. Therefore, TM4SF5-mediated FAK activation can be critical during tumor progression [8]. Given the influence of extracellular cues on cancer cell behavior, the TM4SF5-mediated activation of FAK/c-Src can be compromised by the activity of soluble extracellular factors. Although immune cell-produced cytokines can affect the behavior of cancer cells, it is also known that cancer cells themselves express cytokines that can exert autocrine effects [14]. The current study showed that IL-6/STAT3 signaling might play different roles depending on the degree of malignancy of the hepatocytes. IL-6 has either pro- or anti-inflammatory roles during liver disease [30], and IL6-mediated JAK/STAT3 signaling activity either inhibits or promotes breast tumorigenesis [19]. Therefore, reduced IL-6 expression could be a strategy by which TM4SF5-positive tumors avoid IL-6-mediated anti tumorigenic immunological actions. Furthermore, enhanced IL-6 levels in the Chang-TM4SF5 cells correlated with adhesion-mediated FAK activity and migration, so that crosstalk between the (ectopic) TM4SF5-FAK and IL-6-STAT3 signaling pathways in normal hepatocytes supports homeostatic migration-related signaling activity, although normal hepatocytes only minimally express TM4SF5 [20]. The preincubation of TM4SF5null SNU761

cells with anti-IL-6R antibody reduced migration and invasive ECM degradation, but the antibody preincubation of SNU761-TM4SF5 cells did not change the TM4SF5-dependent migration and invasion capacities. These observations suggested roles of IL-6 endogenously expressed in TM4SF5-null cells that are more important than those in TM4SF5-positive cancer cells, which is shown in the antibody array in Fig.1. Meanwhile, normal or cancer cells with or without TM4SF5 expression showed comparable signaling activities for expression of certain genes downstream of IL-6/IL-6R, suggesting that certain signaling pathways in the cells emanated by the IL-6/IL-6R system were comparably intact. In contrast, adhesion-enhanced FAK activity in the SNU761-TM4SF5 cells was inhibited by IL-6 treatment, indicating that IL-6-mediated regulation of TM4SF5-FAK signaling would not occur because of the reduced IL-6 expression, leading to immunological escape; however, the roles played by immune cell-secreted IL-6 should be considered further. Diverse tumors have enhanced STAT3 activity [31]. Here, STAT3 was shown to be overactivated in suspended SNU761cells even in the absence of IL-6 but not in normal Chang hepatocytes. Furthermore, TM4SF5 was shown to interact with IL-6R, and the interaction appeared to be through their extracellular domains, especially extracellular loop 2, containing N-glycosylation residues, in the case of TM4SF5. These results suggest that the IL-6R/ STAT3 pathway is activated by TM4SF5 even in the absence of ligand binding. TM4SF5 causes Tyr845 phosphorylation of enhanced growth

factor receptor (EGFR) via TM4SF5-mediated c-Src activation even in the absence of EGF [29]. The ligands for most TM4SFs, including TM4SF5, currently are not known. TM4SF5 associates with integrins [8], and interactions between tetraspanins and integrins can regulate integrin functions [7]. These observations suggest that interaction with TM4SF5 mimics ligand binding to IL-6R. Interestingly, the IL-6-independent STAT3 activity appeared to be negatively correlated with FAK activity in the SNU761-TM4SF5 cells. FAK is also hyperactivated in TM4SF5-positive liver cancer cells [10, 20]. Therefore, FAK downstream of TM4SF5 might compete with IL-6-independent STAT3 activity; however, FAK did not affect IL-6-dependent STAT3activity. Growth hormone-mediated FAK activity in CHO cells is not required for STAT3-mediated transcription [32]. Therefore, during TM4SF5-mediated tumorigenesis, a balance between TM4SF5-mediated FAK and STAT3 signaling activity can be subtly modulated. It is currently unknown how TM4SF5 in liver cancer cells activates STAT3 in the absence of IL-6. The negative regulators of STAT3, such as PIAS3 and SOCS3 [31], do not seem to be involved in IL-6-dependent and -independent STAT3 activation in SNU761 cells under the experimental conditions we used, as PIAS3 and SOCS3 levels did not correlate with pY^{705} STAT3 levels. Therefore, instead of the negative regulators, the upstream tyrosine kinases may contribute to the overactivation of STAT3 in TM4SF5-positive cancers. EGF/EGFR activates STAT3, but it does not lead to mitogenic effects [33], and fibronectin-initiated

adhesion activates STAT3, leading to epithelial-mesenchymal transition (EMT) by EGFR-dependent and -independent mechanisms [34]. Interestingly, both FAK and EGFR can associate with TM4SF5 [10, 35]. TM4SF5-mediated c-Src activity [29] also may be a candidate for causing STAT3 overactivation, as c-Src is upstream of STAT3 [36]. Therefore, IL-6-independent STAT3 activation may involve various molecules in TM4SF5-expressing hepatic cancer cells. Because JAK2 inhibition abolished IL-6-independent pY^{705} STAT3 in the SNU761-TM4SF5 cells, presumably integrin/ECM engagement-mediated FAK/JAK2 activity would lead to STAT3 activity [34]. FAK and STAT3 activities in Chang cells did not promote ECM degradation, although the activities in SNU761 cells correlated with migration and invasive ECM degradation. Thus, during TM4SF5-mediated tumor progression, FAK and STAT3 activities can regulate metastatic potentials, presumably via their cross talk during communication between TM4SF5-positive cancer cells and extracellular cues, such as IL-6.

5. Conclusion

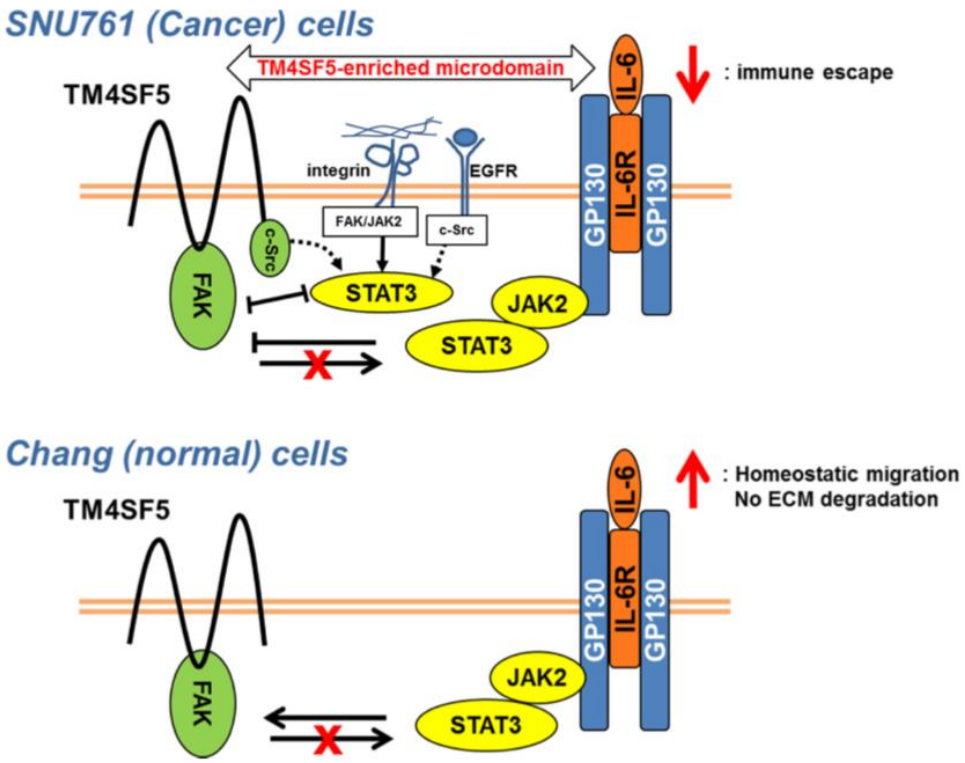

Fig. Ⅱ-7 Crosstalk between the TM4SF5/FAK and IL-6/STAT3 pathways.

In normal and cancerous hepatocytes lacking TM4SF5 expression, IL-6 treatment causes FAK activation (not depicted). TM4SF5-expressing cancer cells exhibited IL-6-independent and -dependent STAT3 activity. IL-6-independent pY^{705} STAT3 presumably is influenced by the FAK/c-Src signaling activity caused by the membrane receptors within the TM4SF5-

enriched microdomain and is competitive with TM4SF5-mediated FAK activity in adhered cells [10]. (Top) IL-6-dependent STAT3 activity in the TM4SF5-positive cancer cells negatively regulates adhesion- and TM4SF5-dependent FAK activity. However, TM4SF5-expressing cancer cells express less IL-6 than TM4SF5-null cells, presumably leading to TM4SF5-mediated immune escape. (Bottom) In normal Chang-TM4SF5 cells, IL-6-dependent STAT3 activity results in TM4SF5/FAK activity and migration, suggesting a regulatory role for IL-6 in homeostatic migration but not in invasive ECM degradation. In both cell lines, FAK activity does not modulate IL-6-dependent STAT3 activity.

6. Reference

1. Yamaguchi H, Condeelis J. 2007. Regulation of the actin cytoskeleton in cancer cell migration and invasion. Biochim. Biophys. Acta 1773:642– 652. http://dx.doi.org/10.1016/j.bbamcr.2006.07.001.

2. Friedl P, Wolf K. 2009. Proteolytic interstitial cell migration: a five-step process. Cancer Metastasis Rev. 28:129–135. http://dx.doi.org/10.1007 /s10555-008-9174-3.

3. Luo M, Guan JL. 2010. Focal adhesion kinase: a prominent determinant in breast cancer initiation, progression and metastasis. Cancer Lett. 289: 127–139. http://dx.doi.org/10.1016/j.canlet.2009.07.005.

4. Chen JS, Huang XH, Wang Q, Chen XL, Fu XH, Tan HX, Zhang LJ, Li W,BiJ.2010. FAK is involved in invasion and metastasis of hepatocellular carcinoma. Clin. Exp. Metastasis 27:71–82. http://dx.doi.org/10.1007 /s10585-010-9306-3.

5. McLean GW, Carragher NO, Avizienyte E, Evans J, Brunton VG, Frame MC. 2005. The role of focal-adhesion kinase in cancer–a new therapeutic opportunity. Nat. Rev. Cancer 5:505–515.

http://dx.doi.org/10.1038 /nrc1647.

6. Zhao J, Guan JL. 2009. Signal transduction by focal adhesion kinase in cancer. Cancer Metastasis Rev. 28:35–49. http://dx.doi.org/10.1007 /s10555-008-9165-4.

7. Berditchevski F. 2001. Complexes of tetraspanins with integrins: more than meets the eye. J. Cell Sci. 114:4143–4151.

8. Lee SA, Park KH, Lee JW. 2011. Modulation of signaling between TM4SF5 and integrins in tumor microenvironment. Front. Biosci. 16: 1752–1758. http://dx.doi.org/10.2741/3818.

9. Wright MD, Ni J, Rudy GB. 2000. The L6 membrane proteins–a new four-transmembrane superfamily. Protein Sci. 9:1594–1600. http://dx .doi.org/10.1110/ps.9.8.1594.

10. Jung O, Choi S, Jang SB, Lee SA, Lim ST, Choi YJ, Kim HJ, Kim DH, Kwak TK, Kim H, Kang M, Lee MS, Park SY, Ryu J, Jeong D, Cheong HK, Park KH, Lee BJ, Schlaepfer DD, Lee JW. 2012. Tetraspan TM4SF5 dependent direct activation of FAK and metastatic potential of hepatocarcinoma cells. J. Cell Sci. 125:5960–5973. http://dx.doi.org/10.1242/jcs .100586.

11. Dougan M, Dranoff G. 2009. Immune therapy for cancer. Annu. Rev.

Immunol. 27:83–117. http://dx.doi.org/10.1146/annurev.immunol .021908.132544.

12. Sansone P, Bromberg J. 2011. Environment, inflammation, and cancer. Curr. Opin. Genet. Dev. 21:80–85. http://dx.doi.org/10.1016/j.gde.2010 .11.001.

13. Kishimoto T. 2005. IL-6: from laboratory to bedside. Clin. Rev. Allergy Immunol. 28:177–186. http://dx.doi.org/10.1385/CRIAI:28:3:177.

14. Waldner MJ, Foersch S, Neurath MF. 2012. Interleukin-6–a key regulator of colorectal cancer development. Int.J.Biol.Sci.8:1248–1253.http: //dx.doi.org/10.7150/ijbs.4614.

15. Yamamoto K, Rose-John S. 2012. Therapeutic blockade of interleukin-6 in chronic inflammatory disease. Clin. Pharmacol. Ther. 91:574–576. http://dx.doi.org/10.1038/clpt.2012.11.

16. Carbia-Nagashima A, Arzt E. 2004. Intracellular proteins and mechanisms involved in the control of gp130/JAK/STAT cytokine signaling. IUBMB Life 56:83–88.http://dx.doi.org/10.1080/15216540410001668064.

17. Rebouissou S, Amessou M, Couchy G, Poussin K, Imbeaud S, Pilati

C, Izard T, Balabaud C, Bioulac-Sage P, Zucman-Rossi J. 2009. Frequent in-frame somatic deletions activate gp130 in inflammatory hepatocellular tumours. Nature 457:200–204. http://dx.doi.org/10.1038/nature07475.

18. Pilati C, Amessou M, Bihl MP, Balabaud C, Van Nhieu JT, Paradis V, Nault JC, Izard T, Bioulac-Sage P, Couchy G, Poussin K, Zucman-Rossi J. 2011. Somatic mutations activating STAT3 in human inflammatory hepatocellular adenomas. J. Exp. Med. 208:1359–1366. http://dx.doi.org /10.1084/jem.20110283.

19. Dethlefsen C, Hojfeldt G, Hojman P. 2013. The role of intratumoral and systemic IL-6 in breast cancer. Breast Cancer Res. Treat. 138:657–664. http://dx.doi.org/10.1007/s10549-013-2488-z.

20. Lee SA, Lee SY, Cho IH, Oh MA, Kang ES, Kim YB, Seo WD, Choi S, Nam JO, Tamamori-Adachi M, Kitajima S, Ye SK, Kim S, Hwang YJ, Kim IS, Park KH, Lee JW. 2008. Tetraspanin TM4SF5 mediates loss of contact inhibition through epithelial-mesenchymal transition in human hepatocarcinoma. J. Clin. Investig. 118:1354–1366. http://dx.doi.org/10 .1172/JCI33768.

21. Pasapera AM, Schneider IC, Rericha E, Schlaepfer DD, Waterman CM. 2010. Myosin II activity regulates vinculin recruitment to focal

adhesions through FAK-mediated paxillin phosphorylation. J. Cell Biol. 188:877– 890. http://dx.doi.org/10.1083/jcb.200906012.

22. Lee SA, Kim TY, Kwak TK, Kim H, Kim S, Lee HJ, Kim SH, Park KH, Kim HJ, Cho M, Lee JW. 2010. Transmembrane 4 L six family member 5(TM4SF5) enhances migration and invasion of hepatocytes for effective metastasis. J. Cell. Biochem. 111:59–66. http://dx.doi.org/10.1002/jcb .22662.

23. Bournazou E, Bromberg J. 2013. Targeting the tumor microenvironment: JAK-STAT3 signaling. JAKSTAT 2:e23828. http://dx.doi.org/10 .4161/jkst.23828.

24. Yu H, Pardoll D, Jove R. 2009. STATs in cancer inflammation and immunity: a leading role for STAT3. Nat. Rev. Cancer 9:798–809. http: //dx.doi.org/10.1038/nrc2734.

25. Kim H, Kang M, Lee SA, Kwak TK, Jung O, Lee HJ, Kim SH, Lee JW. 2010.TM4SF5 accelerates G1/S phase progression via cytosolic p27(Kip1) expression and Rho A activity. Biochim. Biophys. Acta 1803:975–982. http://dx.doi.org/10.1016/j.bbamcr.2010.04.001.

26. Yanez-Mo M, Barreiro O, Gordon-Alonso M, Sala-Valdes M, SanchezMadrid F. 2009. Tetraspanin-enriched microdomains: a functional unit in cell plasma membranes. Trends Cell Biol. 19:434–

446. http://dx.doi .org/10.1016/j.tcb.2009.06.004.

27. Zoller M. 2009. Tetraspanins: push and pull in suppressing and promoting metastasis. Nat. Rev. Cancer 9:40–55. http://dx.doi.org/10.1038 /nrc2543.

28. Lee SA, Kim YM, Kwak TK, Kim HJ, Kim S, Kim SH, Park KH, Cho M, LeeJW. 2009. The extracellular loop 2 of TM4SF5 inhibits integrin alpha2 on hepatocytes under collagen type I environment. Carcinogenesis 30: 1872–1879. http://dx.doi.org/10.1093/carcin/bgp234.

29. Jung O, Choi YJ, Kwak TK, Kang M, Lee MS, Ryu J, Kim HJ, Lee JW. 2013. TheCOOH-terminus of TM4SF5 in hepatoma cell lines regulates c-Src to form invasive protrusions via EGFR Tyr845 phosphorylation. Biochim. Biophys. Acta 1833:629–642. http://dx.doi.org/10.1016/j .bbamcr.2012.11.026.

30. Tilg H, Kaser A, Moschen AR. 2006. How to modulate inflammatory cytokines in liver diseases. Liver Int. 26:1029–1039. http://dx.doi.org/10 .1111/j.1478-3231.2006.01339.x.

31. Wang X, Crowe PJ, Goldstein D, Yang JL. 2012. STAT3 inhibition, a novel approach to enhancing targeted therapy in human cancers. Int. J. Oncol. 41:1181–1191. http://dx.doi.org/10.3892/ijo.2012.1568.

32. ZhuT, GohEL, LobiePE. 1998. Growth hormone stimulates the tyrosine phosphorylation and association of p125 focal adhesion kinase (FAK) with JAK2. Fak is not required for stat-mediated transcription. J. Biol. Chem. 273:10682–10689. http://dx.doi.org/10.1074/jbc.273.17.10682.

33. Guren TK, Abrahamsen H, Thoresen GH, Babaie E, Berg T, Christoffersen T. 1999. EGF-induced activation of Stat1, Stat3, and Stat5b is unrelated to the stimulation of DNA synthesis in cultured hepatocytes. Biochem. Biophys. Res. Commun. 258:565–571. http://dx.doi.org/10 .1006/bbrc.1999.0684.

34. Balanis N, Wendt MK, Schiemann BJ, Wang Z, Schiemann WP, Carlin CR. 2013. Epithelial to mesenchymal transition promotes breast cancer progressionviaafibronectin-dependentSTAT3signalingpathway.J.Biol. Chem. 288:17954–17967. http://dx.doi.org/10.1074/jbc.M113.475277.

35. Lee MS, Kim HP, Kim TY, Lee JW. 2012. Gefitinib resistance of cancer cells correlated with TM4SF5-mediated epithelial-mesenchymal transition. Biochim. Biophys. Acta 1823:514–523. http://dx.doi.org/10.1016/j .bbamcr.2011.11.017.

36. Turkson J, Bowman T, Garcia R, Caldenhoven E, De Groot RP, Jove

R. 1998. Stat3 activation by Src induces specific gene regulation and is required for cell transformation. Mol. Cell. Biol. 18:2545–2552.

요약 (국문초록)

간질환 심화과정에서 TM4SF5/STAT3의 상호작용과 그 역할에 관한 연구

TM4SF5는 세포막 단백질로 여러 가지 암 종에서 발현되고 있는데 그 중에서도 간암이나 간경화에서 높게 발현되고 있는 것은 이미 선행연구에서 확인되었다. 하지만 지방간에서의 TM4SF5의 역할은 밝혀진 바가 없으며 간질병의 진행 정도에 따른 TM4SF5/STAT3의 상호작용으로 인한 역할 또한 밝혀내고자 한다. 본 연구에서 TM4SF5가 과 발현 되어있는 마우스모델에서 52주령이 되었을 때 지방간이 유도되는 것을 확인하였고, 이것이 더 심화되어 78주령이 되었을 때는 간경화가 보이는 지방간 염증을 발견하였다. 이 때 TM4SF5와 STAT3의 상호작용에 의해서 질병이 심화된다고 생각되어 신호전달을 확인한 결과, 지방간에서는 TM4SF5가 STAT3보다는 지방대사와 관련된 단백질 중 하나인 SREBP1을 증가시키게 되어 지방간을 유도하는데 반대로 STAT3의 인산화는 줄어드는 것을 확인하였다. 그래서 지방축적과 관련 있는 동시에 STAT3의 활성을 저해하는 것으로 알려진 SOCS1,3의 발현을 확인하였더니 TM4SF5가 있을 때 조직과 간세포 모두에서 증가하는 것을 보았다. 이것은 SOCS1,3의 발현이 올라가고 또한 STAT3와 SREBP1이 서로 상반되는 역할을 함으로써 지방간을 유도하는 것이라고 보여 진다. 그리고 78주령 마우스에서 보여 지는 지방간 염증은 지방간에서와는 다르

게 SREBP1의 수준은 낮아지고 SOCS1,3의 발현 또한 TM4SF5 유무와 상관없이 비슷한 수준으로 나타나는 것을 확인하였다. 그러면서 STAT3의 인산화가 다시 증가하고 간경화의 주요인자 중 하나인 ECM이 높게 발현하여 질병을 심화시키게 되는 것이라고 예상된다. 여기서 세포의 종류에 따라서 발현하는 ECM이 다르다는 것을 알게 되었는데 간세포에서는 collagen 보다 Laminin이 상대적으로 높게 발현되어 있고 이것은 TM4SF5와 STAT3에 의해서 조절될 수 있다는 것을 확인하였다.

이러한 결과는 각 간질병 진행 상태에 따라서 TM4SF5의 역할이 다르게 움직임으로써 전달하는 신호가 다르다고 생각되어지는데 이전 연구결과에서는 간암세포의 TM4SF5 발현이 Integrin과의 crosstalk을 통하여 FAK/STAT3와 함께 혈관형성의 activity나 세포증식속도와 면역회피에 영향을 주는 것으로 증명되었다. 그래서 이후의 연구에서는 간암세포나 간경화가 일어난 세포에서 TM4SF5의 발현유무에 따라서 STAT3를 통한 ECM(collagen, laminin, fibronectin 등)의 발현 양이 달라지는 것을 확인하였고 또한 TM4SF5의 억제제를 이용한 세포실험이나 동물실험을 통해서도 TM4SF5의 발현을 낮춤으로써 STAT3의 인산화와 ECM의 발현 양이 감소하는 것을 확인하였다. 그리고 지방간에서도 TM4SF5/STAT3를 조절하여 지방의 축적을 저해시킬 수 있다는 것을 알 수 있었다. 이 연구는 두 가지 basic하고 clinical 관점에서 중요성을 내포하고 있는데 각 질병에 관련된 세포의 미세 환경을 조절함으로써 지방간, 간경화, 암 전이의 진행속도를 낮출 수 있다는 것을 규명할 수 있다.

주요어: Animal models, Collagen I, Fibrosis, Hepatic cancer, Laminin, Nonalcoholic fatty liver disease (NAFLD), SOCS, SREBP1, STAT3, TM4SF5, FAK, IL-6

학 번 : 2011-21717